Olga Marisa da Silva Pereira

The effects of anti-leukemia chemotherapy on LKB1-AMPK pathway functioning in acute myeloid leukemia cell lines

UMinho|2013

Universidade do Minho
Escola de Ciências da Saúde

Olga Marisa da Silva Pereira

The effects of anti-leukemia chemotherapy on LKB1-AMPK pathway functioning in acute myeloid leukemia cell lines

Os efeitos da quimioterapia anti-leucémica na funcionalidade da via LKB1-AMPK em linhas celulares de leucemia mielóide aguda

Agosto de 2013

Universidade do Minho
Escola de Ciências da Saúde

Olga Marisa da Silva Pereira

The effects of anti-leukemia chemotherapy on LKB1-AMPK pathway functioning in acute myeloid leukemia cell lines

Os efeitos da quimioterapia anti-leucémica na funcionalidade da via LKB1-AMPK em linhas celulares de leucemia mielóide aguda

Dissertação de Mestrado
Mestrado em Ciências da Saúde

Trabalho realizado sob a orientação da
Professora Doutora Paula Cristina da Costa Alves Monteiro Ludovico
e co-orientação da
Mestre Isabel Maria da Silva Castro

Agosto de 2013

The work presented in this thesis was performed in the Microbiology and Infection Research Domain in the Life and Health Sciences Research Institute (ICVS), School of Health Sciences, University of Minho, Braga, Portugal (ICVS/3B's – PT Government Associate Laboratory, Braga/Guimarães, Portugal). The financial support was given by Fundação para a Ciência e Tecnologia (FCT)/MCTES (PIDDAC) and co-supported by Fundo Europeu de Desenvolvimento Regional (FEDER) though the COMPETE-Programa Operacional Factores de Competitividade (POFC) means of a project PTDC/BIA-MIC/114116-2009.

AGRADECIMENTOS

À Professora Doutora Paula Ludovico, pela oportunidade, conhecimento e apoio transmitidos ao longo deste projecto. Obrigada!

À Doutora Isabel Castro, pela ajuda e apoio durante este projecto.

À Belém e à Ângela, pela ajuda constante, apoio incondicional, palavras de amizade e momentos de boa disposição que passamos juntas. Obrigada!

Ao Bernardo, pela disponibilidade e prontidão em ajudar, sempre!

Ao João Amorim, pelos momentos de descontracção, boa disposição e gargalhadas sem fim que me proporcionou.

À Ana Rita e à Joana pelas gargalhadas e momentos de boa disposição que passamos juntas.

A todos os colegas do ICVS com quem tive oportunidade de conviver, aprender e crescer enquanto pessoa.

Aos meus pais, que me apoiaram incondicionalmente ao longo de todo o meu percurso académico.

Aos meus irmãos, pelo apoio incondicional, palavras de carinho, momentos de descontracção e por nunca me deixarem desistir. Obrigada!

Aos meus sobrinhos, que são das pessoas que mais amo neste mundo e que sempre me deram força para lutar pelos meus objectivos.

ABSTRACT

Acute myeloid leukemia (AML) is a clonal disorder characterized by genetic alterations in hematopoietic stem and/or progenitor cells, leading to the accumulation of leukemic myeloblasts. Current AML therapies rely mainly on high doses of cytarabine and doxorubicin, which promote good outcomes for young patients but that are highly toxic and have limited application and poor outcomes among old individuals. Thus, the elucidation of the mechanisms underlying AML cell's response to conventional chemotherapy is still a major challenge.

Studies showed that some anticancer agents that induce DNA damage activate a DNA damage response (DDR), involving the phosphorylation of proteins such as AMP-activated protein kinase (AMPK), that leads to autophagy induction as a pro-survival mechanism. Cytarabine and doxorubicin are inducers of DNA damage and DDR, however, the study of their effects in AML cells is still very scarce. Our preliminary data showed that AML cells treated with conventional chemotherapy displayed cell cycle arrest in G0/G1 and S phases associated with autophagy induction. Therefore, this work aimed to understand if the activation of AMPK pathway with consequent cell cycle arrest and autophagy induction could act as a pro-survival mechanism in AML cells. For such purpose, two AML cell lines (HL-60 and KG-1) were used as *in vitro* models and their response to conventional chemotherapy, cytarabine and/or doxorubicin was evaluated. The effect of conventional chemotherapy combination with rapamycin or chloroquine (CQ), autophagy activator or inhibitor, respectively, was also determined.

Results suggested that cytarabine or doxorubicin promote DNA damage in HL-60 cells, which leads to the activation of AMPK pathway culminating in G0/G1 cell cycle arrest and autophagy induction as a pro-survival mechanism. Whether anti-leukemia agents promote DNA damage in KG-1 cells is inconclusive due to the high endogenous levels of DNA damage displayed by these cells, however, our data showed that doxorubicin alone or combined with cytarabine promote AMPK pathway activation, S phase cell cycle arrest and autophagy induction as a tumor suppressor mechanism. Results obtained with the combination of anti-leukemia agents with CQ showed a decrease in HL-60 cell viability but an increase in KG-1 cell viability, supporting the hypothesis that this process may function as a pro-survival in HL-60 cells but a pro-death in KG-1 cells. Therefore, different approaches involving the combination of conventional chemotherapy with AMPK/autophagy modulators could be a good strategy for combined chemotherapy in AML.

RESUMO

A leucemia mielóide aguda (LMA) é uma doença clonal caracterizada por alterações genéticas nas células estaminais e/ou progenitoras hematopoiéticas, resultando numa acumulação de mieloblastos leucémicos. A actual terapia anti-leucémica consiste principalmente na aplicação de elevadas doses de citarabina e doxorubicina. Apesar deste regime terapêutico ser eficiente em pacientes jovens, a sua aplicação é limitada e tem resultados insatisfatórios em pacientes idosos. Desta forma, a elucidação dos mecanismos celulares de resposta das células de LMA à quimioterapia convencional é ainda um grande desafio.

Diferentes estudos demonstraram que alguns agentes anticancerígenos indutores de danos no DNA activam uma resposta celular a estes danos, que envolve a fosforilação de proteínas tais como "AMP-activated protein kinase" (AMPK), resultando numa indução de autofagia como mecanismo de adaptação e sobrevivência. A citarabina e a doxorubicina são conhecidos indutores de danos no DNA e da resposta celular a estes danos, no entanto, os dados sobre estes efeitos em células de LMA são ainda muito escassos. Dados preliminares do nosso grupo demonstraram que células de LMA tratadas com quimioterapia convencional exibem uma paragem do ciclo celular nas fases G0/G1 e S associada com a indução de autofagia. Assim, este trabalho pretende determinar se a activação da via AMPK com consequente paragem do ciclo celular e indução de autofagia pode constituir um mecanismo de adaptação e sobrevivência das células de LMA. Para isso, duas linhas celulares de LMA (HL-60 e KG-1) foram usadas como modelos *in vitro*, sendo sujeitas a tratamento com citarabina e/ou doxorubicina. O efeito da combinação da quimioterapia convencional com rapamicina ou cloroquina (CQ), um activador ou inibidor da autofagia, respectivamente, foi também avaliado.

Os resultados obtidos indicaram que a citarabina e a doxorubicina promovem danos no DNA nas células HL-60, os quais levam à activação da via do AMPK culminando numa paragem do ciclo celular nas fases G0/G1 e indução de autofagia como mecanismo de sobrevivência. Apesar de os resultados serem inconclusivos no que diz respeito à indução de danos no DNA nas células KG-1, principalmente devido aos elevados níveis endógenos de danos no DNA apresentados por estas células, os nossos resultados indicam que a doxorubicina sozinha ou combinada com a citarabina promove activação da via AMPK, paragem no ciclo celular na fase S e indução de autofagia como mecanismo associado à morte celular. Os resultados obtidos com a combinação da terapia convencional com a CQ mostraram uma diminuição da viabilidade das

células HL-60 mas um aumento da viabilidade das células KG-1, suportando a hipótese de que a autofagia funciona como um mecanismo de sobrevivência nas células HL-60 mas como um mecanismo associado à morte nas células KG-1. Assim, diferentes metodologias envolvendo a combinação da quimioterapia convencional com moduladores do AMPK/autofagia poderão ser uma boa estratégia terapêutica para pacientes com LMA.

TABLE OF CONTENTS

LIST OF TABLES AND FIGURES

Tables: **Pag.**

Figures:

HSC - hematopoietic stem cell

AML - acute myeloid leukemia

ALL - acute lymphoid leukemia

LSC - leukemic stem cell

CMP - common myeloid progenitor

MDS - myelodysplastic syndrome

FAB - French-American-British system

WHO - World Health Organization system

AML-MRC - AML with myelodysplasia-related chances

t-MN - therapy-related myeloid neoplasms

CR - complete remission

HDAC - high doses of cytarabine

HSCT - hematopoietic stem cell transplantation

OS - overall survival

MDR - multi-drug resistance

APL - acute promyelocytic leukemia

ATRA - all-trans retinoic acid

RXR - retinoic X receptor

ATO - arsenic trioxide

Ara-C- 1-β-arabinofuranosylcytosine/cytarabine

DDR - DNA damage response

PIKKs - phosphoinositide 3-kinase related protein kinases

ATM - ataxia-telangiectasia mutated

ATR - ATM and Rad3 related

dsDNA breaks - double-strand DNA breaks

ssDNA breaks - single-strand DNA breaks

LKB1 - liver kinase B1

AMPK - AMP-activated protein kinase

MDM2 - murine double minute 2

Sesn 1/2 - Sestrins 1 and 2

TSC - tuberous sclerosis

Rheb - Ras homolog enriched in brain

mTORC1 - mammalian target of rapamycin complex 1

CDKI - cyclin-dependent kinase inhibitor

Chk - checkpoint kinase

Cdc25A - Cell division cycle 25 homolog A

GADD45 - growth arrest and DNA damage 45

Atg - autophagy-related genes

hVPS34 - vacuolar protein sorting 34

PE - phosphatidylethanolamine

3-MA - 3-Methyladenine

CQ - chloroquine

HU - hydroxyurea

PI - propidium iodide

IC_{50} - half maximal inhibitory concentration

INTRODUCTION

1. Acute Leukemia

Acute leukemia comprises a group of clonal disorders characterized by an uncontrolled expansion of hematopoietic stem cells (HSCs) and/or committed progenitor cells that fail to differentiate normally, resulting in the accumulation of nonfunctional immature cells [1-3]. This group of disorders is divided into two different subtypes depending on their cell of origin: leukemia evolving from myeloid precursors is named acute myeloid leukemia (AML), while lymphocytic precursors give rise to acute lymphoid leukemia (ALL) [4].

1.1. Acute myeloid leukemia

1.1.1. Etiology and epidemiology

AML is a clonal hematopoietic disorder characterized by an extreme proliferation and accumulation of abnormal leukemic myeloblasts in the bone marrow, which interfere with the normal production of blood cells [5-8]. Alterations in HSCs, committed myeloid progenitors cells or both can be responsible for the transformation of normal hematopoietic cells into leukemic myeloblasts [3, 9] and three different scenarios can be described [3]: A) HSC undergoes a first mutation leading to the formation of a pre-leukemic stem cell. Then, secondary mutation(s), epigenetic changes and/or aberrant microenvironment signals promote the transformation of the pre-leukemic stem cell into a leukemic stem cell (LSC) (Fig.1A); B) a first mutation occurs at the HSC level resulting in the formation of a pre-leukemic myeloid progenitor cell. This cell gives rise to LSC after secondary mutation(s), epigenetic changes and/or aberrant microenvironment signals (Fig.1B); C) HSC first differentiates into a common myeloid progenitor (CMP) cell, which then undergoes primary and secondary mutations to ultimately generate LSC (Fig.1C). For all of the three scenarios, the generation of LSC with self-renewal capability, abnormal/arrested differentiation and resistance to death signals leads to the formation and accumulation of leukemic myeloblasts in the bone marrow (Fig.1). This accumulation disrupts the normal production of white and red blood cells and platelets [5-8]. During the progression of the disease, leukemic myeloblasts accumulation occurs not only in the bone marrow, but also in the blood

and organs such as brain, skin and gums, which may lead to infection, anemia, bleeding or organ infiltration [5-8].

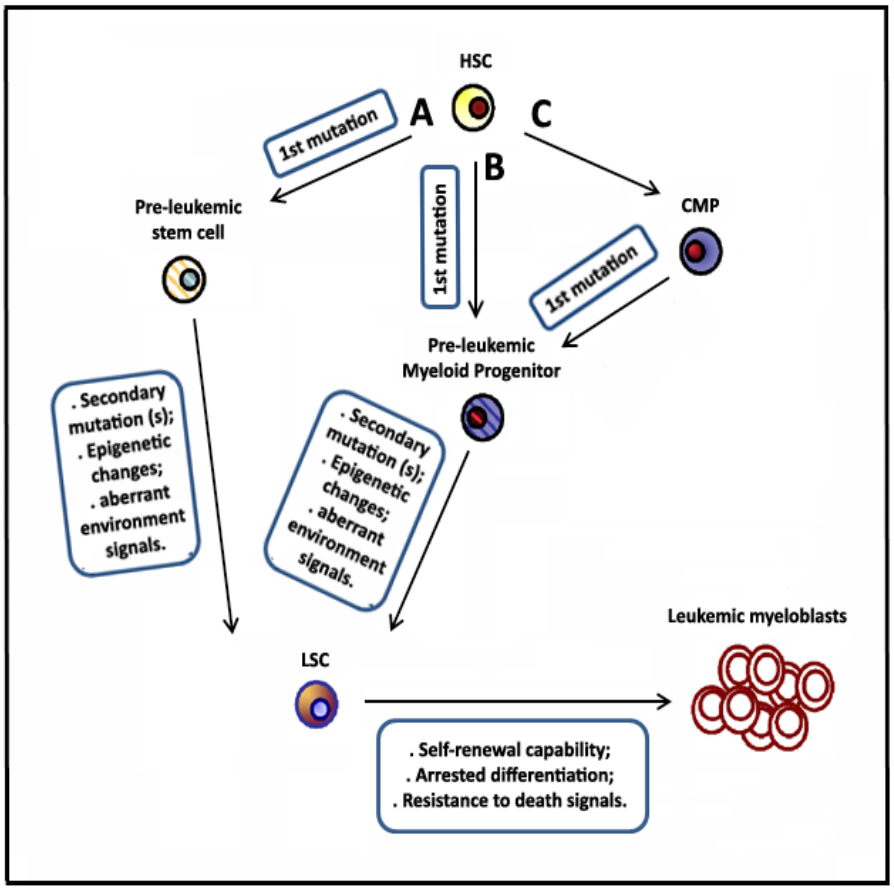

Figure 1 – Schematic representation of the models for acute myeloid leukemia (AML) development. Three different scenarios can occur during AML evolution (A-C). HSCs, CMP cells or both are potential targets for primary and secondary mutations, epigenetic changes and/or aberrant microenvironment signals that lead to the acute myeloid disease development. Cells bearing a single mutation are termed "pre-leukemic", which upon undergoing subsequent mutations, epigenetic changes and/or aberrant microenvironment signals give rise to LSCs. LSCs in turn give rise to the majority of malignant cells found in the leukemia population – myeloblasts. From [3].

AML can arise *de novo* or secondarily either due to the progression of other malignant disorders, such as myelodysplastic syndrome (MDS) or chronic bone marrow stem cell disorders, [10, 11] or due to the treatment with cytotoxic agents or radiotherapy (10-15% of patients with AML develop this disease after treatment with cytotoxic chemotherapy used in solid tumors) [12, 13].

AML comprises about 40% of all leukemia in the Western world [8] and 25% of all leukemia diagnosed in adults [14]. In fact, AML is the most common type of acute leukemia in adults [14], with a median age of diagnosis of 65 years [8, 15, 16]. The incidence of AML increases with age [17-19], being rarely diagnosed before the 40 years (Fig.2) [18, 19]. From 2006 to 2010, the U.S. incidence in the <65 years' age group was only 1.5 cases per 100,000 people, whereas in the ≥ 65 years' age group was 18.3 cases per 100,000 people (Fig.2) [19]. AML in adults has a slight male predominance and from 2006 to 2010, the U.S. incidence in the male´s group was 7.9 per 100,000 people, whereas only 5.1 per 100.000 people was in females (Fig.2) [19]. AML incidence is expected to increase in the future in line with age population [17, 18].

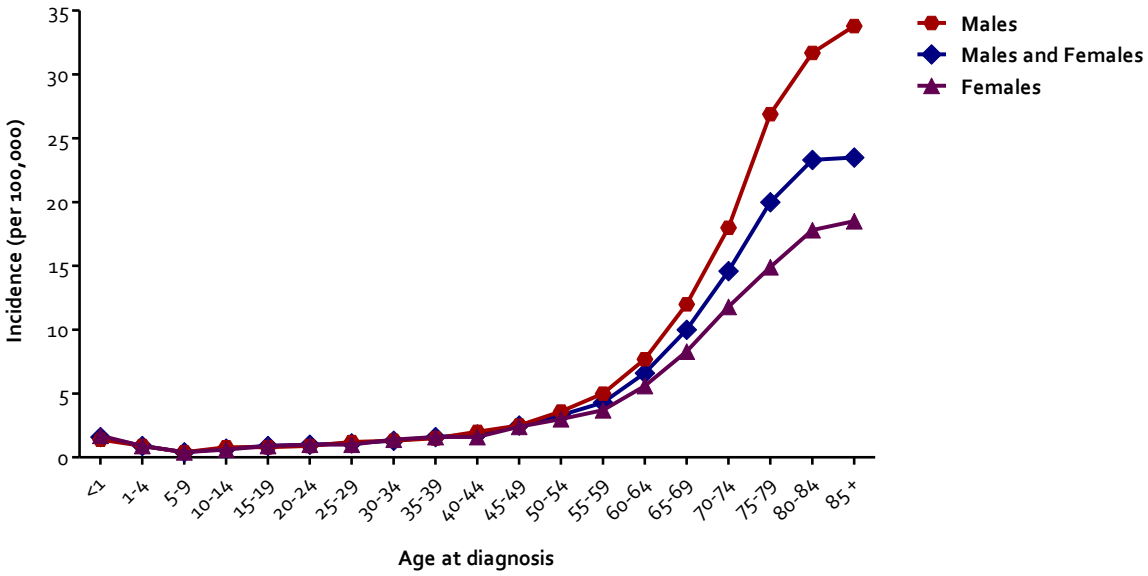

Figure 2 - Acute Myeloid Leukemia (AML): Age-Specific Incidence Rates by Sex in the U.S. population (2006-2010). The horizontal axis shows 5-year age intervals. The vertical axis shows the frequency of new cases of AML per 100,000 people in a given age and sex-group. Red, purple and blue represents males, females and males plus females, respectively. From [19].

1.1.2. Clinical presentation

The AML symptoms are nonspecific and include loss of weight and appetite, weakness and fatigue, lethargy, dyspnea, fever and bleeding [4, 20]. Pains in the bones may occur as result of

bone marrow infiltration with blasts [4, 20]. Hepatosplenomegaly may also occur when blasts infiltrate organs [4].

Common physical features may include pallor, epistaxis, gingivitis, splenomegaly, hepatomegaly or bone tenderness [4].

1.1.3. Diagnosis and classification

The 2 systems commonly used in the classification of AML are the French-American-British (FAB) system, initially proposed in 1976 [21], and the World Health Organization (WHO) system, introduced by the first time in 1999 [20, 22]. The FAB classification is based on morphology, cytochemistry and degree of maturation of malignant blasts [23, 24], whereas WHO classification combines not only morphologic and cytochemistry features but also genetic, immunophenotypic, biologic and clinical information [25-27].

The FAB classification recognizes eight subtypes of AML (M0 to M7) (Table 1) [4, 20, 23], while 2008 WHO classification identifies four main subgroups: i) AML with recurrent genetic abnormalities; ii) AML with myelodysplasia-related changes (AML-MRC); iii) therapy-related myeloid neoplasms (t-MN) and iv) those that do not fall into any of these groups (Table 2) [26-28].

Table 1 - Classification of acute myeloid leukemia (AML) according to FAB classification system [20].

FAB subtype	Morphological classification
M0	Undifferentiated acute myeloid leukemia
M1	Acute myeloid leukemia with minimal maturation
M2	Acute myeloid leukemia with maturation
M3	Acute promyelocytic leukemia
M4	Acute myelomonocytic leukemia
M4 eos	Acute myelomonocytic leukemia with eosinophilia
M5	Acute monocytic leukemia
M6	Acute erythroid leukemia
M7	Acute megakaryoblastic leukemia

The WHO system created several subclasses of AML (Table 2), allowing physicians to identify subgroups of patients who might benefit from specific treatment strategies [20].

Table 2 - Classification of acute myeloid leukemia (AML) according to 2008 WHO classification system [26-28].

AML with recurrent genetic abnormalities		**AML with myelodysplasia-related changes (AML-MRC)**	**Therapy-related myeloid neoplasms (t-MN: t-AML; t-MDS; t-MDS/MPN)**	**AML not otherwise specified (AML NOS)**	
AML with t(8;21)(q22;q22); *RUNX1-RUNX1T1*	AML with inv(3)(q21; q26.2) or t(3;3)(q21;q26.2); *RPN1-EVI1*	AML cases with a history of MDS (myelodysplastic syndrome) or MDS/MPN (myelodysplastic syndrome/myeloproliferative neoplasm)	Direct mutational effect of cytotoxic agents and/or radiation	AML with minimal differentiation	Acute erythroid leukemia (erythroid/myeloid and pure erythroleukemia) *
AML with inv(16)(p13.1; q22) or t(16;16)(p13.1;p22); *CBFB-MYH11*	AML (megakaryoblastic) with t(1;22)(p13;q13); *RBM15-MKL1*	Without antecedent MDS or MDS/MPN, but with dysplasia in at least 50% of cells in two or more myeloid lineages	Immunosuppression from prior or current therapy	AML without maturation	Acute megakaryocytic leukemia
Acute promyelocytic leukemia with t(15;17)(q22;q12); *PML-RARα*	Provisional entities: AML with mutated *NPM1*; AML with mutated *CEBPA*	AML cases with myelodysplasia-related cytogenetic abnormalities	Ineffective bone marrow microenvironment because of injury to vascular supply or increasing fibrosis (caused by prior treatment)	AML with maturation	Acute basophilic leukemia
AML with t(9;11)(p22;q23); *MLLT3-MLL*			Host genetic predisposition	Acute myelomonocytic leukemia	Acute panmyelosis with myelofibrosis
AML with t(6;9)(p23;q34); *DEK-NUP214*			High frequency of unfavorable cytogenetic abnormalities	Acute monoblastic/ acute monocytic leukemia	

Footnote:

* The 2008 WHO system recognizes two different subtypes of acute erythroid leukemia depending on the presence or absence of a significant myeloblastic component: acute erythroid/myeloid leukemia and pure erythroleukemia. The first subtype is characterized by: i) myeloblasts <20% of all bone marrow cells but $\geq$ 20% of the nonerythroid cells; ii) at least 50% erythroid precursors in the bone marrow nucleated cell population [28]. In the second subtype 80% or more of the bone marrow cells are immature erythroid precursors with minimal differentiation and no significant myeloblastic component [25].

According to WHO classification, a myeloid neoplasm with 20% or more blasts in the peripheral blood or bone marrow is identified as AML, in contrast with the FAB system where this threshold increases to 30% [25, 26].

1.1.4. Cytogenetic abnormalities

AML is a heterogeneous hematological disorder with respect to chromosome abnormalities, gene mutations and changes in expression of multiple genes and microRNAs [20]. Cytogenetic abnormalities are detected in 50% to 60% of the newly diagnosed AML patients [29], being the majority associated with non-random chromosomal translocations [30]. These translocations often result in gene rearrangements that involve a locus encoding a transcriptional activator that leads to the expression of a fusion protein [30]. In many cases, this fusion protein functions as a transcriptional factor capable of interacting with a co-repressor complex [30]. Thus, in the presence of aberrant recruitment of a co-repressor to a locus of active transcription, this fusion protein changes expression of target genes necessary for myeloid development, which contribute for leukemic transformation [31, 32]. The three most common chromosomal translocations that occur in AML are t (15; 17) and t (8; 21) with an occurrence of 10% and inv (16) with an occurrence of 5% [20, 29]. The t (15; 17), t (8; 21) and inv (16) result in the expression of PML-RARα, RUNX1-RUNX1T1 (also called AML1-ETO [33]) and CBFβ-MYH11 oncofusion proteins, respectively. These proteins, by different mechanisms (reviewed in [20, 29, 33]), act as transcriptional repressors that interfere with the expression of genes involved in important processes such as differentiation, impairing the hematopoietic myeloid cells maturation [34-38]. AML patients with these alterations are classified into the group with a favorable prognosis [29].

Around 40%-50% of AML patients present a normal karyotype and are included into the intermediate-risk group [39]. However, not all these patients exhibit the same response to treatment, mainly due to the presence of a large variability in gene mutations. These mutations can be divided into two classes, class I and class II [20]. Class I comprises the mutations that activate signal transduction pathways responsible for proliferation, survival or both in hematopoietic myeloid progenitor cells. Mutations in *KIT* (feline sarcoma viral oncogene homolog), *FLT3* (Fms-like tyrosine kinase 3) and *RAS* (rat sarcoma viral oncogene homolog) fall into this group [20]. On the other hand, class II includes the mutations that affect transcription

factors or components of the cell cycle machinery blocking normal myeloid differentiation. Mutations in *MLL* (mixed lineage leukemia), *BAAL* (brain and acute leukemia), *WT1* (Wilms tumor 1), *CEBPα* (enhancer-binding protein α) and *NPM1* (nucleoplasmin 1) genes belong to this group [20].

The detailed knowledge about cytogenetic and molecular characterization of AML patients comprises crucial information for a better diagnosis, prognosis and treatment strategies.

1.1.5. Therapy and outcomes

Acute leukemia is a fatal disease that if untreated has a median survival of 3 months or less [4]. Therefore, the early diagnosis and treatment are fundamental for obtain better outcomes.

The treatment of AML is divided into two phases: the remission induction therapy (with possible post-induction phase) and the post-remission therapy [4, 20]. In the induction therapy, the goal is to achieve a marked reduction in the number of malignant cells in the bone marrow and peripheral blood in order to establish normal hematopoiesis [4, 20]. The post-remission therapy is administered weeks after the induction therapy has ended with the intention of preventing relapse [4, 20]. The basis for the current AML treatment was developed nearly 30 years ago and consists in the combination of an anthracycline (DNA intercalating agent and topoisomerase II inhibitor), such as daunorubicin or idarubicin, and cytarabine (a nucleoside analog) [40-43]. The standard regimen used during the remission induction therapy of AML includes 7 days of continuous infusion of cytarabine (100-200 mg/m^2) combined with daunorubicin or idarubicin (45-60 mg/m^2) administered intravenously for 3 days, referred to as "7 + 3" regimen [40-43]. After this first phase, it is expected that AML patients achieve complete remission (CR), which is defined as a bone marrow with less than 5% of blasts and a neutrophil and platelet count greater than 1000 and 100 000, respectively [44]. However, only 65%-75% of patients aged < 60 years [40-42, 45] and 40%-50% of patients aged > 60 years reach CR [45-47]. In order to improve the CR rate, several studies have been conducted using alternative anthracyclines, the anthracenedione mitoxantrone, high doses of cytarabine (HDAC) (cumulative dose 18-24 g/m^2) or additional cytotoxic agents such as etoposide, fludarabine, cladribine or topotecan [6, 7, 20]. However, despite theoretical benefits, none of these regimens have convincingly shown a survival advantage over "7 + 3" standard regimen [6, 7, 20]. Therefore,

patients who fail to achieve CR after remission induction therapy, should participate in the post-induction therapy [20]. On the other hand, patients who achieve CR should advance to the next phase, the post-remission therapy, since studies have shown that patients who don´t receive post-remission therapy relapse within 6 to 9 months [48]. The post-remission therapy includes chemotherapy, autologous hematopoietic stem cell transplantation (HSCT) or allogeneic HSCT [7]. The choice of the treatment depends on patient age, comorbidities, chance of relapse based on cytogenetics and whether or not the patient has a suitable donor for HSCT [7]. For patients aged < 60 years, the standard consolidation chemotherapy consists in high doses of cytarabine (2-3 g/m^2) [7, 20] twice a day on days 1, 3 and 5, for a total of 3 to 4 cycles [7]. However, patients older than 60 years receive a less intensive chemotherapy based in 5 days of cytarabine (100 mg/m^2) and 2 days of daunorubicin (45 mg/m^2), for a total of 2 cycles [6, 7]. Previous studies showed that high doses of cytarabine induce higher toxicity, mainly cerebellar toxicity, in patients aged > 60 years, making this approach an unacceptable option [49, 50]. HSCT is also associated with increased risks of transplant-related morbidity and mortality. Therefore, this approach is less common in patients aged > 60 years, being used in patients aged < 60 years who have a substantial risk of relapse [51].

In addition to AML treatment recommendations also AML outcomes differ depending on whether patients are above or below 60 years old [52, 53]. Patients aged > 60 years have lower CR rates, shorter disease-free survival and overall survival (OS) and higher incidence of early death during chemotherapy when compared to patients aged < 60 years (Table 3) [7, 46, 47, 54]. These poor outcomes occur because old patients present higher prevalence of unfavorable cytogenetics and myelodysplasia, a greater incidence of multi-drug resistance (MDR) and more frequent comorbidities, which often make them unsuitable for intensive treatment [7]. Thus, while young patients tolerate intensified treatment strategies and have good outcomes, AML treatment is highly toxic and has limited application and poor outcomes among old individuals.

Table 3 - Treatment outcomes in acute myeloid leukemia (AML) based on age criteria [20].

	Age < 60 years	**Age > 60 years**
Complete remission (CR) (%)	65-75	40-50
Disease-free survival (%)	45	20
Early death (%)	10	25
Overall survival (OS) (%)	30	10

The net incidence of AML in older patients is expected to increase as the population continues to age, making essential the development of new therapeutic strategies [55]. Current clinical trials have focused on less-intensive therapies with the potential to be efficacious without impairing patients' quality of life [53]. The growing understanding of specific gene mutations, chromosomal translocations and alterations in signaling pathways and gene transcription in AML has led to the development of a number of targeted agents [53, 56]. These include histone deacetylase inhibitors, FLT3 inhibitors, proteosome inhibitors, DNA methyl transferase inhibitors, among others (Table 4) [53, 56]. In addition, several studies have also been done to optimize traditional chemotherapeutics [20]. Alterations in the concentrations and new formulations are examples of these optimizations [20].

Table 4 - Therapeutic strategies investigated in the treatment of acute myeloid leukemia (AML) [20].

Therapeutic approach	Examples
• **Epigenetic regulation**	• Histone deacetylase inhibitors: vorinostat, panobinostat, belinostat; • DNA methyl transferase inhibitors: Vidaza, Dacogen.
• **Differentiation-inducing therapeutics**	• Retinoid X receptor agonists; • Arsenic trioxide.
• **Angiogenesis inhibition**	• Inhibition of angiogenesis: Velcade; • Thalomid, Revlimid.
• **Inhibition of signaling pathways**	• Tyrosine kinase inhibitors: midostaurin, lestaurtinib, sorafenib, KW-2449, AC220; • Cell cycle inhibitors: ON 01910.Na; • Farnesyl transferase inhibitors: Zarnestra, Sarasar; • mTOR inhibitors: Afinitor, PI-103, temsirolimus, GSK21110183; • PARP inhibitors: ABT-888; • MEK1/2 inhibitors: AZD6244, AS703026, PD98059, GSK1120212; • Bcl-2 inhibitors: oblimersen, obatoclax, ABT-263; • XIAP inhibitor: AEG-35156; • Aminopeptidase inhibitors (tosedostat);
• **Modulation of drug resistance**	• Valspodar, zosuquidar
• **Modified traditional chemotherapeutics**	• Nucleoside analogs: clofarabine, sapacitabine, elacytarabine; • Alkylating drugs: irofulven, Temodar, Onrigin; • Topoisomerase inhibitors: Hycamtin
• **Immune therapy**	• Antibodies: Mylotarg, lintuzumab, Avastin, T-cell targeted therapy

Despite the fact that standard treatment strategies, above mentioned, are applied to the most AML subtypes, acute promyelocytic leukemia (APL) is differently treated [57]. APL is characterized by the t(15;17) chromosomal translocation and consequent expression of the fusion protein PML-RARα [57, 58]. In normal conditions and in the absence of the all-trans retinoic acid (ATRA), RARα interacts with the nuclear receptor RXR (Retinoid X receptor) forming the RARα/RXR heterodimer that binds to DNA recruiting co-repressor complexes that blocks transcription of its target genes [59, 60]. However, in the presence of physiological concentrations of ATRA, the co-repressor complexes undergo a conformational alteration that triggers their dissociation and promotes the recruitment of co-activators important for the transcription of genes involved in processes such as differentiation [61, 62]. In APL, PML-RARα

binds to RXR and acts as a constitutive repressor that is insensitive to physiological concentrations of ATRA [57, 63, 64]. Thus, the transcription of genes involved in differentiation is disrupted blocking the normal promyelocytic maturation [57, 63, 64]. In an attempt to overcome this problem, APL patients are treated with ATRA, a noncytotoxic agent capable of differentiate abnormal promyelocytes into mature granulocytes [65, 66]. However, despite the high CR rates (80%-90%) [65, 66], this effect is transient, lasting weeks or months, when ATRA is administered as a single agent [66, 67]. Therefore, the current standard approach consists in the administration of ATRA plus anthracycline-based chemotherapy [68]. APL patients treated with this approach present the similar high CR rates but lower relapse rate when compared to those treated with ATRA monotherapy [69]. These better outcomes seem to suggest an additive or synergistic effect of both treatment modalities [69]. Recently, some studies have demonstrated that arsenic trioxide (ATO) has also activity against APL [70], showing a CR rate >80% [71, 72]. A more recent study also showed that APL patients treated with ATRA, ATO or ATRA plus ATO present the same CR rates (> 80%), however, in patients submitted to the combination treatment, the time to achieve CR was significantly shorter and the reduction of the disease burden was greater [73]. Nevertheless, despite these results, the current recommendation for induction therapy in newly diagnosed APL remains the standard approach with ATRA plus chemotherapy [68].

2. Cytarabine and doxorubicin

2.1. Mechanisms of action

Malignant cells are characterized by high nuclear DNA replication rates and consequent extreme proliferation when compared to surrounding healthy cells [74]. Interference in DNA replication of malignant cells leads to unsuccessful DNA replication that creates DNA replication stress, which may culminate in cell death, inhibiting tumor cell expansion [75]. Therefore, the mechanistic basis for several anticancer agents consists in the interference with the machinery required for DNA replication [76]. Cytarabine (1-β-D-arabinofuranosylcytosine [ara-C]), one of the most effective chemotherapeutic agents used in the treatment of acute leukemia [77], is a nucleoside/deoxycytidine analogue that is easily taken up by transformed cells and subsequent metabolized into the nucleoside triphosphate form (ara-CTP) [78], which is a substrate for DNA

polymerase [79]. Several studies have reported that the incorporation of ara-CTP instead of deoxycytidine into nascent DNA strand during DNA replication is responsible for the inhibition of DNA strand elongation and unsuccessful DNA replication [80]. Moreover, evidence showed that ara-CTP - deoxycytidine substitution occurs mainly in the Okazaki fragments, inhibiting their elongation and consequently the elongation of the lagging strand during DNA replication [80]. However, the knowledge of how the ara-CTP incorporation interferes with the Okazaki fragments extension is still very scarce. Studies showed that ara-CTP incorporation affects the local structure and/or stability of newly replicated DNA, inhibiting the extension of the nascent DNA at a point distal from the site of substitution [80, 81]. Gmeiner *et al.* described that ara-CTP incorporation provokes an increase in the bend of the helical axis at the site of ara-CTP substitution, which may contribute to the inhibition of DNA extension [76]. Nevertheless, additional studies are required to better understand this mechanism and to improve chemotherapeutic regimens [76].

Doxorubicin, a hydroxylated daunorubicin derivate used against a broad spectrum of solid tumors, lymphomas and leukemias [82], has also been described as impairing important cellular processes involving DNA, such as DNA replication and transcription [83]. This chemotherapeutic agent is rapidly taken up into the nucleus where it binds with high affinity to DNA by classical intercalation between base pairs [84]. However, its precise mechanism of action is not fully understood and several hypotheses have been proposed [83, 85-88]. The mechanism of action most widely accepted is that doxorubicin acts as a DNA topoisomerase II inhibitor [89-91]. DNA topoisomerases II are enzymes involved in the unwinding of DNA during the replication and transcription processes [92]. These enzymes modify the topology of DNA through different steps [92]: 1) DNA topoisomerase II cleaves one strand of the DNA duplex introducing a transient enzyme-bridged DNA gate; 2) a second DNA segment passes through the enzyme-bridged DNA gate; 3) DNA topoisomerase II catalyzes the re-ligation of the cleavage duplex/double-strand DNA break and the products of the reaction are released from the enzyme. The anthracycline doxorubicin is commonly described as an inhibitor of the re-ligation reaction, leading to the accumulation of enzyme-linked double-strand DNA break complexes [89-92], which are extremely toxic to the cells [83].

2.2. Activation of a DNA damage response (DDR)

Dividing cells are under continuous assault either by environmental agents, such as UV light, or by products of normal metabolism, such as reactive oxygen intermediates, which may damage the DNA impairing the proper replication and segregation of the genome to daughter cells [93-95]. To preserve the integrity of the genome, eukaryotic cells have evolved checkpoint control mechanisms capable of detect DNA damage [93-95]. The identification of DNA damage results in the activation of a DNA damage response (DDR), which is a complex network of interacting signal transduction pathways that coordinate cell cycle transitions, DNA replication, DNA repair and cell death [96]. The major regulators of the DDR pathways are the phosphoinositide 3-kinase related protein kinases (PIKKs), including ataxia-telangiectasia mutated (ATM) and ATM and Rad3 related (ATR) [96]. ATM is mainly activated in response to double-strand DNA (dsDNA) breaks [97], while ATR is mainly activated by the presence of single-strand DNA (ssDNA) breaks, induced for example by DNA replication stress [98, 99] (Fig.3). Once activated, both ATM and ATR preferentially phosphorylate serine or threonine residues that are followed by glutamine ("SQ"/"TQ" motifs). Therefore, these proteins cross-talk and target an overlapping set of substrates that promote cell cycle arrest and activation of specific repair pathways in order to repair the damaged DNA and guarantee that progeny cells receive two accurate copies of the genome at the time of cell division [96, 99] (Fig.3). However, when DNA damage is extensive and impossible to repair, DDR pathways activate the expression of genes that induce programmed cell death, mainly described as being of apoptotic nature [96, 100] (Fig.3).

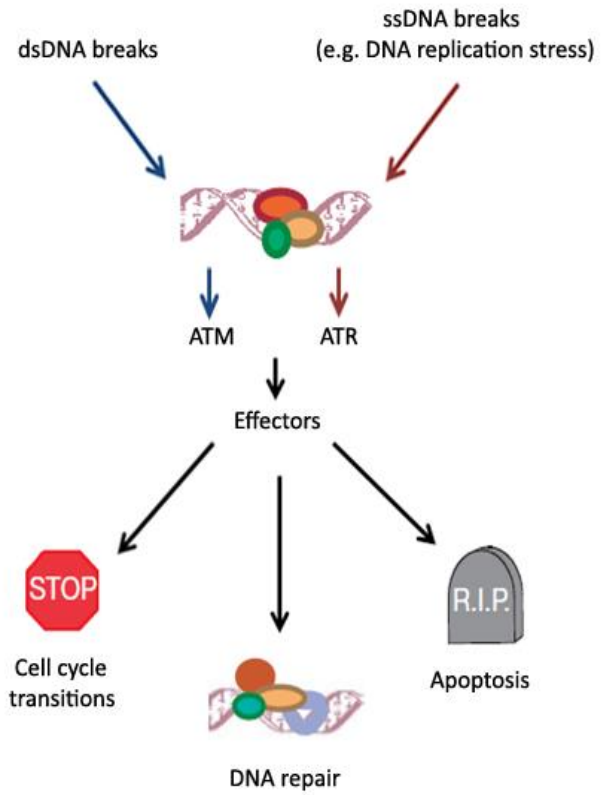

Figure 3 – General outline of the DNA damage response (DDR). In the presence of DNA damage, such as dsDNA and ssDNA breaks, a DDR is activated in order to repair these abnormal structures. The central components of the DDR are the ATM protein, activated by dsDNA breaks, and ATR protein, triggered by ssDNA breaks. Activated ATM and ATR target an overlapping set of substrates/effectors that block cell cycle transitions and stimulate DNA repair. Apoptosis is induced through these pathways when DNA damage is impossible to repair. Blue and red arrows represent ATM and ATR pathway activation, respectively. Cell-cycle arrest is illustrated as a stop sign, DNA repair is represented with a DNA helix with several oval-shaped subunits and apoptosis with a tombstone. From [96].

Cytarabine and doxorubicin are chemotherapeutic agents described as inducers of DNA damage [80, 81, 89-91] and DDR pathways [101-103]. As previous referred, cytarabine inhibits the strand elongation during DNA replication [80], which results in ssDNA breaks [104] (Fig.4). On the other hand, doxorubicin inhibits the re-ligation reaction catalyzed by DNA topoisomerase II during the unwinding of DNA, leading to dsDNA breaks [89-91] (Fig.4). Therefore, the lesions induced by cytarabine result in the activation of ATR pathway [101], while the damage caused by doxorubicin activates ATM pathway [103] (Fig.4).

Under normal conditions, ATM protein resides in the nucleus as an inactive dimer or higher order multimer [105]. However, upon introduction of dsDNA breaks, induced for example by

doxorubicin [89-91], ATM suffers autophosphorylation at Ser1981 [103, 105], which leads to ATM dimer dissociation into monomers and ATM activation [105] (Fig.4). Although ATM protein is activated by autophosphorylation at Ser1981 upon dsDNA breaks, some studies reported that this protein is also activated by ATR, through phosphorylation at Ser1981, upon DNA replication stress induction [106] (Fig.4). Moreover, ATM protein has also been described as inducer of ATR activation [107] (Fig.4). Therefore, ATR and ATM proteins crosstalk and phosphorylate an overlapping set of substrates [106, 107] (Fig.4).

Once activated, ATM protein phosphorylates the histone H2AX at Ser139 [108], being this modification the currently most widely used marker to detect DNA damage [109-111] (Fig.4). A cyclic process is responsible for the phosphorylation of the histone H2AX over megabases of DNA flanking dsDNA breaks and for the consequent formation of an expanding platform for the recruitment of additional damage-response proteins [108], which act as scaffolding proteins that make some non-chromatin-associated substrates accessible to the activated ATM protein [112, 113]. Thus, beyond histone H2AX [108], ATM protein also phosphorylates several other effectors, such as p53 at Ser15 [114, 115], Liver kinase B1 (LKB1) at Thr366 [116] and AMP-activated protein kinase (AMPK) at Thr172 [117, 118] (Fig.4). AMPK is a heterotrimeric complex composed by one catalytic subunit, AMPKα, and two regulatory subunits, AMPKβ and AMPKγ [119] (Fig.4). Therefore, in response to DNA damage, ATM phosphorylates AMPK at Thr172 located in the α catalytic subunit [117, 118] (Fig.4). In addition to ATM and in response to DNA damage, AMPK is also phosphorylated at Thr172 (AMPKα) by LKB1 [120] (Fig.4), a serine/threonine protein kinase that was discovered 12 years ago as mutated in the Peutz-Jeghers Syndrome [121], a rare disorder that predisposes patients to multiple benign and malignant tumors including gastrointestinal, pancreatic and lung tumors [122].

.

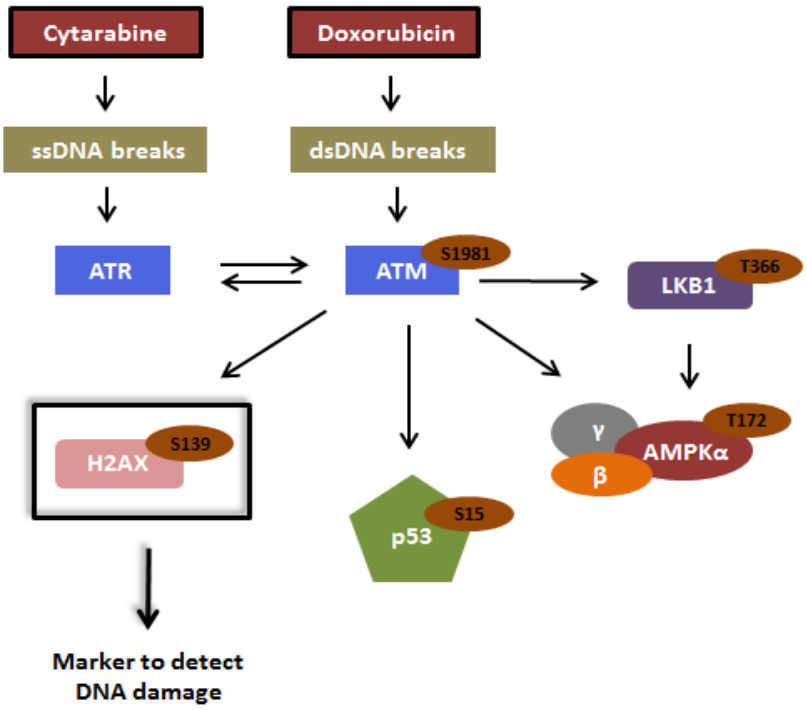

Figure 4 – Partial schematic representation of the DNA damage response (DDR) pathway activated by the chemotherapeutic agent's cytarabine and doxorubicin. Cytarabine induces ssDNA breaks, which result in the activation of ATR protein. On the other hand, doxorubicin leads to the formation of dsDNA breaks, which promote the phosphorylation at Ser1981 and consequent activation of ATM. Furthermore, ATR is also activated by ATM, as well as, ATM is stimulated by ATR (through phosphorylation at Ser1981). Once activated, ATM protein phosphorylates the histone H2AX at Ser139, being this modification widely used to detect DNA damage. Beyond histone H2AX, other several substrates are phosphorylated by ATM, namely p53 at Ser15, LKB1 at Thr366 and AMPK at Thr172 (AMPKα). In response to DNA damage, AMPK is also phosphorylated at Thr172 (AMPKα) by the LKB1 protein.

p53 is an important checkpoint protein that plays a crucial role in the maintenance of genome integrity [123]. Under physiological conditions, p53 is kept at basal levels through interaction with the murine double minute 2 (MDM2) protein, an ubiquitin E3 ligase that promotes p53 ubiquitination and degradation by the proteasome [124]. However, in the presence of a stress stimulus, p53 undergoes post-translational modifications, such as the phosphorylation at Ser15 by ATM in response to DNA damage [114, 115], which disrupt p53-MDM2 complex and promotes p53 stabilization and accumulation. Once activated, p53 acts as a transcription factor that regulates the transcription of several target genes leading to cell cycle arrest, DNA repair and apoptosis if the damage is too severe to be repaired [115] (Fig.5).

Recently, it was also reported that activation of p53 in response to DNA damage might promote the transcription and expression of the evolutionarily conserved stress-sensitive genes Sestrins 1 and 2 (Sesn 1/2), which form a complex with AMPK and TSC (tuberous sclerosis) 1:TSC2 heterodimer [125] (Fig.5). In this complex, Sesn 1/2 promote the activation of AMPK by induced proximity-dependent autophosphorylation at Thr172 (AMPKα), which, once activated, phosphorylates TSC2, present in the TSC1:TSC2 heterodimer, at Thr1227 and Ser1345 [125] (Fig.5). After activation, TSC2 functions as a GTPase-activating protein for the Ras homolog enriched in brain (Rheb) GTPase, inducing a decrease in the Rheb-GTP levels [125] (Fig.5). As the GTP-bound form of Rheb is required for mammalian target of rapamycin complex 1 (mTORC1) activation, through phosphorylation at Ser2448 [126], in response to DNA damage, mTORC1 is inactivated [125] (Fig.5). The mTORC1 complex, constituted by mTOR, raptor, PRAS40 and mLST8, regulates several important biological processes [127], such as: positively regulates protein synthesis [128, 129] and negatively regulates autophagy (a catabolic process) [130]. Therefore, in response to DNA damage occurs the inhibition of protein synthesis [125] and the activation of autophagy [131] (Fig.5). Upon DNA damage induction, AMPK not only directly phosphorylates TSC2 [125], but also phosphorylates p53 at Ser15 [132], which suggests the existence of a positive regulatory loop to further increase the activation of TSC2 with consequent inhibition of mTORC1 and induction of autophagy (Fig.5). In addition, it was also reported that, in response to DNA damage, AMPK phosphorylates p27 at Thr198 [133] (Fig.5). p27 is a member of the cyclin-dependent kinase inhibitors (CDKIs) family that functions, in the nucleus, to negatively regulate Cdk2 on Cyclin E (A)/Cdk2 complexes, preventing the progression of the cell cycle by induction of G0/G1 cell cycle arrest [134]. Nonetheless, in response to stress stimuli, including DNA damage, the phosphorylation of p27 at Thr198 by AMPK promotes p27 stabilization, exportation and sequestration in the cytoplasm, where it promotes autophagy induction [135] (Fig.5). However, the precise mechanism by which p27 stimulates autophagy is not yet known.

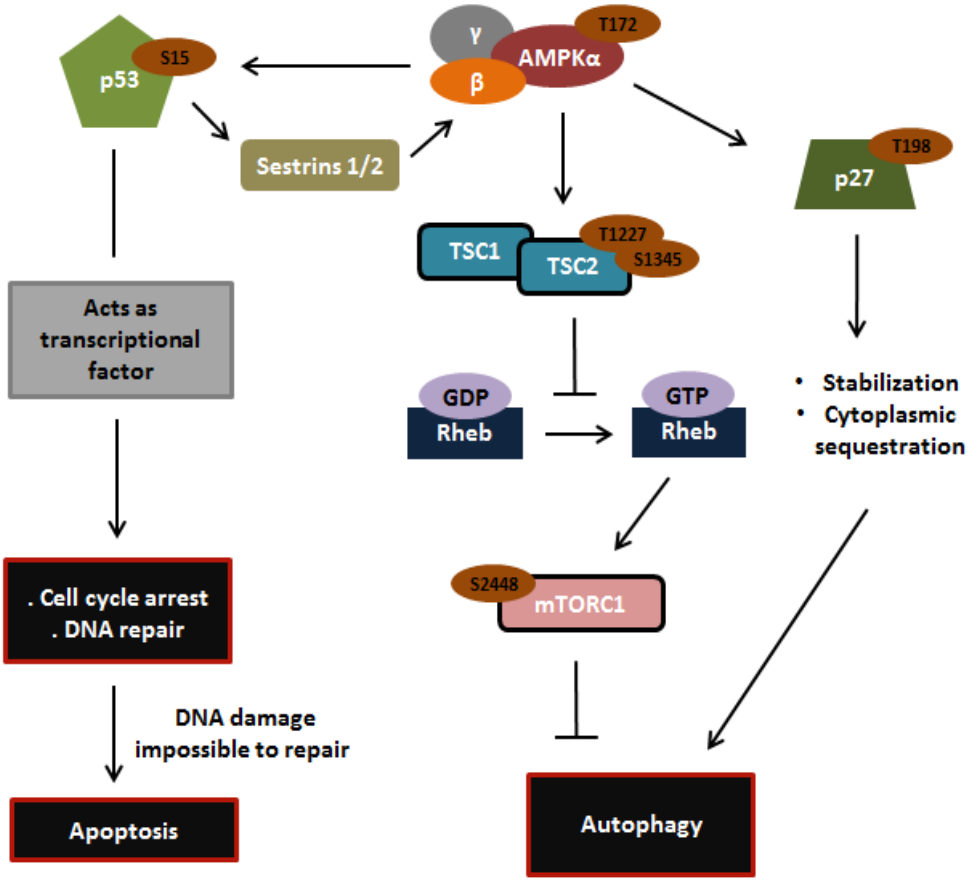

Figure 5 - Schematic representation of the interplay between AMPK and p53 and p27 in response to DNA damage. After DNA damage, p53 is phosphorylated at Ser15 and consequently activated. After activation, p53 functions as a transcription factor that regulates the transcription of several target genes leading to cell cycle arrest, DNA repair and apoptosis when the damage is impossible to repair. As transcriptional factor, p53 may also promote the transcription and expression of Sesn 1/2, which form a complex with AMPK and TSC1:TSC2 heterodimer. In this complex, Sesn 1/2 promote the activation of AMPK by induced proximity-dependent autophosphorylation at Thr172 (AMPKα), which, once activated, phosphorylates TSC2 at Thr1227 and Ser1345. After activation, TSC2 acts as a GTPase-activating protein for the Rheb GTPase, leading to a decrease in the Rheb-GTP levels. As the GTP-bound form of Rheb is required for mTORC1 activation, through phosphorylation at Ser2448, in response to DNA damage, mTORC1 is inhibited with consequent activation of autophagy. After DNA damage induction, AMPK also phosphorylates p53 at Ser15, suggesting the existence of a positive regulatory loop to further increase the activation of TSC2 with consequent inhibition of mTORC1 and induction of autophagy. In addition, activated AMPK also phosphorylates p27 at Thr198 promoting p27 stabilization and cytoplasmic sequestration, leading to autophagy induction.

The information above referred shows us that AMPK is a central/crucial player in the DDR, since this protein allows the interconnection of several molecules involved in this complex pathway.

In addition to DNA damage, the LKB1-AMPK pathway is also activated in response to metabolic/energy stresses, such as nutrient starvation (e.g. glucose or amino acid deprivation), growth factor withdrawal, hypoxia or agents that affect ATP synthesis (reviewed in [136]). These cellular stresses reduce ATP production or accelerate ATP consumption, causing a rise in the AMP:ATP ratio (reviewed in [136]). The accumulation of AMP results in the allosteric binding of AMP to the regulatory γ subunit of AMPK, which induces conformational changes in the AMPK heterotrimeric complex, improving the ability of the catalytic α subunit of AMPK to serve as a substrate for upstream kinases (reviewed in [136, 137]). LKB1 is one of the most important upstream kinases that activate AMPK, through phosphorylation at Thr172 (AMPKα), in response to energy depletion [138]. Once activated, and similar to that described for DDR (Fig.5), AMPK phosphorylates p53 at Ser15 [139], TSC2 at Thr1227 and Ser1345 [140] and p27 at Thr198 [141]. The activation of p53 induces cell cycle arrest and consequent cell proliferation inhibition [139], while the stimulation of TSC2 suppresses mTORC1 complex, which results in the inhibition of anabolic processes, such as protein synthesis [140] and activation of catabolic processes, such as autophagy [130]. The phosphorylation of p27 at Thr198 by AMPK is also described as inducing autophagy in response to metabolic stress [141]. Furthermore, recently, it was also reported that, in response to energy deprivation, AMPK can inhibit mTORC1 independently of TSC2 by phosphorylating raptor, a component of the mTORC1 complex, at Ser722 and Ser792 [142] (Fig.6). Moreover, it was also described that AMPK is capable of phosphorylating ULK1 at Ser317 and Ser777, leading to autophagy induction [143] (Fig.6).

Therefore, AMPK functions as an important sensor of cellular energy status that allows cells to coordinate energy availability with cell proliferation and regulation of anabolic and catabolic processes [136, 139, 141].

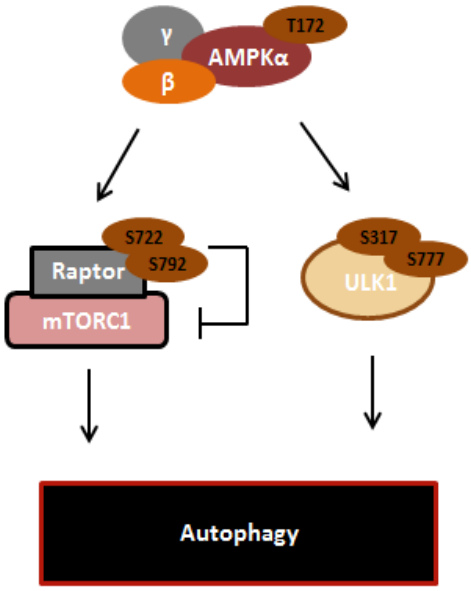

Figure 6 – Schematic representation of the interaction of AMPK with raptor and ULK1 in response to metabolic stress. After energy depletion, AMPK is activated through phosphorylation at Thr172 (AMPKα). Then, AMPK can phosphorylate raptor at Ser722 and Ser792 or ULK1 at Ser317 and Ser777, promoting autophagy induction.

Given the similarities observed between the downstream effectors of AMPK in response to DNA damage and metabolic stress, it is possible that, in response to DNA damage, AMPK also phosphorylates raptor and ULK1 leading to autophagy induction (Fig.6).

Therefore, at the end of the complex DDR three main processes are affected and regulated: cell cycle, DNA repair and autophagy (Fig.7).

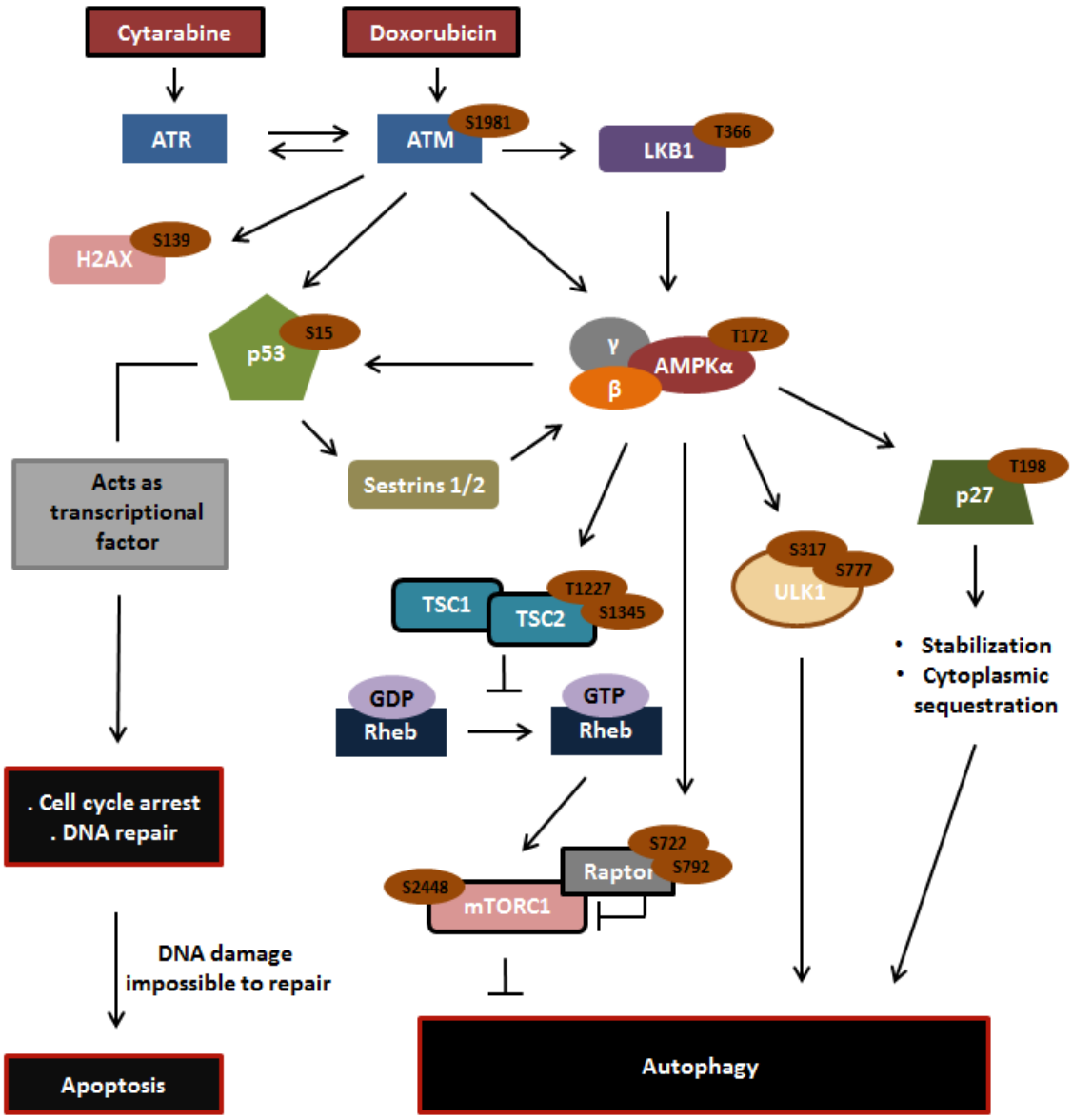

Figure 7 – Schematic representation of the interplay between DNA damage response, activated by the chemotherapeutic agent's cytarabine and doxorubicin, and LKB1-AMPK pathway. After DNA damage, cytarabine activates ATR, while doxorubicin activates ATM (phosphorylation at Ser1981). Furthermore, ATR is also activated by ATM, as well as, ATM is stimulated by ATR (through phosphorylation at Ser1981). Once activated, ATM phosphorylates several substrates such as histone H2AX at Ser139, p53 at Ser15, LKB1 at Thr366 and AMPK at Thr172 (AMPKα). In response to DNA damage, LKB1 is also capable of phosphorylating AMPK at Thr172 (AMPKα). p53 acts as a transcription factor that after phosphorylation at Ser15 regulates the transcription of genes involved in cell cycle arrest, DNA repair and apoptosis (when the damage is impossible to repair). Furthermore, the activation of p53 results in the transcription and expression of Sesn 1/2, which form a complex with AMPK and TSC1:TSC2 and promote the activation of AMPK by induced proximity-dependent autophosphorylation at Thr172 (AMPKα). The interaction between Sesn1/2, AMPK and TSC1:TSC2 allows the phosphorylation of TSC2 at Thr1227 and Ser1345 by activated AMPK. After activation, TSC2 functions as a GTPase-

activating protein that activates the Rheb GTPase, leading to a decrease in the Rheb-GTP levels and consequent mTORC1 inhibition. As mTORC1 is a negative regulator of autophagy, its inhibition results in autophagy induction. Once activated, AMPK also phosphorylates p53 at Ser15, suggesting the existence of a positive regulatory loop to further increase the activation of TSC2, and p27 at Thr198. Phosphorylation of p27 promotes the stabilization and cytoplasmic sequestration of this protein, leading to autophagy induction. Although not yet demonstrated in the DDR, it is known that in response to metabolic stress, AMPK activation, through phosphorylation at Thr172 (AMPKα), by LKB1 results in the phosphorylation of ULK1 at Ser317 and Ser777 and mTORC1 inhibition through raptor phosphorylation at Ser722 and Ser792, which stimulates autophagy induction. Therefore, it is possible that in response to DNA damage these two pathways also occur in order to promote autophagy. Adapted from Paula Ludovico (2012).

3. Cell cycle regulation in response to DNA damage

Activation of DDR promotes an arrest in the cell cycle progression, providing time for DNA repair or apoptosis induction when the damage is impossible to repair [144]. This arrest is mediated by a network of signaling pathways termed cell cycle checkpoints, which include G1, intra-S and G2/M checkpoints [144]. G1 is the first checkpoint and prevents cells with damaged DNA from entering into the S phase and replicate the abnormal DNA [145]. During this checkpoint, the activation of ATM in response to dsDNA breaks promotes the phosphorylation of checkpoint kinase 2 (Chk2), while the activation of ATR in response to ssDNA breaks results in Chk1 phosphorylation [146]. ATM and ATR may also phosphorylate MDM2 [147, 148] and p53 [114, 115] at different residues. Once activated, Chk1 or Chk2 phosphorylates Cdc25A (Cell division cycle 25 homolog A) phosphatase and p53 [144]. The phosphorylation of Cdc25A leads to its enhanced ubiquitination and proteasome-mediated degradation, which prevents the dephosphorylation of Cdk2 on Cyclin E (A)/Cdk2 complexes, promoting Cdk2 inhibition and preventing the initiation of DNA synthesis [145, 149, 150]. This checkpoint pathway targeting Cdc25A occurs rapidly and is relatively transient, arresting cell cycle progression for only some hours [149, 150]. The prolonged maintenance of G1 cell cycle arrest is achieved through a complementary pathway that involves p53 [144, 145]. The phosphorylation of p53 and MDM2, through the proteins previous mentioned, induces the stabilization and accumulation of p53, increasing its activity as transcription factor [144]. One of the key targets of p53 during G1 checkpoint is the gene that codifies the CDKI p21. After transcription and expression, p21 inhibits Cdk2 activity on Cyclin E (A)/Cdk2 complexes, preventing the transcription of genes

required for S phase entry [151-153]. As result, cells undergo G1 cell cycle arrest. Although the phosphorylation of Cdc25A and p53 occurs rapidly, the impact of these events on cell cycle machinery is faster in the case of Cdc25A pathway than p53, since contrarily to Cdc25A the p53 pathway requires the transcription, expression and accumulation of new proteins, namely p21 [144, 145]. Therefore, the checkpoint pathway involving p53 complements and eventually replaces the transient inhibition of Cdk2 promoted by Cdc25A degradation, leading to a sustained G1 cell cycle arrest [144]. Cells that overcome the G1 checkpoint will be subjected to another, the intra-S checkpoint. This checkpoint occurs during the S phase of the cell cycle progression and slows down DNA synthesis and replication after DNA damage detection [144]. Contrarily to G1 checkpoint, the intra-S checkpoint is independent of p53 and therefore does not induce the sustained cell cycle arrest. Thus, in response to genotoxic insults the intra-S checkpoint only induces a transient arrest in the S phase of the cell cycle [144]. Similar to observed with G1 checkpoint, the intra-S checkpoint also involves the ATM/ATR - Chk2/Chk1 - Cdc25A transient cascade [149, 150, 154]. Cells that overtake the intra-S checkpoint will undergo the G2/M checkpoint. This checkpoint prevents cells that suffer DNA damage to progress into G2 with unrepaired DNA damage and to initiate mitosis and segregate damaged DNA into daughter cells [144]. Similar to G1 checkpoint, in response to DNA damage, G2/M checkpoint also induces an acute and transient cell cycle arrest, which involves post-translational modifications of effector proteins, and a delayed and sustained cell cycle arrest, which in addition to post-translational modifications also involves alterations of transcriptional programs [144]. The acute and transient G2 cell cycle arrest involves two main pathways: ATM/ATR - Chk2/Chk1 - Cdc25A [155, 156] and ATM/ATR - Chk2/Chk1 - Cdc25C [155, 157]. In the first pathway Cdc25A suffers proteasome-mediated degradation [155], while in the second pathway the phosphatase Cdc25C is exported from nucleus to cytoplasm [158-160]. These both processes prevent the dephosphorylation of Cdk1 on Cyclin B (A)/Cdk1 complexes, preventing cells from entering in mitosis [155, 160]. Similar to that observed during the sustained G1 cell cycle arrest, the mechanism that contributes for the sustained G2 cell cycle arrest also involves the p53 transcription factor. Once stabilized and activated, p53 promotes the transcription and expression of the CDKI p21, which by the inhibition of Cdk1 activity prevents the transcription of genes required for the initiation of mitosis [161]. However, in addition to p21, p53 also promotes the transcriptional up-regulation of additional target genes, namely 14-3-3σ and GADD45 (growth arrest and DNA damage 45). After expression, 14-3-3σ [162] and GADD45 [163] proteins bind to

Cdk1 inducing its cytoplasmic sequestration and consequent impairment of the initiation of the mitotic process.

4. Autophagy: a pro-survival or a pro-death mechanism?

In addition to cell cycle, autophagy has also been described as a process target by DDR [131, 135]. Autophagy is an evolutionarily conserved self-degradative process by which cytoplasmic content, including cellular proteins and organelles, are delivered to the lysosomes for degradation [164-167]. This cellular catabolic pathway involves at least five steps (Fig.8): 1 - induction (isolation of a membrane to form a phagophore); 2 - expansion (elongation of the phagophore); 3 - completion (maturation of the autophagosome); 4 - fusion (between autophagosome and lysosome) and 5 - degradation of autolysosome content [164]. Several Atg (autophagy-related genes) proteins are involved in this process and constitute the core of the "autophagy machinery" essential for the execution of this dynamic process [164-167].

The induction of autophagy is mainly regulated by two complexes: type I PI3K-Akt-mTOR and type III PI3K hVPS34 (vacuolar protein sorting 34)/Beclin1 (Fig.8). Inhibition of mTOR leads to the activation of ULK1, which may be involved in the isolation of a small membrane called phagophore (Fig.8). On the other hand, the activation of hVPS34/Beclin1 may be responsible for the recruitment of the Atg5 and Atg12 proteins into the phagophore (Fig.8). The expansion of this crescent structure requires the conjugation of the Atg12 to Atg5 and LC3-I to phosphatidylethanolamine (PE), which is catalyzed by Atg7 and Atg3 proteins (Fig.8). The LC3-I is synthesized through a larger precursor called pro-LC3. Therefore, before LC3-I/PE conjugation the cysteine protease Atg4 cleaves the C-terminal portion of nascent pro-LC3 leading to the formation of LC3-I (Fig.8). After conjugation, Atg12/Atg5 complex binds to Atg16 forming the Atg12/Atg5/Atg16 trimeric complex, which binds to phagophore (Fig.8). This trimeric complex recruits cytosolic LC3-I/PE (also referred as LC3-II) to the edges of phagophore, allowing the elongation and curvature of this structure (Fig.8). Moreover, the cargo may also contribute to the induction and expansion of the phagophore by serving as a scaffold. During maturation of autophagosome, the trimeric complex redistributes and concentrates mostly on the outer side of the phagophore, while LC3-II is distributed symmetrically on both sides of this structure (Fig.8). Then, the proteins present in the outer side of the membrane are released into the cytosol and

the uncoated autophagosome fuses with the lysosome originating the autolysosome (Fig.8). The acid hydrolases supplied by the lysosome promote the acidification of the autophagosome environment, which allows the degradation of autolysosome content, namely the cargo and the LC3-II trapped in the lumen of this structure (Fig.8). The macromolecules resulting from this degradation are transported through permeases to cytoplasm for recycling or energy production [164-167].

The LC3-II present in the autophagosomes can be easily monitored by immunoblotting and immunofluorescence, therefore, this is the best and most widely used marker for autophagy detection [168].

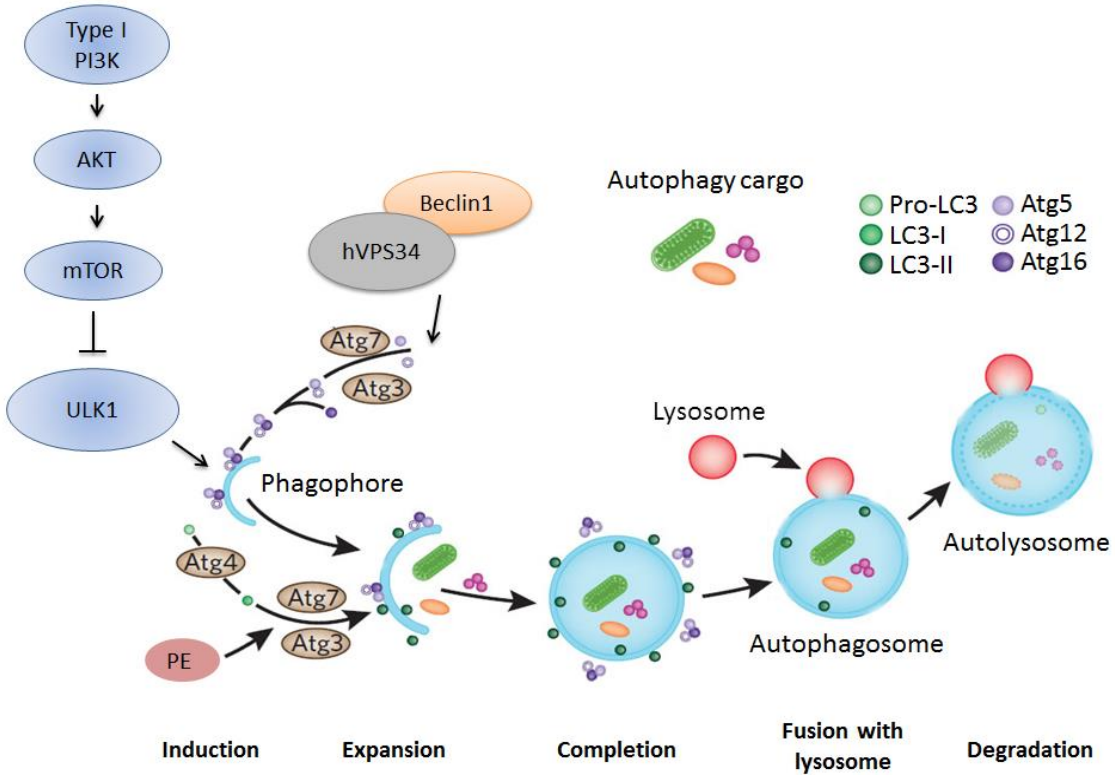

Figure 8 – Schematic representation of the several stages of autophagy: induction, expansion, completion, fusion of autophagosome with lysosome and degradation of autolysosome content. The induction step is regulated by two important complexes, type I PI3K-Akt-mTOR and type III PI3K hVPS34/Beclin1. The inhibition of mTOR promotes ULK1 activation, which participates in the isolation of the phagophore, while the activation of hVPS34/Beclin1 may be involved in the recruitment of Atg5 and Atg12 proteins into this structure. In the next step, expansion of the phagophore, pro-LC3 is converted to LC3-I by the cysteine protease Atg4 and the conjugation of Atg12 to Atg5 and LC3-I to PE is mediated by Atg7 and Atg3 proteins. The recruitment of Atg12/Atg5/Atg16 and LC3-I/PE (LC3-II) conjugates to phagophore allows the elongation and curvature of this structure. During the

completion of autophagosome, Atg12/Atg5/Atg16 complex concentrates mostly on the outer side of the phagophore, while LC3-II is distributed symmetrically on both sides of this structure. Then, the proteins present in the outer side of the membrane are released into the cytosol, which allows the fusion of uncoated autophagosome to lysosome, originating the autolysosome. Finally, the acid hydrolases supplied by the lysosome allows the degradation of autolysosome content. Adapted from [164, 169].

Under physiological conditions, autophagy occurs at basal levels for the turnover of long-lived proteins and also for the removal of superfluous or damaged organelles, playing an essential role in the maintenance of normal cellular homeostasis [165, 170]. On the other hand, in the presence of stressful conditions, such as starvation (e.g. amino acid and nutrient deprivation) and hypoxia, this "self-eating" process is rapidly up-regulated functioning as an adaptive response that recycles and generates basic components, such as amino acids, fatty acids and nucleotides, to sustain core metabolic functions, allowing the temporary cell survival until the end of the unfavorable conditions [171-173]. Therefore, autophagy primarily functions as a pro-survival mechanism. However, this cytoprotective role of autophagy does not occur indefinitely and when the cellular stress leads to continuous or excessively autophagy, this process can be lethal, possibly as result of the inability of cells to survive to the degradation of large amounts of cytoplasmic contents [172-174]. Accordingly, it is extremely important that autophagy be tightly regulated [174], since cell survival or death can ensue depending on the duration and severity of this process [172].

In the last years, the role of autophagy as a pro-survival or pro-death mechanism in cancer research has been a subject of intense debate and controversy (reviewed in [172, 175]). Accumulating evidence suggests that autophagy functions as a cytoprotection that allows the adaptation and survival of tumor cells to adverse conditions, such as radiotherapy and chemotherapy. Examples of such evidence are: the combination of 3-Methyladenine (3-MA), an autophagy inhibitor, with radiotherapy resulted in an increased susceptibility of liver cancer cells (*in vitro* study) and in a significant repression of liver tumor growth (*in vivo* study), suggesting that cancer cells could be responding to radiotherapy with an increase of autophagy as a self-protective mechanism [176]; studies with chloroquine (CQ), also an autophagy inhibitor, showed that this autophagy modulator potentiated the effectiveness of the chemotherapeutic agents in colon cancer cells [177] and glioblastoma [178], indicating a cytoprotective role of autophagy in cancer cells response to chemotherapy; the inhibition of autophagy by pharmacological inhibitors

(3-MA, CQ or bafilomycin A1) or genetic knockdown of autophagy genes (*ATG5* and *ATG7*) was also described as enhancing cell death induced by Imatinib in chronic myeloid leukemia cells [179]; in Myc-induced model of lymphoma the combination of CQ or *ATG5* siRNA with chemotherapy also enhanced the ability of chemotherapeutic agents to induce tumor cell death [180]. However, the pro-death function of autophagy has also been described in tumor cells submitted to stress conditions: the treatment of malignant glioma cells with arsenic trioxide promoted autophagy induction and consequent tumor glioma cell death [181]; tamoxifen was also described as inducing autophagic cell death in breast cancer cells [182]; several molecules, including morphinone (morphine derivate), vitamin K2 and Eupalinin A (sesquiterpene lactone), were also reported as inducing autophagic cell death in HL-60 AML cell line [183]. Moreover, the link between autophagy and tumor cell death has also been demonstrated using pharmacological (e.g. 3-MA) and genetic approaches (*BECLIN1*, *ATG5* or *ATG7* silencing) for suppression of autophagy [172].

Although studies suggest that autophagy functions as a tumor pro-death mechanism, it is believed that this process primarily acts as a pro-survival mechanism that becomes lethal when the autophagic degradation of the cytoplasmic contents becomes extensive. Thus, it is possible that the induction of tumor cell death promoted by autophagy in response to stress conditions is a mechanism by which the cells are trying to survive [171, 175]. Therefore, autophagy is a double-edged sword that may induce tumor cell survival or death depending on the cellular context, such as type of tumor and duration/severity of autophagy process [171, 175].

In recent years, studies have emerged reporting that some DNA-damaging anticancer agents induce a DDR that involves the activation of crucial proteins, such as AMPK, resulting in autophagy induction [184-186]. In these studies the induction of autophagy resulted in a pro-survival mechanism that conferred chemoresistance to cancer cells:

- 2009, Harhaji-Trajkovic *et al.* described that cisplatin triggered AMPK activation associated with mTOR inhibition and autophagy induction, which protected human glioma cells from cell death [184];
- 2011, Xie *et al.* reported that etoposide induced AMPK activation associated with autophagy induction, which promoted human hepatoma cells adaptation and survival to new stress conditions [185];

- 2012, Li *et al.* showed that topotecan induced p53 activation associated with Sestrins and AMPK activation that promoted autophagy induction and human colon cancer cell survival [186].

However, other studies showed that AMPK activation associated with autophagy induction resulted in a pro-death mechanism that allows the eradication of malignant cells:

- 2012, Shi *et al.* reported that the activation of AMPK, through metformin, induced mTOR inhibition and autophagy induction, which promoted lymphoma cells sensitization and death [187];
- 2013, Huo *et al.* showed that C6 ceramide triggered AMPK activation associated with autophagy induction, which promoted cytotoxic effects in human colorectal cancer cells [188].

Taken together, these studies clearly show that the association of AMPK activation with autophagy induction plays an important role in the response of cancer cells to chemotherapeutic agents. Therefore, it becomes crucial to understand the exact role of this cellular process in cancer context in order to develop new and more efficient therapies.

5. LKB1-AMPK pathway and autophagy in acute myeloid leukemia: a pro-survival or a pro-death mechanism?

Over the past few years, studies have emerged reporting the relevance of LKB1-AMPK pathway and autophagy on AML cells survival [189-192]. In 2010, Green *et al.* showed that the LKB1-AMPK axis is consistently functional in primary AML cells [189]. Using the AMPK activator metformin, Green *et al.* also showed that LKB1-AMPK pathway acts as a tumor suppressor pathway, since the treatment with this compound resulted in a decrease of AML cells survival (primary samples) and a significant reduction in the growth of AML tumors in mice [189]. This study suggested that the induction of LKB1-AMPK pathway could be a good strategy to fight AML disease. In fact, in 2000, Yokozawa *et al.* had reported that AML patients with low p27 (a direct substrate of AMPK) protein levels were associated with poor prognosis and disease progression, while patients with high p27 protein levels had a significantly increased disease-free survival, suggesting that p27 functions as a tumor suppressor in AML cells [192]. However, in 2011,

Borthakur *et al.* described that AML patients display higher LKB1 protein levels associated with shorter overall survival and that high LKB1 and Beclin1 (an autophagy related protein) protein levels negatively impacts clinical outcomes in AML patients [190]. Therefore, given the scarce studies about the LKB1-AMPK pathway and autophagy functions in AML cells, it becomes essential a more detailed knowledge about these processes in order to develop more effective therapeutic approaches.

Our preliminary results showed that anti-leukemia conventional chemotherapy, cytarabine and/or doxorubicin, promoted cell cycle arrest in G0/G1 and S phases associated with autophagy induction in AML cells (unpublished data). Therefore, for this master work we proposed the hypothesis that cytarabine and/or doxorubicin treatment activates LKB1-AMPK pathway that culminates in cell cycle arrest and autophagy induction as a pro-survival mechanism that confers chemoresistance to AML cells. If this hypothesis is confirmed, or even if we find that this pathway acts as a pro-death mechanism, the combination of conventional chemotherapy with manipulation of AMPK pathway or its outcomes may be used to develop more effective therapeutic strategies.

AIMS

In the present work we aimed to investigate the role of DNA damage response and its interplay with LKB1-AMPK pathway in AML cells subjected to conventional chemotherapy, cytarabine and doxorubicin. For that, the following purposes were achieved:

1) Evaluate the DNA damage in AML cells exposed to conventional chemotherapy;
2) Characterize the AMPK pathway functioning in AML cells response to anti-leukemia agents;
3) Evaluate the AMPK pathway outcomes, cell cycle and autophagy activity, after AML cells treatment with conventional chemotherapy;
4) Evaluate the impact of autophagy pharmacological manipulation in AML cells viability and cell cycle profile after treatment with conventional chemotherapy;
5) Characterize the DNA damage in AML cells submitted to the combination of anti-leukemia agents with autophagy modulators.

Cell cultures - Two distinct types of cell lines, HL-60 and KG-1, were used during this work. HL-60 is an acute myeloid leukemia (AML) cell line, a French-American British (FAB) - M2 [193], and was established in 1976 from a 35-year-old female [194]. These cells grow in culture suspensions, display a doubling time between 25h to 45h and exhibit myeloblastic morphology, particularly large cells with 2 to 4 rounded nuclei and basophilic cytoplasm [194]. KG-1 is an erythroleukemia cell line, a subtype of AML and a FAB - M6, and was established in 1977 from a 59-year-old male. These cells also grow in culture suspensions, present a doubling time between 40h to 50h and display morphology and physiology similar to dendritic myeloid cells [195].

HL-60 and KG-1 cell lines were obtained from German Collection of Microorganisms and Cell cultures (DMSZ, Deutsche Sammlung von Mikroorganismen und Zellkulturen in German). These cells were culture in Roswell Park Memorial Institute (RPMI) 1640 medium (Biochrom®) supplemented with 10% heat-inactivated fetal bovine serum (Biochrom®) and 1% antibiotic-antimitotic mix (Invitrogen®, San Diego, CA, USA) in a humidified, 37°C, 5% CO_2 atmosphere. Cells between 5 and 20 passages were used for all the experiments.

Treatments - The standard regimen used in AML treatment consists in the combination of an anthracycline, such as doxorubicin, and cytarabine. Therefore, doxorubicin and cytarabine were used and obtained from Sigma-Aldrich® (St. Louis, USA). Aqueous solutions of both compounds were prepared (at a final concentration of 400 µM and 100,000 µM for doxorubicin and cytarabine, respectively) and storage at - 80^0C during 6 months. Other drugs used during this work were chloroquine diphosphate salt (CQ) and rapamycin, modulators of autophagy process [196-198], which were purchased from Sigma-Aldrich® (St. Louis, USA) and prepared in dH_2O and DMSO, respectively. Hydroxyurea (HU), an inducer of DNA damage [199], was also used. This drug was obtained by Sigma-Aldrich® (St. Louis, USA) and resuspended in dH_2O. 350,000 cells/well were plated and subject to treatments during 18h.

Measurement of cell survival

- **MTS assay –** Cell viability was assessed using 'Cell Titer 96 Aqueous One Solution Cell Proliferation Assay (MTS)', which was acquired from Promega® (Madison, WI, USA). MTS is a colorimetric method widely used to determine the number of viable cells, since the mitochondrial dehydrogenases present in metabolically active cells have the ability to reduce the MTS, a yellow tetrazolium salt, into purple formazan [200]. Therefore, this method measures mitochondrial metabolic rate, which indirectly reflects the number of viable cells [200].

  The number of viable cells in culture was determined after 18h of treatment exposure. Control cells without treatment were maintained at the same conditions. Cells were plated in 96-well plates at volume of 100 µl/well of each sample and 10 µl of MTS solution (1.90 mg/ml) was added to each well. Absorbance at 490 nm was recorded after 4 hours of incubation in a humidified, 37°C, 5% CO_2 atmosphere. Results were expressed as relative MTS activity compared to control (cells without treatment) and at least three biological replicates were used.

- **Annexin V/PI assay –** The Annexin V/PI assay is widely used to identify and quantify viable and non-viable cells characterizing the mode of cell death. This technique allows us to distinguish three distinct cellular populations: viable cells, cells in early apoptosis and cells in late apoptosis or necrosis [201]. Viable cells are characterized by an asymmetric distribution of the phospholipids between the inner and outer leaflets of the plasma membrane and the phosphatidylserine is almost exclusively observed in the inner surface of the membrane [201, 202]. However, cells in early apoptosis undergo changes in the plasma membrane structure, such as the translocation of the phosphatidylserine from the inner to the outer leaflet of the plasma membrane, while the membrane integrity remains unchallenged [202]. Late apoptosis and necrosis are characterized by fragmentation of the plasma membrane [201]. Therefore, these three populations can be identified using Annexin V, a Ca^{2+} dependent protein that has high affinity for phosphatidylserine, and propidium iodide (PI), a membrane impermeable compound that penetrates cells with compromised plasma membrane binding the nucleic acids [201]. Thus, viable cells are Annexin V-negative and PI-negative, early apoptotic cells are Annexin V-positive but PI-negative and late apoptotic or necrotic cells are Annexin V-positive and PI-positive [201].

After 18h of treatment, cells were washed twice with PBS and resuspended in binding buffer solution (100 mM HEPES (pH 7.4), 140 mM NaCl and 2.5 mM $CaCl_2$) at a concentration of $1x10^6$ cells/ml. After that, 100 µl of each sample ($1x10^5$ cells), 5 µl of Annexin V (BD Biosciences®) and 10 µl of PI (50 µg/ml) (Invitrogen®, San Diego, CA, USA) were transferred to cytometer tubes. The samples were incubated in the dark for 15 minutes at room temperature and then 200 µl of binding buffer solution was added to each tube. PI signals were measured using FACS LSRII flow cytometer (BD Biosciences®) with a 488 nm excitation laser. The Annexin V signal was collected through a 488 nm blocking filter, a 550 nm long-pass dichroic with a 525 nm band pass. Signals from 10,000 cells/sample gated in the singlets population were captured at a flow rate of 1,000 cells/s. Data collected with the FACS LSRII flow cytometer were analyzed with FlowJo 7.6 (Tree Star®, Ashland, OR) software. Three biological replicates were used.

Immunoblot analysis - For detection of protein levels in total cellular extracts, untreated or treated cells were collected after 18h of treatment and disrupted: 50 µl of lysis buffer (1% NP-40, 500 mM Tris HCl, 2.5 M NaCl, 20 mM EDTA, phosphatase and protease inhibitors from Roche®, at pH 7.2) was used and samples were sonicated to protein extraction. Total cellular protein was quantified by Bradford (from BioRad®) method with BSA (from Sigma-Aldrich®) as the standard and 20 µg of protein was resolved on a 12% sodium dodecyl sulfate polyacrylamide gel electrophoresis (SDS-PAGE). Proteins were transferred using the Trans-Blot Turbo® transfer system (BioRad®) to a Nitrocellulose membrane, which was boiled for 15 minutes in a water bath. Then, membranes were blocked for 1h at room temperature in PBS-T containing 3% skim milk Molico® and incubated overnight at 4°C with monoclonal primary antibodies at 1:1000: Rabbit anti-phospho-histone H2AX (Ser139), Rabbit anti-histone H2AX, Rabbit anti-phospho-AMPKα (Thr172), Rabbit anti-AMPKα (all from Cell Signaling®), Rabbit anti-phospho p27 (Thr198), Rabbit anti-p27 (both from Abcam®), Rabbit anti-LC3A/B (from Cell Signaling) and Mouse anti-Actin (from Milipore®). In the next step, membranes were washed with TBS-T and incubated with the corresponding secondary antibodies for 1:30h at room temperature and 1:5000: IgG anti-Mouse for Actin (from BioRad®) and IgG anti-Rabbit for all the others (from Cell-Signaling®). Protein levels were detected with ChemiDoc XRS system (BioRad®) after incubation with SuperSignal® West Femto Maximum Sensitivity Substrate (from Thermo Scientific®) and

protein bands quantified with Image Lab® Software. At least three biological replicates were used.

Cell cycle analysis by flow cytometry – After 18h of treatment exposure, cells were washed with PBS, resuspended in absolute ethanol at 70% of final concentration and incubated for at least 30 minutes at 4^0C. After that, the samples were washed with PBS and incubated with staining solution (0.1% triton-X-100, 20 µg/ml of PI and 250 µg/ml of RNase in PBS) in the dark for 1h at 50^0C. Cell cycle analysis was performed through DNA content assessment and PI signals were measured using FACS LSRII flow cytometer (BD Biosciences®) with a 488 nm excitation laser. Signals from 10,000 cells/sample gated in the singlets population were captured at a flow rate of 1,000 cells/s. Data collected with the FACS LSRII flow cytometer were analyzed with the Modifit® Software. Three biological replicates were used.

Statistical Analysis – All the experiments were performed using at least three biological replicates. Significant differences between treatments and the respective controls were determined based on Two-way ANOVA with Bonferroni post hoc test for Annexin V/PI and cell cycle analysis. For all the other methods this difference was evaluated using the Student's *t*-test. Data is reported as the mean ± standard error of the mean (SEM) and a *p*-value lower than 0.05 was assumed to denote a significant difference. Statistical analyses were performed using Prism software (Graph-Pad Software, San Diego, CA).

1. Detection of DNA damage induced by conventional chemotherapy in AML cells

Cytarabine and doxorubicin, chemotherapeutic agents used in acute myeloid leukemia (AML) treatment, are described as inducers of DNA damage [80, 81, 89-91] and DNA damage response (DDR) [101-103]. However, the study of these effects in AML cells is still very scarce. Therefore, we decided to evaluate the occurrence of DNA damage, reflected by the phosphorylation of histone H2AX (Ser139) [109, 110], elicited by conventional chemotherapy (cytarabine and/or doxorubicin) in the AML cell lines HL-60 and KG-1.

In a first approach, the cytotoxicity and the determination of the half maximal inhibitory concentration (IC_{50}) of cytarabine and doxorubicin were performed for both HL-60 and KG-1 cells. The study of the cytotoxicity of drugs in tumor cell lines commonly uses IC_{50} values due to the good relation between stress response and cell death that these concentrations allow [203, 204] and therefore these were the drugs concentrations used throughout this study.

1.1. HL-60 cells (AML - FAB M2 leukemia)

1.1.1. Cytarabine and doxorubicin cytotoxicity and IC_{50} determination

As mentioned above, previous to the determination of the DNA damage induced by cytarabine and/or doxorubicin in HL-60 cells, the IC_{50} values of these anti-leukemia agents were determined. For that, HL-60 cells were exposed to these drugs, either individually or combined, during 18h. After that, MTS (Cell Titer 96 Aqueous One Solution Cell Proliferation Assay) and Annexin V/PI assays were performed to assess cell viability.

The results showed that cell survival obtained by MTS was not correlated with Annexin V/PI data when HL-60 cells were treated with cytarabine and/or doxorubicin (Fig.9). The drugs concentration that decreased cell viability to about 50% by MTS assay (Fig.9A) (cytarabine = 1000 μM; doxorubicin = 1 μM) only induced a decrease of about 30% by Annexin V/PI assay (Fig.9B). MTS is a method that measures mitochondrial metabolic rate, through the reduction of tetrazolium salt into formazan, which indirectly reflects the number of viable cells [200]. However, in the last years, cytotoxicity studies have reported that some chemicals have the ability to interfere with mitochondrial function, leading to alterations in the reduction of tetrazolium salt

into formazan and consequent cytotoxicity erroneous conclusions [205-207]. Cytarabine [208] and doxorubicin [209] have also been described as affecting mitochondrial function of HL-60 cells. Thus, the differences between MTS and Annexin V/PI results observed in this study could be explained by the loss of mitochondrial function induced by these anti-leukemia agents, which may impair the reduction of tetrazolium into formazan, resulting in false positives. Therefore, according to this hypothesis and based on Annexin V/PI assay, which is a more accurate method [201, 202], we can suggest that the IC_{50} values determined by MTS assay do not correspond to real IC_{50} values.

Data obtained by MTS assay also revealed that conventional chemotherapy combination promoted a statistical significant decrease in HL-60 cell's viability when compared to cytarabine but not doxorubicin treatment (Fig.9A). However, Annexin V/PI results showed that the combination of these anti-leukemia agents induced a statistical significant decrease in HL-60 cell's viability when compared either with cytarabine or doxorubicin individual treatment (Fig.9B), suggesting that the combination of these drugs may generate a synergistic cytotoxic effect. Nevertheless, in future, specific software analysis, such as CalcuSyn [210], will be performed in order to confirm the synergistic effect of drugs combination.

According to Annexin V/PI data, cytarabine and/or doxorubicin promoted both early apoptotic (Annexin V+/PI-) and late apoptotic/necrotic (Annexin V+/PI+) cell death (Fig.9B). However, the combination of the two anti-leukemia agents only induced a statistical significant increase in the late apoptotic/necrotic HL-60 cell population when compared to cytarabine treatment (Fig.9B), suggesting that the most efficient drug is doxorubicin and that cytarabine only potentiates its cell death effects.

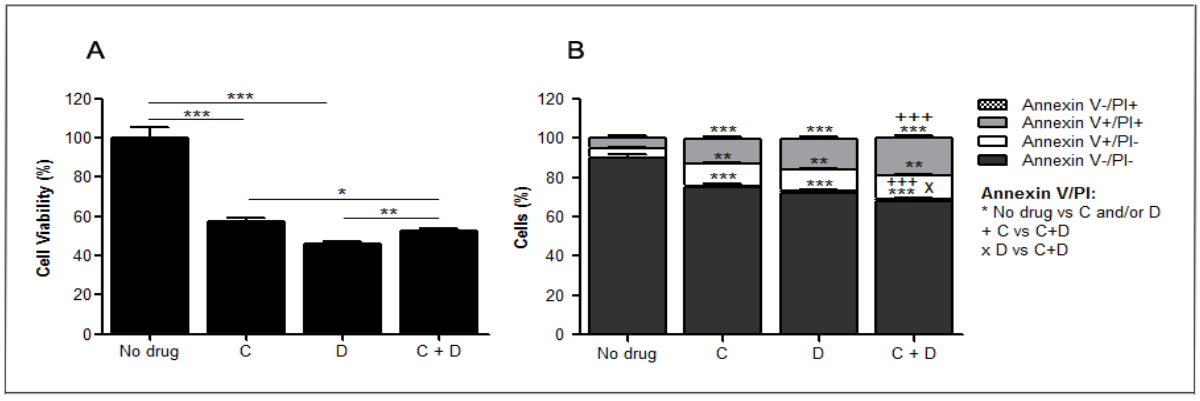

Figure 9 – Cytotoxicity of cytarabine and/or doxorubicin in HL-60 cells. Cells were incubated during 18h with cytarabine and/or doxorubicin, and after this time, cell viability was measured by MTS (A) and Annexin V/PI (B)

assays, as described in Material and Methods section. The results of MTS and Annexin V/PI assays were obtained from comparison with non-treated cells (no drug) and are represented as mean+/-SEM of at least three biological replicates. The comparison between non-treated group and treated groups and within treated groups was performed using the Student´s *t*test for MTS results and the Two-way ANOVA with Bonferroni post hoc test for Annexin V/PI results. The statistical analysis was performed using the Prism software (Graph-Pad Software, San Diego, CA) and */x $p < 0.05$; ** $p < 0.01$; ***/+++ $p < 0.001$. C – cytarabine; D – doxorubicin; C+D – cytarabine combined with doxorubicin.

As hydroxyurea (HU) is a well-known inducer of DNA damage [199], we used this drug as a positive control. For that, a sub-lethal and a lethal concentration of this cytotoxic agent were determined through MTS and Annexin V/PI assays after 18h of treatment. In this case, a good correlation between MTS (Fig.10A) and Annexin V/PI (Fig.10B) data was observed and 100 µM and 500 µM were the concentrations chosen for the following experiments. This good correlation between MTS and Annexin V/PI supports the hypothesis that cytarabine and doxorubicin may interfere with mitochondrial activity of HL-60 cells resulting in false positives by MTS assay. Annexin V/PI results also showed an evident increase in the percentage of late apoptotic/necrotic HL-60 cells with increasing HU concentration (Fig.10B).

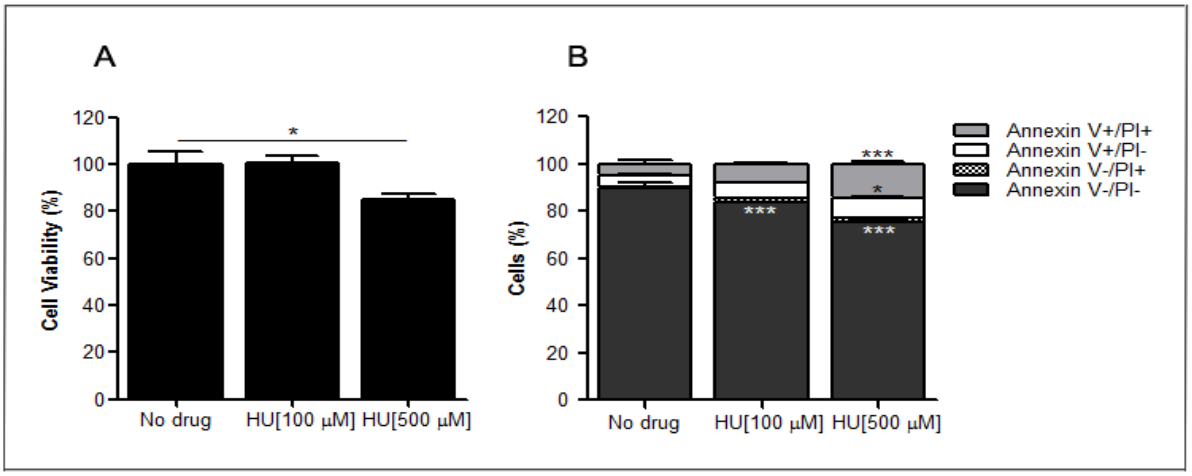

Figure 10 – Hydroxyurea (HU) cytotoxicity in HL-60 cells. Cells were incubated during 18h with HU, and after this time, cell viability was measured by MTS (A) and Annexin V/PI (B) assays, as described in Material and Methods section. The results of MTS and Annexin V/PI assays were obtained from comparison with non-treated cells (no drug) and are represented as mean+/-SEM of at least three biological replicates. The comparison between non-treated group and treated groups was performed using the Student´s *t*test for MTS results and the Two-way ANOVA with Bonferroni post hoc test for Annexin V/PI results. The statistical analysis was performed using the Prism

software (Graph-Pad Software, San Diego, CA) and *p <0.05; ***p <0.001. HU [100 μM] - hydroxyurea 100 μM; HU [500 μM] - hydroxyurea 500 μM.

The conventional chemotherapy IC_{50} values and the sub-lethal and lethal HU concentrations selected for the following assays are described in table 5. The HU concentrations were chosen based on both MTS and Annexin V/PI assays. However, IC_{50} values for cytarabine and doxorubicin were selected based only on MTS assay, since the IC_{50} values of cytarabine and doxorubicin determined by this approach (table 5) are the most commonly used in studies performed with HL-60 cells [203, 204]. Nevertheless, in the future, new studies have to be performed with the IC_{50} values determined by Annexin V/PI assay.

Table 5 - IC_{50} values of cytarabine and doxorubicin determined by MTS assay and sub-lethal and lethal concentrations of hydroxyurea (HU) determined by MTS and Annexin V/PI assays in HL-60 cells.

HL-60			
Cytarabine	**IC_{50} Concentration**	1000	[μM]
Doxorubicin		1	
HU	**Sub-lethal concentration**	100	
	Lethal concentration	500	

1.1.2. Detection of DNA damage through the evaluation of H2AX phosphorylation

The phosphorylation of histone H2AX at Ser139 occurs as result of DNA damage induction and thus this event has been widely used as biomarker for this genotoxic insult [109-111]. Therefore, after 18h of treatment with cytarabine and/or doxorubicin or HU (as a control), immunoblotting analysis of pH2AX (Ser139) and total H2AX were performed to evaluate DNA damage.

The results showed that the pH2AX/H2AX ratio increased after treatment of HL-60 cells with cytarabine and/or doxorubicin (Fig.11A). However, a statistical significant increase was only

observed when both anti-leukemia agents (C+D) were combined (Fig.11A), re-enforcing the use of drugs combination to achieve the desired synergistic effect and the more effective loss of cell survival observed by Annexin V/PI assay (Fig.9B). As expected from a positive control, both HU concentrations promoted a statistical significant increase in pH2AX/H2AX ratio, which is dose-dependent and thus higher for the highest HU concentration (Fig.11B).

These results suggested that cytarabine or doxorubicin individual treatment, at the concentrations tested, might be inducing DNA damage in HL-60 cells. Nevertheless, the DNA damage, as reflected by the pH2AX/H2AX ratio, was higher and statistical significant only when both drugs were combined. Since these chemotherapeutic agents are well described as inducers of DNA damage [80, 81, 89-91], the results obtained were expected. In addition, the non-significant increase of pH2AX/H2AX ratio in HL-60 cells treated with cytarabine or doxorubicin, individually, could be explained by the fact that the IC_{50} values used for these anti-leukemia agents do not correspond to real IC_{50} values. Therefore, it is possible that using IC_{50} values determined by Annexin V/PI assay the DNA damage inflicted by these drugs individually becomes more pronounced. Thus, in future approaches, the evaluation of DNA damage promoted by cytarabine and/or doxorubicin, using IC_{50} values obtained by Annexin V/PI assay, will be performed.

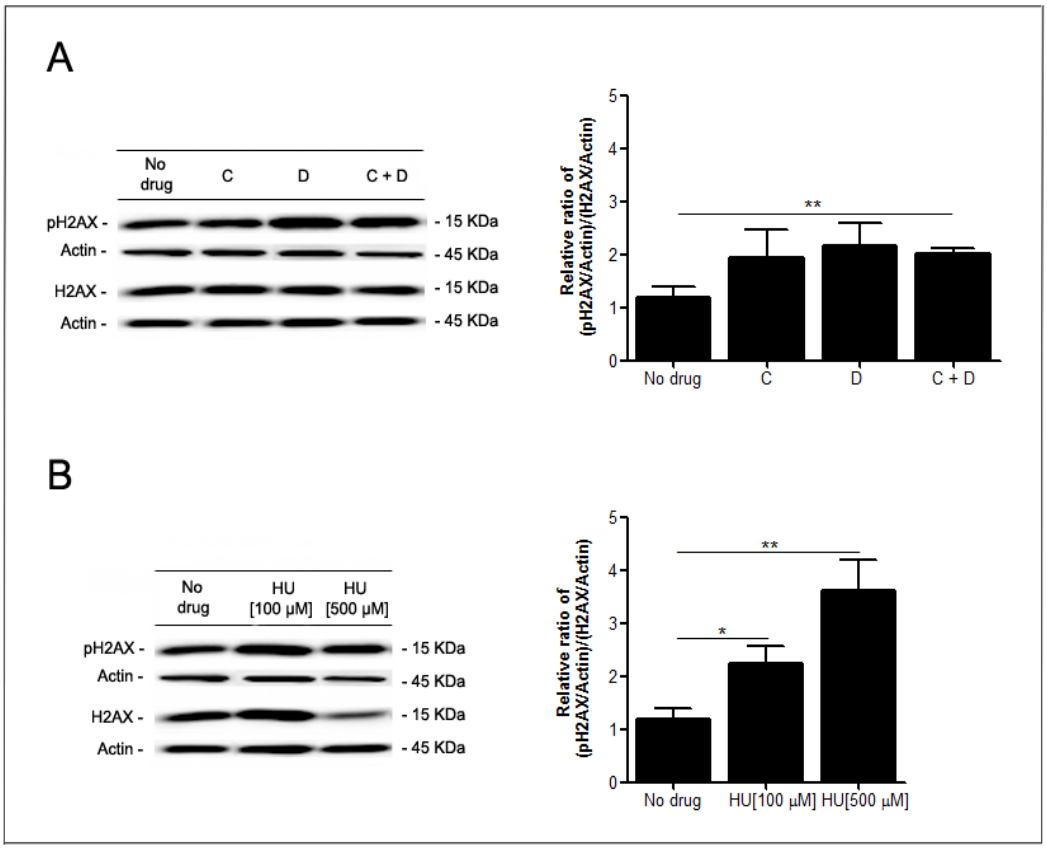

Figure 11 – pH2AX (Ser139) and total H2AX protein levels and densitometric analysis of pH2AX/H2AX in HL-60 cells treated with cytarabine and/or doxorubicin (A) or hydroxyurea (HU) (B). Cells were incubated during 18h with each of the agents as represented, and after this time, immunoblotting analysis of pH2AX (Ser139) and total H2AX, as described in Material and Methods section, was performed to assess DNA damage. The protein bands were quantified in the Image Lab® Software. The comparison between non-treated group and treated groups and within treated groups was performed using the Student´s *t*-test and the Prism software (Graph-Pad Software, San Diego, CA). Densitometric analysis is shown as mean+/-SEM of at least three biological replicates. *p <0.05; **p <0.01. C – cytarabine; D – doxorubicin; C+D – cytarabine combined with doxorubicin; HU [100 µM] - hydroxyurea 100 µM; HU [500 µM] - hydroxyurea 500 µM.

1.2. KG-1 cells (erythroleukemia - FAB M6 leukemia)

1.2.1. Cytarabine and doxorubicin cytotoxicity and IC_{50} determination

Similar to the approach used for HL-60 cells, the IC_{50} values of cytarabine and doxorubicin were determined in KG-1 cells. For that, cells were treated during 18h with those drugs, either individually or combined, and MTS and Annexin V/PI assays were performed to measure cell

viability and to determine the IC_{50} values. KG-1 cells were also treated with HU to determine a sub-lethal and a lethal concentration.

In contrast to HL-60 cells, in KG-1 cells a good correlation between the MTS and Annexin V/PI data was obtained (Fig.12). The IC_{50} concentration for cytarabine (1000 μM) and doxorubicin (2 μM) promoted a decrease in cell viability to about 50-60% and the combination of these drugs further decreased the viability of KG-1 cells to about 30-40% as reflected by the results obtained by both assays (Fig.12A and 12B). Therefore, these results suggested that, in contrast to HL-60 cells, cytarabine and doxorubicin do not have major effects on the mitochondrial function of KG-1 cells, suggesting that these two types of AML cells are distinctly affected by the anti-leukemia agent's treatment. Moreover, results also suggested that the combination of both anti-leukemia agents promotes a synergistic cytotoxic effect in KG-1 cells. However, as described for HL-60 cells, CalcuSyn analysis has to be performed to confirm this effect.

Annexin V/PI results also demonstrated that cytarabine and/or doxorubicin treatment resulted in both early apoptotic and late apoptotic/necrotic KG-1 cells, however, there was an evident increase in the percentage of early apoptotic cells promoted by these drugs either alone or combined (Fig.12B). This data suggested that in KG-1 cells the conventional chemotherapy is mainly inducing apoptotic cell death and once again reinforces that HL-60 and KG-1 cells respond differently to anti-leukemia therapy, since the predominant type of cell death promoted by these agents was distinct for each cell line.

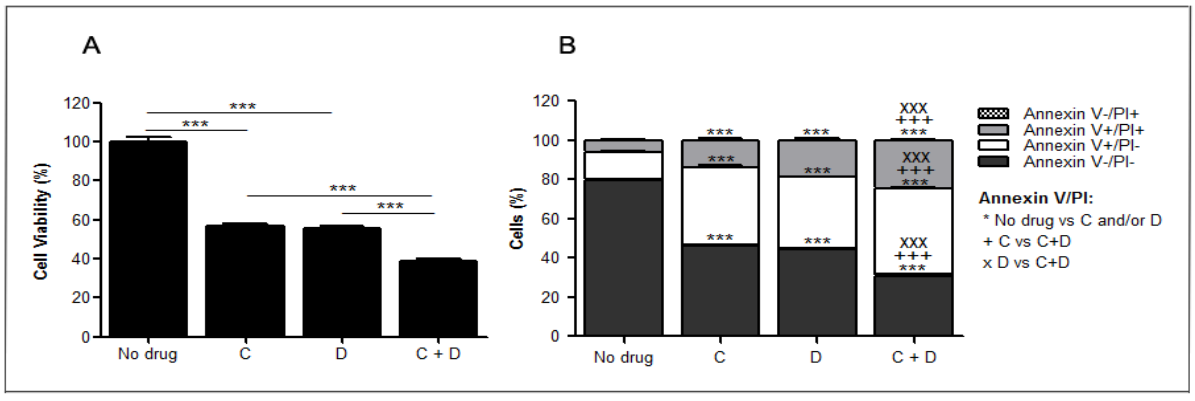

Figure 12 – Cytotoxicity of cytarabine and/or doxorubicin in KG-1 cells. Cells were incubated during 18h with cytarabine and/or doxorubicin, and after this time, cell viability was measured by MTS (A) and Annexin V/PI (B) assays, as described in Material and Methods section. The results of MTS and Annexin V/PI assays were obtained from comparison with non-treated cells (no drug) and are represented as mean+/-SEM of at least three biological

replicates. The comparison between non-treated group and treated groups and within treated groups was performed using the Student´s *t*test for MTS results and the Two-way ANOVA with Bonferroni post hoc test for Annexin V/PI results. The statistical analysis was performed using the Prism software (Graph-Pad Software, San Diego, CA) and ***/+++/xxx p <0.001. C – cytarabine; D – doxorubicin; C+D – cytarabine combined with doxorubicin.

Regarding HU, the results from MTS (Fig.13A) and Annexin V/PI (Fig.13B) assays were also similar and 100 µM and 500 µM were, respectively, the sub-lethal and lethal concentrations chosen for the following experiments. Moreover, these results also showed that 500 µM of HU promoted an evident and statistical significant increase in the percentage of early apoptotic KG-1 cells (Fig.13B).

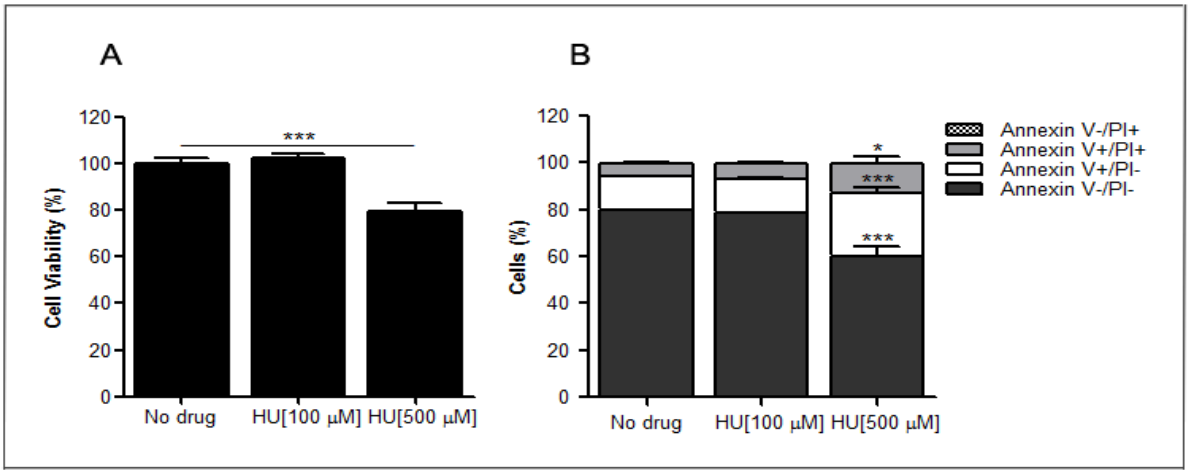

Figure 13 – Hydroxyurea (HU) cytotoxicity in KG-1 cells. Cells were incubated during 18h with HU, and after this time, cell viability was measured by MTS (A) and Annexin V/PI (B) assays, as described in Material and Methods section. The results of MTS and Annexin V/PI assays were obtained from comparison with non-treated cells (no drug) and are represented as mean+/-SEM of at least three biological replicates. The comparison between non-treated group and treated groups was performed using the Student´s *t*test for MTS results and the Two-way ANOVA with Bonferroni post hoc test for Annexin V/PI results. The statistical analysis was performed using the Prism software (Graph-Pad Software, San Diego, CA) and *p <0.05; ***p <0.001. HU [100 µM] - hydroxyurea 100 µM; HU [500 µM] - hydroxyurea 500 µM.

The conventional chemotherapy IC_{50} values and the sub-lethal and lethal HU concentrations selected for the following experiments were chosen based on both MTS and Annexin V/PI assays and are described in table 6.

Table 6 - IC_{50} values of cytarabine and doxorubicin and sub-lethal and lethal concentrations of hydroxyurea (HU) determined by MTS and Annexin V/PI assays in KG-1 cells.

KG-1			
Cytarabine	**IC_{50} Concentration**	1000	[μM]
Doxorubicin		2	
HU	**Sub-lethal concentration**	100	
	Lethal concentration	500	

1.2.2. Detection of DNA damage through the evaluation of H2AX phosphorylation

In the next step, we determined the protein levels of H2AX and its phosphorylated form by immunoblotting. The pH2AX/H2AX ratio was also calculated to compare the DNA damage levels in KG-1 cells after conventional chemotherapy treatment. Cells were also submitted to HU treatment in the conditions mentioned before and the same parameters were evaluated.

The results showed that KG-1 non-treated cells displayed high basal levels of H2AX phosphorylation and low levels of total H2AX, resulting in a high pH2AX/H2AX ratio (Fig.14) and suggesting that these cells may exhibit endogenous DNA damage. In fact, Boehrer *et al.* reported that KG-1 cells display signs of endogenous DNA damage, such as the phosphorylation of ATM (Ser1981) and histone H2AX (Ser139) [211]. Furthermore, data obtained also demonstrated that cytarabine and/or doxorubicin did not promote major alterations in pH2AX/H2AX ratio (Fig.14A). Curiously, this phenomenon was also observed by Boehrer *et al.*, that when submitted KG-1 cells to different doses of irradiation did not observe major alterations in the phosphorylation of ATM and histone H2AX in comparison to non-treated cells [211]. Therefore, this data suggested that either these drugs do not induce DNA damage in KG-1 cells or it is not detectable due to the high endogenous DNA damage levels displayed by these cells. One interesting hypothesis that could be raised is whether the high endogenous levels of DNA damage of KG-1 cells confer them resistance to DNA damage agents consistently with an hormesis effect. Although the results obtained only allows us to speculate, the data obtained with HU, a well-known inducer of DNA replication stress [199] that also did not affect the pH2AX/H2AX ratio (Fig.14B), claims for further studies to clarify these observations.

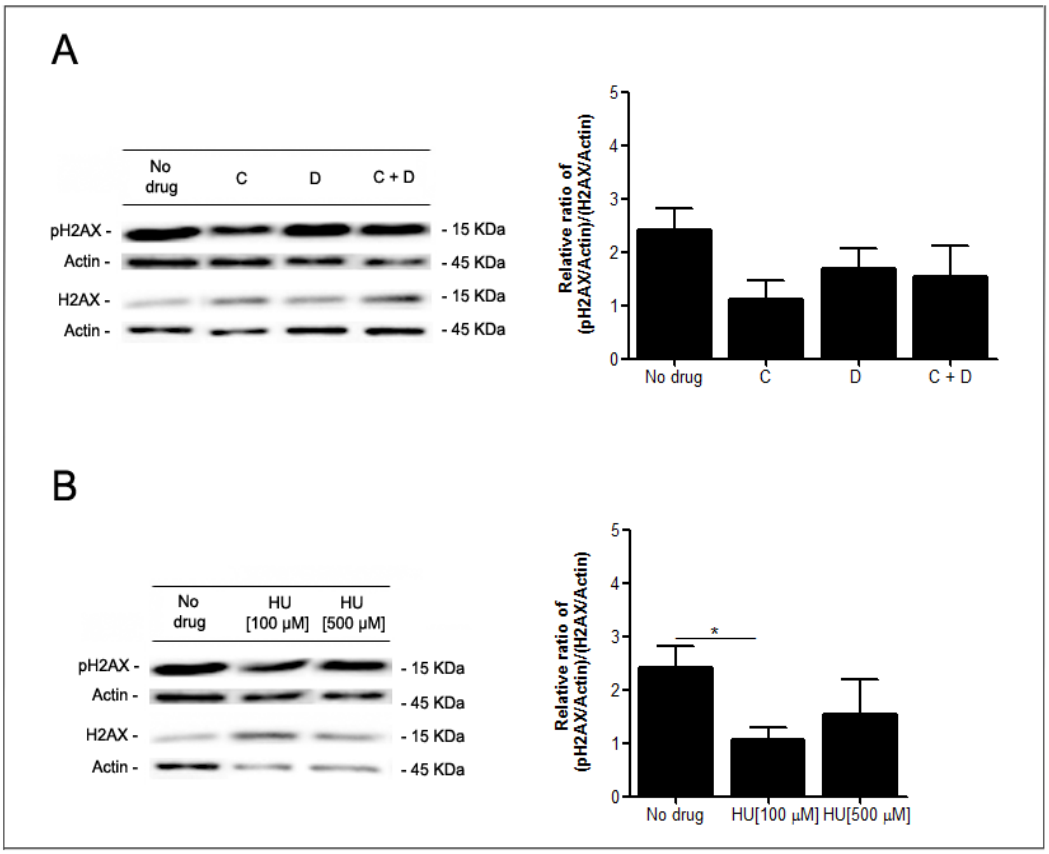

Figure 14 – pH2AX (Ser139) and total H2AX protein levels and densitometric analysis of pH2AX/H2AX in KG-1 cells treated with cytarabine and/or doxorubicin (A) or hydroxyurea (HU) (B). Cells were incubated during 18h with each of the agents as represented, and after this time, immunoblotting analysis of pH2AX (Ser139) and total H2AX, as described in Material and Methods section, was performed to assess DNA damage. The protein bands were quantified in the Image Lab® Software. The comparison between non-treated group and treated groups and within treated groups was performed using the Student´s *t*-test and the Prism software (Graph-Pad Software, San Diego, CA). Densitometric analysis is shown as mean+/-SEM of at least three biological replicates. *p <0.05. C – cytarabine; D – doxorubicin; C+D – cytarabine combined with doxorubicin; HU [100 µM] - hydroxyurea 100 µM; HU [500 µM] - hydroxyurea 500 µM.

Taken together, results of sections 1.1.2 and 1.2.2 suggested that the conventional chemotherapy used in AML treatment (cytarabine and doxorubicin), alone or in combination, promote DNA damage in HL-60 cells, an *in vitro* model of AML with differentiation. Nevertheless, without further deep analysis, the data is inconclusive in what regards KG-1 cells, an *in vitro* model of erythroleukemia.

2. Determination of AMPK pathway functioning in AML cells response to conventional chemotherapy

2.1. HL-60 cells (AML - FAB M2 leukemia)

In section 1.1.2 we showed that cytarabine or doxorubicin treatment promoted a slight increase in pH2AX/H2AX ratio in HL-60 cells, suggesting the occurrence of DNA damage. We also demonstrated that conventional chemotherapy combination induced a statistical significant increase in this ratio. In the last years, studies have reported that the DNA damage induced by some chemotherapeutic agents could promote AMP-activated protein kinase (AMPK) activation [184-186]. Therefore, we decided to evaluate the impact of cytarabine and/or doxorubicin in the AMPK pathway functioning in HL-60 cells. For that, the activation of this pathway was determined through the immunoblotting analysis of phosphorylated AMPK (Thr172) and total AMPK. As p27 is a direct substrate of AMPK [141], we also evaluated the p27 phosphorylation (Thr198). Similar to the previous sections, HU treatment was used as a control to understand the connections between DNA damage and the functioning of AMPK pathway.

The results showed that cytarabine or doxorubicin individual treatment promoted a statistical significant increase in pAMPK/AMPK ratio of HL-60 cells, being the effect of cytarabine more pronounced than doxorubicin (Fig.15A). Surprisingly, the combination of both drugs resulted in a statistical significant decrease of pAMPK/AMPK ratio when compared to cytarabine and a decrease, although without statistical significance, when compared to doxorubicin (Fig.15A). However, a slight and not statistical significant increase in pAMPK/AMPK ratio was observed when both drugs were combined in comparison to non-treated cells (Fig.15A). HL-60 cells treated with HU also displayed an increase, although not significant, in pAMPK/AMPK ratio, being the effect of the lower HU concentration more evident than the higher concentration (Fig.15B). Therefore, these results suggested that while cytarabine or doxorubicin induces AMPK pathway activation in HL-60 cells, the combination of both drugs only promotes a slight activation.

Altogether, this data and the data of section 1.1 seem to indicate that the combination of both anti-leukemia agents promotes more cytotoxicity (determined by Annexin V/PI assay; Fig.9B) and DNA damage (Fig.11A) associated with less AMPK pathway activation (Fig.15A), suggesting that this pathway may function as a pro-survival mechanism in HL-60 cells. In fact, this hypothesis is supported by results obtained with HU, since these demonstrated that the higher HU concentration, which promoted more HL-60 cell death (Fig.10) and DNA damage

(Fig.11B) in comparison to the lower concentration, induced a trend for a less AMPK pathway activation (Fig.15B).

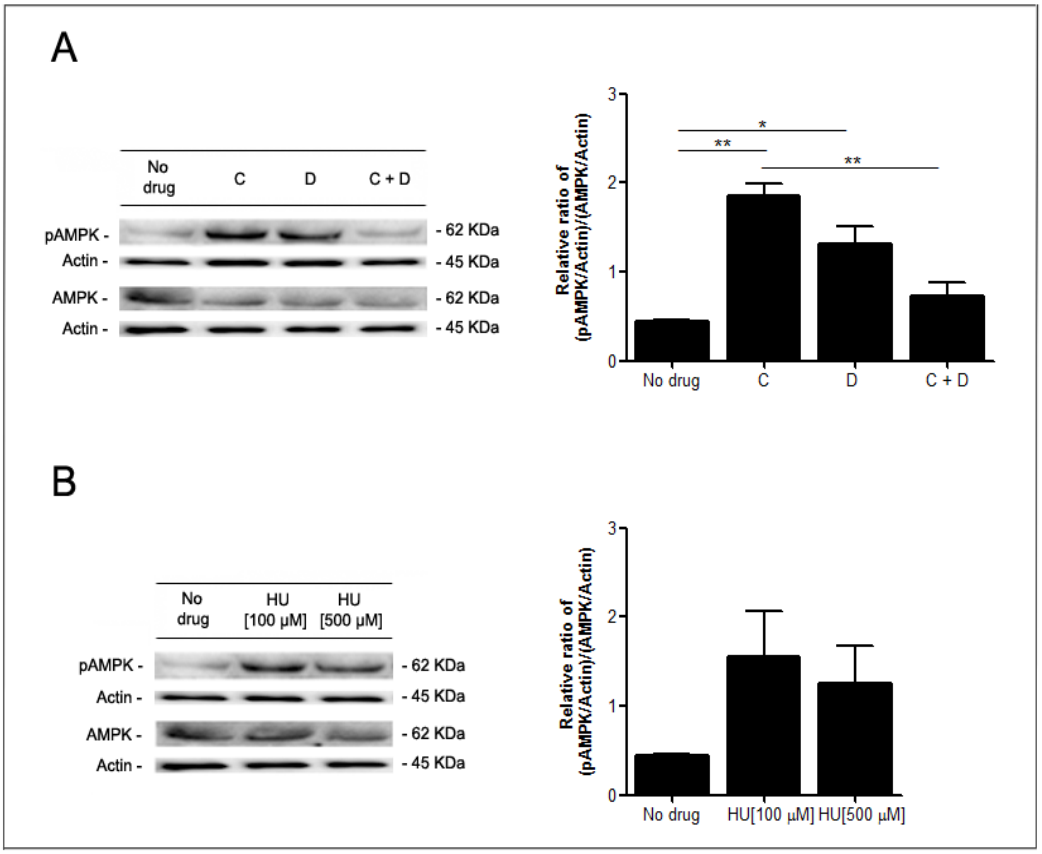

Figure 15 – pAMPK (Thr172) and total AMPK protein levels and densitometric analysis of pAMPK/AMPK in HL-60 cells treated with cytarabine and/or doxorubicin (A) or hydroxyurea (HU) (B). Cells were incubated during 18h with each of the agents as represented, and after this time, immunoblotting analysis of pAMPK (Thr172) and total AMPK, as described in Material and Methods section, was performed to assess AMPK activation. The protein bands were quantified in the Image Lab® Software. The comparison between non-treated group and treated groups and within treated groups was performed using the Student´s *t*-test and the Prism software (Graph-Pad Software, San Diego, CA). Densitometric analysis is shown as mean+/-SEM of at least three biological replicates. *p <0.05; **p <0.01. C – cytarabine; D – doxorubicin; C+D – cytarabine combined with doxorubicin; HU [100 µM] - hydroxyurea 100 µM; HU [500 µM] - hydroxyurea 500 µM.

Regarding the phosphorylation of p27, the results showed that treatment of HL-60 cells with cytarabine and/or doxorubicin did not altered pp27/p27 ratio (Fig.16A). The same holds true for the treatment of the cells with HU, although the higher concentration resulted in a non-statistical

significant increase of pp27/p27 ratio (Fig.16B). Therefore, these results suggested that cytarabine and/or doxorubicin treatment do not promote p27 phosphorylation in HL-60 cells. Nevertheless, its cellular compartmentalization has still to be studied.

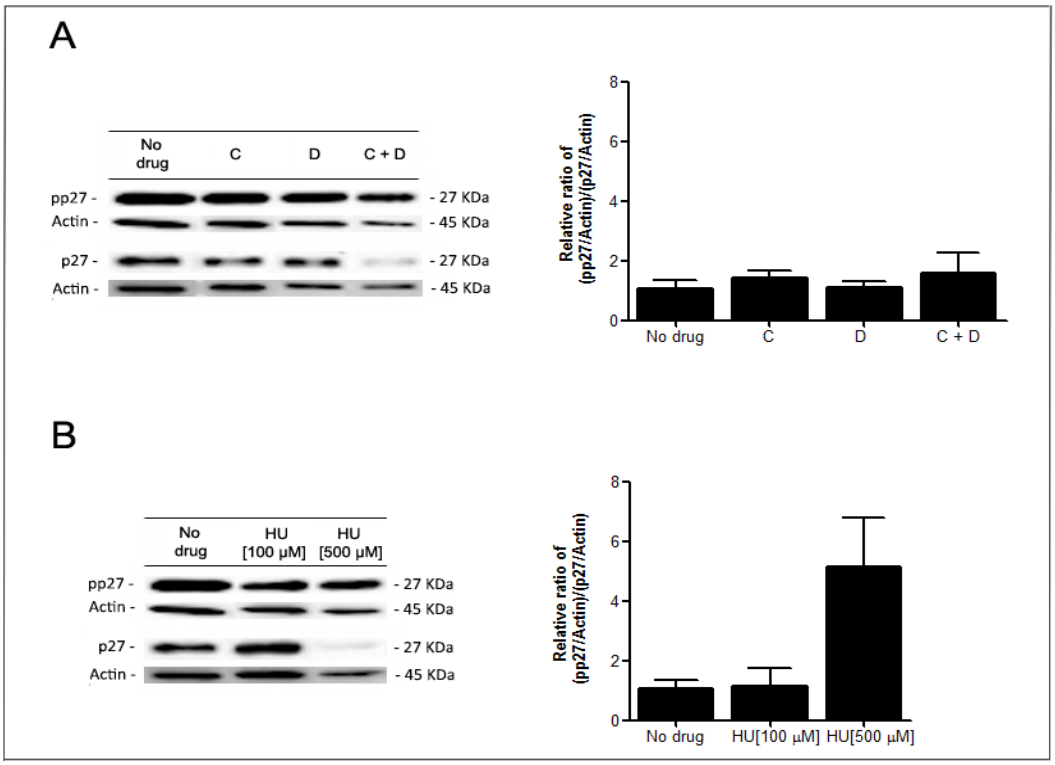

Figure 16 – pp27 (Thr198) and total p27 protein levels and densitometric analysis of pp27/p27 in HL-60 cells treated with cytarabine and/or doxorubicin (A) or hydroxyurea (HU) (B). Cells were incubated during 18h with each of the agents as represented, and after this time, immunoblotting analysis of pp27 (Thr198) and total p27, as described in Material and Methods section, was performed to assess p27 activation. The protein bands were quantified in the Image Lab® Software. The comparison between non-treated group and treated groups and within treated groups was performed using the Student´s *t*-test and the Prism software (Graph-Pad Software, San Diego, CA). Densitometric analysis is shown as mean+/-SEM of at least three biological replicates. C – cytarabine; D – doxorubicin; C+D – cytarabine combined with doxorubicin; HU [100 µM] - hydroxyurea 100 µM; HU [500 µM] - hydroxyurea 500 µM.

So far, data concerning HL-60 cells indicated that cytarabine or doxorubicin promotes a slight induction of DNA damage and AMPK pathway activation, which does not result in the phosphorylation of p27. Moreover, results also suggested that the higher cytotoxic effect induced

by the combination of these drugs is associated with an increased DNA damage but lower AMPK pathway activation, suggesting that, in HL-60 cells, this pathway may act as a pro-survival mechanism.

2.2. KG-1 cells (erythroleukemia - FAB M6 leukemia)

Although results exhibited in section 1.2.2 are inconclusive about the induction of DNA damage by cytarabine and/or doxorubicin in KG-1 cells, we decided to proceed with the analysis of AMPK functioning. In fact, due to the high endogenous DNA damage levels of KG-1 cells, AMPK could be also constitutively activated, or different regulatory mechanisms, such as the increase in AMP/ATP ratio [136, 137], could have relevant functions in this context. Thus, similar to HL-60 cells, we decided to evaluate AMPK and p27 functioning in KG-1 cells response to conventional chemotherapy. For that, cells were treated during 18h with cytarabine and/or doxorubicin and immunoblotting analysis of pAMPK (Thr172), pp27 (Thr198), total AMPK and p27 was performed. The results showed that either cytarabine or doxorubicin individual treatment promoted an increase in pAMPK/AMPK ratio of KG-1 cells, although without statistical significance (Fig.17A). Data also revealed that conventional chemotherapy combination induced a marked increase in pAMPK/AMPK ratio when compared to cytarabine or doxorubicin alone (Fig.17A), nonetheless, these alterations did not reach statistical significance. Regarding HU treatment of KG-1 cells, results demonstrated that both concentrations promoted an increase in pAMPK/AMPK ratio, however, only the higher HU concentration induced a statistical significant increase (Fig.17B). These results suggested that cytarabine and/or doxorubicin promote AMPK pathway activation in KG-1 cells, being the effect of the drugs combination more pronounced than the individual drugs.

Taken together, this data and the data of section 1.2.1 seem to indicate that the higher cytotoxic effect induced by the combination of both anti-leukemia agents (Fig.12) is associated with an elevated AMPK pathway activation (Fig.17A), suggesting that AMPK, contrarily to HL-60 cells, may function as a tumor suppressor in KG-1 cells. Indeed, results with HU support this conclusion, since the higher HU concentration, which promoted higher cytotoxicity (Fig.13), induced an increase in AMPK activation (Fig.17B).

Over again, these results suggested that HL-60 and KG-1 cells are two distinct types of AML that respond differently to conventional chemotherapy treatment, since HL-60 cells seem to activate AMPK pathway mediated by the induction of DNA damage as a pro-survival mechanism, while KG-1 cells seem to stimulate this pathway as a tumor suppressor pathway.

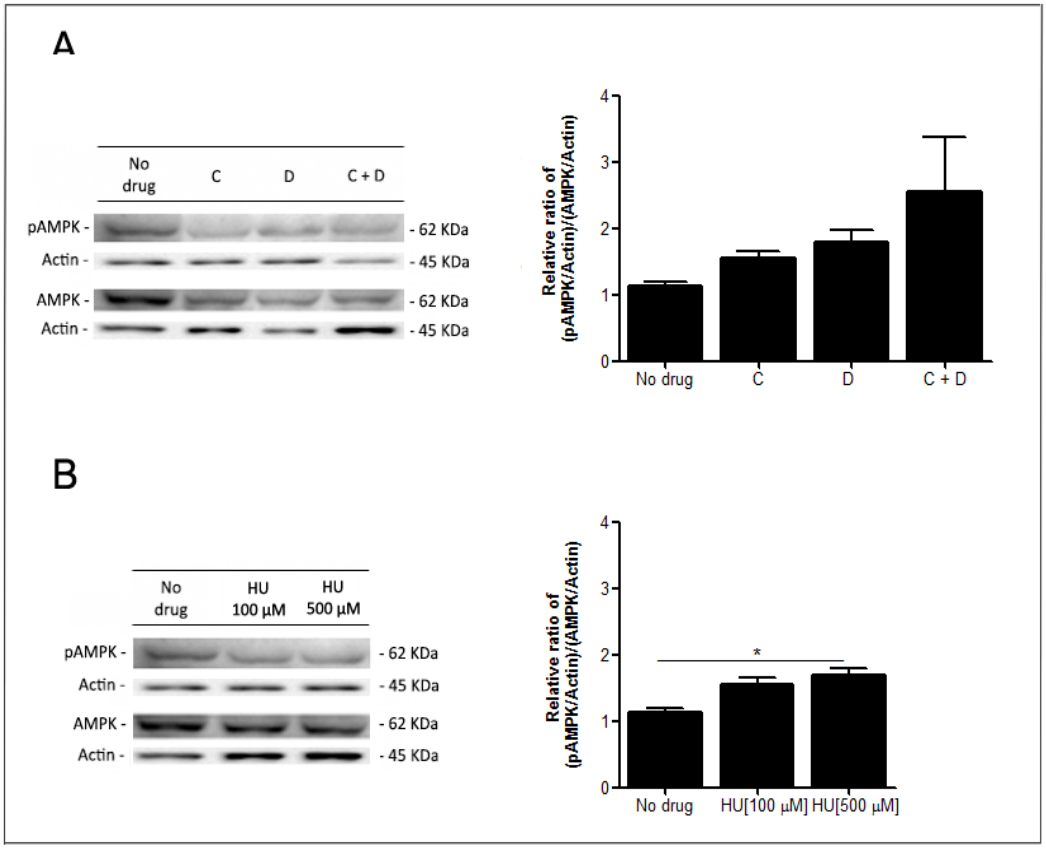

Figure 17 – pAMPK (Thr172) and total AMPK protein levels and densitometric analysis of pAMPK/AMPK in KG-1 cells treated with cytarabine and/or doxorubicin (A) or hydroxyurea (HU) (B). Cells were incubated during 18h with each of the agents as represented, and after this time, immunoblotting analysis of pAMPK (Thr172) and total AMPK, as described in Material and Methods section, was performed to assess AMPK activation. The protein bands were quantified in the Image Lab® Software. The comparison between non-treated group and treated groups and within treated groups was performed using the Student´s *t*-test and the Prism software (Graph-Pad Software, San Diego, CA). Densitometric analysis is shown as mean+/-SEM of at least three biological replicates. *p <0.05. C – cytarabine; D – doxorubicin; C+D – cytarabine combined with doxorubicin; HU [100 µM] - hydroxyurea 100 µM; HU [500 µM] - hydroxyurea 500 µM.

Concerning p27 immunoblotting analysis, results showed that KG-1 cells, similar to that observed with H2AX phosphorylation (Fig.14), also displayed high basal levels of p27 phosphorylation (Fig.18), suggesting that these cells may exhibit endogenous DNA damage associated with a constitutive DDR involving p27. Although Boehrer *et al.* described that KG-1 cells display an intrinsic DDR activation [211], until now, none study reported the participation of p27 in this pathway.

Moreover, data obtained also demonstrated that neither cytarabine nor doxorubicin nor the combination of both drugs induced statistical significant alterations on pp27/p27 ratio (Fig.18A). In the same way, HU treatment did not affect pp27/p27 ratio (Fig.18B). Therefore, these results indicated that, similar to HL-60 cells, anti-leukemia agents do not promote p27 phosphorylation in KG-1 cells. However, its cellular compartmentalization has still to be studied.

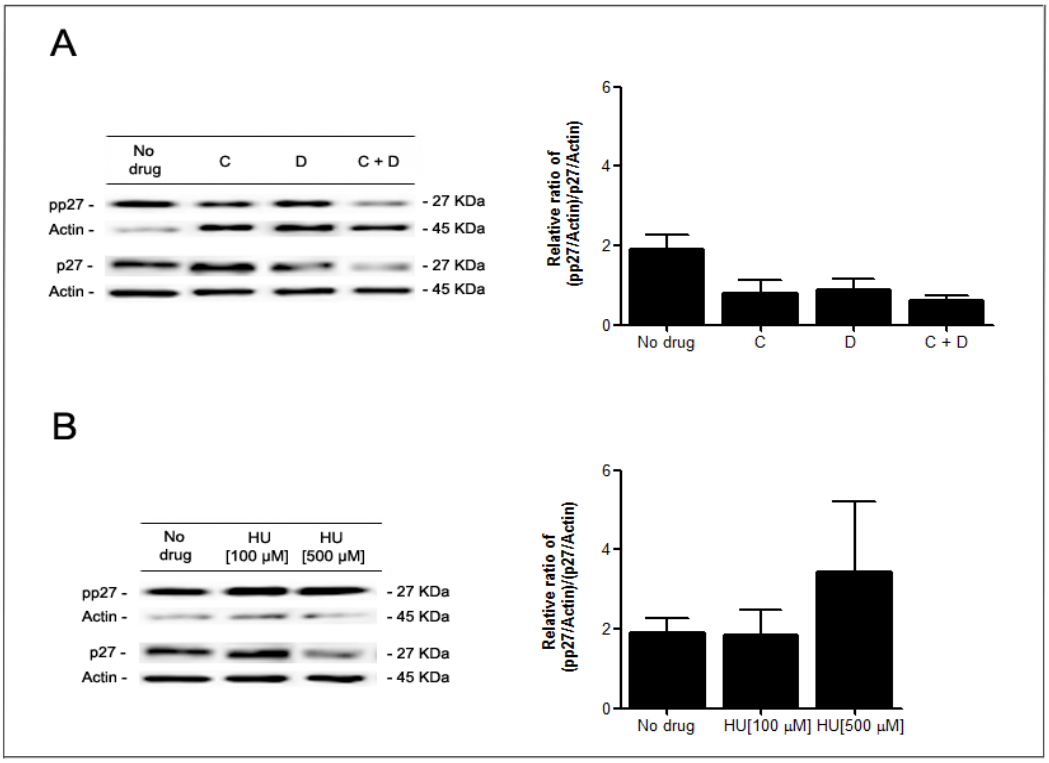

Figure 18 – pp27 (Thr198) and total p27 protein levels and densitometric analysis of pp27/p27 in KG-1 cells treated with cytarabine and/or doxorubicin (A) or hydroxyurea (HU) (B). Cells were incubated during 18h with each of the agents as represented, and after this time, immunoblotting analysis of pp27 (Thr198) and total p27, as described in Material and Methods section, was performed to assess p27 activation. The protein bands were quantified in the Image Lab® Software. The comparison between non-treated group and treated groups and within treated groups was performed using the Student´s *t*-test and the Prism software (Graph-Pad Software, San Diego, CA). Densitometric analysis is shown as mean+/-SEM of at least three biological replicates. C –

cytarabine; D – doxorubicin; C+D – cytarabine combined with doxorubicin; HU [100 μM] - hydroxyurea 100 μM; HU [500 μM] - hydroxyurea 500 μM.

In summary, data concerning KG-1 cells suggested that cytarabine or doxorubicin promotes a slight AMPK activation, which does not result in p27 phosphorylation. Moreover, results also indicated that the higher cytotoxic effect promoted by drugs combination is associated with higher AMPK activation, suggesting that AMPK pathway may function as a pro-death mechanism in KG-1 cells.

3. Analysis of AMPK pathway outcomes, cell cycle profile and autophagy activity, in AML cells challenged with conventional chemotherapy

3.1. HL-60 cells (AML-FAB M2 leukemia)

Studies in different solid tumor cells (e.g. human hepatoma cells, human/rat glioma cells and human colon cancer cells) showed that the activation of AMPK results in autophagy induction as a pro-survival mechanism [184-186]. Our preliminary data showed that cytarabine or doxorubicin treatment promoted cell cycle arrest in G0/G1 and S phases associated with autophagy induction in AML cells (unpublished data). In section 2.1, results also suggested that AMPK pathway activation may function as a pro-survival mechanism in HL-60 cells. Therefore, we decided to evaluate the impact of conventional chemotherapy in the cell cycle profile and autophagy activity, two processes that might be regulated by AMPK activation. For that, HL-60 cells were treated with cytarabine and/or doxorubicin during 18h and the cell cycle profile was determined by assessing DNA content by flow cytometry. As LC3 is the best and most widely used marker for autophagy detection [168], immunoblotting analysis of LC3 (I and II) was performed to assess autophagy. As previously mentioned, pro-LC3 is processed to LC3-I, which is conjugated to phosphatidylethanolamine (PE) forming LC3-PE (or LC3-II) [164, 165, 167]. Nevertheless, as LC3-II is degraded in the autolysosome, the amount of this protein would not provide accurate information about alterations on autophagy. Therefore, chloroquine (CQ), a lysosomotropic agent that raises intralysosomal pH [196] impairing the autophagic protein degradation [197], is used to avoid LC3-II degradation [212]. Thus, after 16h of treatment with the conventional chemotherapy, CQ was added to inhibit LC3-II degradation, allowing its

accumulation and accurate information about its levels. HL-60 cells were also treated with HU in the same conditions explained before and the same parameters were evaluated.

Data obtained showed that cytarabine or doxorubicin treatment promoted cell cycle arrest in G0/G1 phases in HL-60 cells, being the effect of cytarabine more evident than the one induced by doxorubicin (Fig.19A). Moreover, results also revealed that although conventional chemotherapy combination promoted a G0/G1 cell cycle arrest when compared to non-treated cells, in comparison to cytarabine or doxorubicin treatment, it induced a cell cycle arrest in S phase (Fig.19A). This is supported by the increased percentage of cells in S phase and lower percentage of cells in G2/M phases (Fig.19A). Data obtained with conventional chemotherapy did not correlate to that obtained with HU treatment. Indeed, HU did not seem to be inducing major alterations on cell cycle profile although at the lower HU concentration there was an increase in the percentage of cells in G2/M phases (Fig.19B). These results were unexpected, since HU is a well-known inducer of DNA replication stress that promotes cell cycle arrest in S phase [213]. In fact, studies reported that HL-60 cells treated with similar HU concentrations used in this work undergo DNA damage predominantly during the S phase of the cell cycle [199]. However, one possible explanation for these results could be that HL-60 cells progress into G2 phase with some unrepaired DNA damage inflicted by HU in the previous S phase, resulting in the activation of G2/M checkpoint and G2/M cell cycle arrest in an attempt to repair the DNA damage.

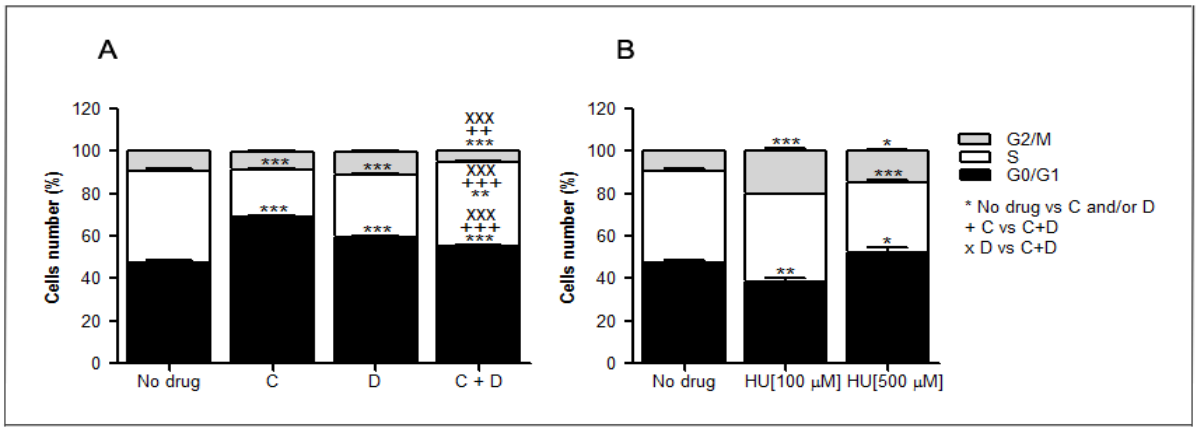

Figure 19 - Cell cycle profile of HL-60 cells treated with cytarabine and/or doxorubicin (A) or hydroxyurea (HU) (B). Cells were incubated during 18h with each of the agents as represented, and after this time, cell cycle profile was determined through DNA content assessment, as described in Material and Methods section. Cell cycle analysis was performed using the Modifit® Software. The comparison between non-treated group

and treated groups and within treated groups was performed using the Two-way ANOVA with Bonferroni post hoc test and the Prism software (Graph-Pad Software, San Diego, CA). Cell cycle analysis is shown as mean+/-SEM of at least three biological replicates. *p <0.05; **/++ p <0.01; ***/+++/xxx p <0.001. C – cytarabine; D – doxorubicin; C+D – cytarabine combined with doxorubicin; HU [100 µM] - hydroxyurea 100 µM; HU [500 µM] - hydroxyurea 500 µM.

Regarding the effect of anti-leukemia drugs on autophagy in HL-60 cells, our data showed that cytarabine or doxorubicin treatment promoted a slight increase, without statistical significance, in LC3-II/LC3-I ratio and that the effect of cytarabine was slightly more pronounced than that of doxorubicin (Fig.20A). The results also demonstrated that the combination of both drugs had no particular evident effect in the LC3-II/LC3-I ratio when compared to control conditions (Fig.20A). HU results revealed that while the lower concentration promoted a slight but not statistical significant increase in LC3-II/LC3-I ratio, the higher HU concentration displayed a LC3-II/LC3-I ratio similar to that of non-treated cells (Fig.20B).

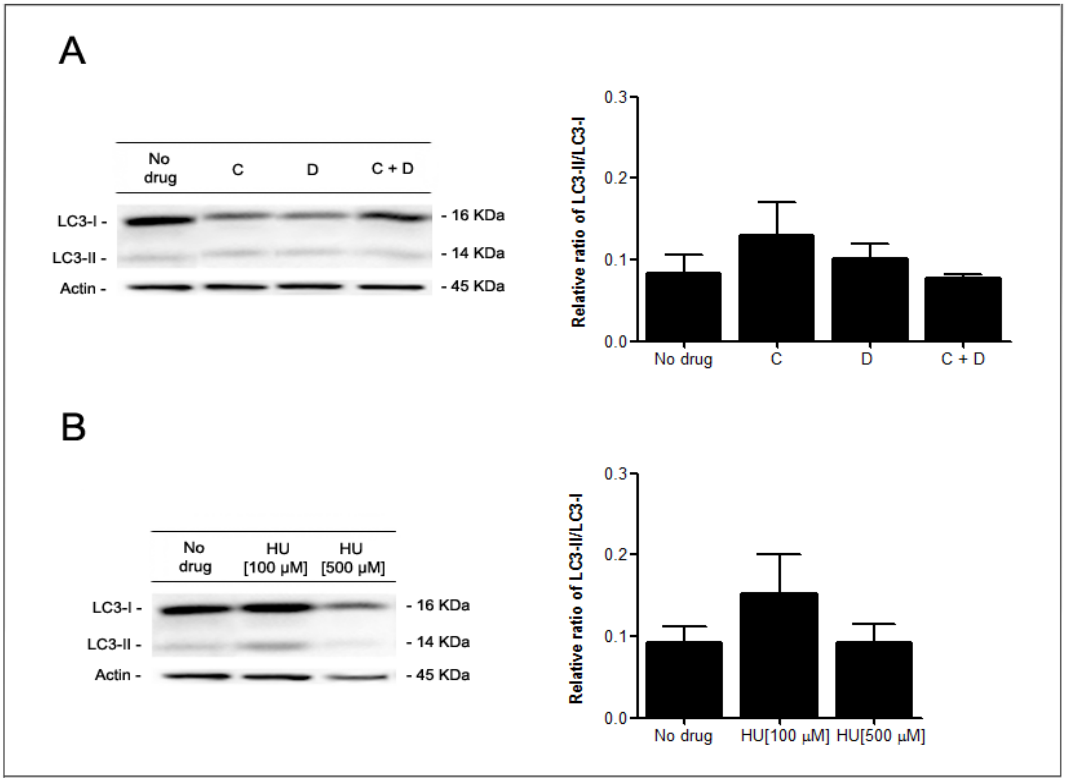

Figure 20 – LC3-I and LC3-II protein levels and densitometric analysis of LC3-II/LC3-I in HL-60 cells treated with cytarabine and/or doxorubicin (A) or hydroxyurea (HU) (B). Cells were incubated during 18h with each of the agents as represented and 2h before the end of the treatment CQ (4.4 µM) was added to block the

autophagy flux and to allow LC3-II accumulation. After the treatment time, immunoblotting analysis of LC3 (I and II), as described in Material and Methods section, was performed to assess autophagy activity. The protein bands were quantified in the Image Lab® Software. The comparison between non-treated group and treated groups and within treated groups was performed using the Student´s *t*-test and the Prism software (Graph-Pad Software, San Diego, CA). Densitometric analysis is shown as mean+/-SEM of at least three biological replicates. C – cytarabine; D – doxorubicin; C+D – cytarabine combined with doxorubicin; HU [100 μM] - hydroxyurea 100 μM; HU [500 μM] - hydroxyurea 500 μM.

Altogether, results suggested that cytarabine or doxorubicin promote a slight induction of DNA damage, which results in the activation of AMPK associated with G0/G1 cell cycle arrest and a moderate induction of autophagy. Interesting, the combination of both anti-leukemia agents, which promoted higher cytotoxicity and DNA damage in comparison to individual drugs, resulted in lower AMPK activation, lower cell cycle arrest in G0/G1 phases and had no impact on autophagy, reinforcing the idea that AMPK pathway activation may function as a pro-survival mechanism. Data obtained with HU supports this hypothesis, since the higher concentration of this compound promoted more HL-60 cell death and DNA damage associated with less AMPK activation and without impact on autophagy.

3.2. KG-1 cells (erythroleukemia - FAB M6 leukemia)

In contrast with that described in section 3.1, different studies have also reported that AMPK activation could be associated with autophagy induction and tumor cell death [187, 188]. In section 2.2, results also indicated that AMPK pathway activation may act as a tumor suppressor in KG-1 cells. Therefore, similar to the approach used for HL-60 cells, we decided to evaluate the impact of conventional chemotherapy in the cell cycle profile and autophagy activity of KG-1 cells. The results showed that while cytarabine promoted a G0/G1 cell cycle arrest, doxorubicin induced an arrest in S phase (Fig.21A). Moreover, data also demonstrated that conventional chemotherapy combination resulted in a cell cycle profile similar to that exhibited by doxorubicin treatment, an arrest in S phase (Fig.21A). Regarding HU, results showed that HU had a modest effect on cell cycle and only the higher HU concentration was able to promote a cell cycle arrest in G0/G1 phases (Fig.21B).

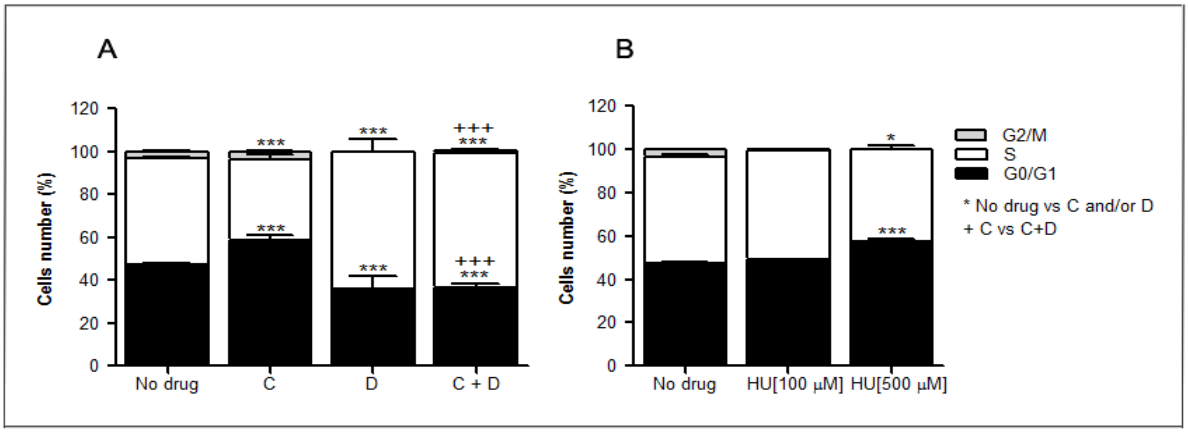

Figure 21 - Cell cycle profile of KG-1 cells treated with cytarabine and/or doxorubicin (A) or hydroxyurea (HU) (B). Cells were incubated during 18h with each of the agents as represented, and after this time, cell cycle profile was determined through DNA content assessment, as described in Material and Methods section. Cell cycle analysis was performed using the Modifit® Software. The comparison between non-treated group and treated groups and within treated groups was performed using the Two-way ANOVA with Bonferroni post hoc test and the Prism software (Graph-Pad Software, San Diego, CA). Cell cycle analysis is shown as mean+/-SEM of at least three biological replicates. *p <0.05; ***/+++ p <0.001. C – cytarabine; D – doxorubicin; C+D – cytarabine combined with doxorubicin; HU [100 µM] - hydroxyurea 100 µM; HU [500 µM] - hydroxyurea 500 µM.

Regarding the effect of conventional chemotherapy in the autophagy levels of KG-1 cells, our data showed that cytarabine did not induce alterations in LC3-II/LC3-I ratio while doxorubicin promoted a statistical significant increase in this ratio (Fig.22A). A slight increase in LC3-II/LC3-I ratio was also observed when both drugs were combined (Fig.22A). Data obtained also revealed that both HU concentrations induced a statistical significant increase in LC3-II/LC3-I ratio, being the effect of the higher concentration more pronounced that the lower concentration (Fig.22B).

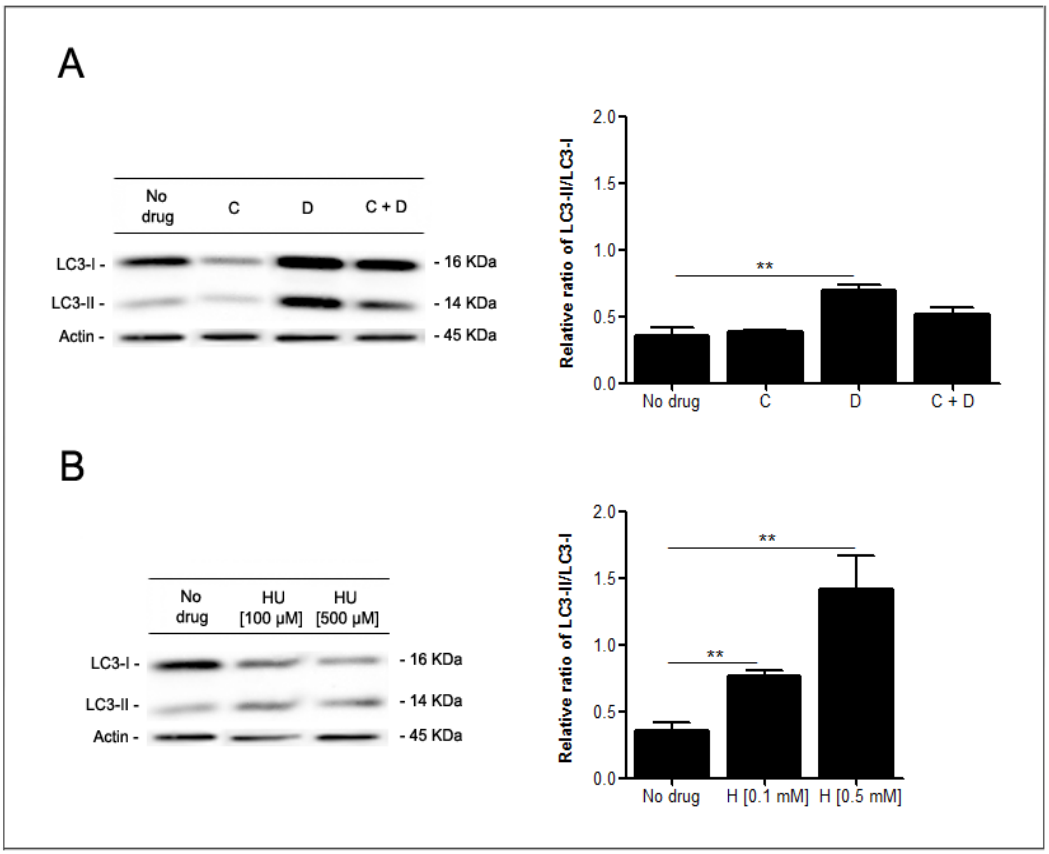

Figure 22 – LC3-I and LC3-II protein levels and densitometric analysis of LC3-II/LC3-I in KG-1 cells treated with cytarabine and/or doxorubicin (A) or hydroxyurea (HU) (B). Cells were incubated during 18h with each of the agents as represented and 2h before the end of the treatment CQ (4.4 µM) was added to block the autophagy flux and to allow LC3-II accumulation. After the treatment time, immunoblotting analysis of LC3 (I and II), as described in Material and Methods section, was performed to assess autophagy activity. The protein bands were quantified in the Image Lab® Software. The comparison between non-treated group and treated groups and within treated groups was performed using the Student´s *t*-test and the Prism software (Graph-Pad Software, San Diego, CA). Densitometric analysis is shown as mean+/-SEM of at least three biological replicates. **p <0.01. C – cytarabine; D – doxorubicin; C+D – cytarabine combined with doxorubicin; HU [100 µM] - hydroxyurea 100 µM; HU [500 µM] - hydroxyurea 500 µM.

In summary, data concerning KG-1 cells suggested that doxorubicin alone or combined with cytarabine promotes AMPK activation associated with cell cycle arrest in S phase and autophagy induction. Data obtained with HU also showed that AMPK pathway activation was associated with autophagy induction. Given that the higher cytotoxicity induced by the higher HU concentration

was associated with higher AMPK activation and autophagy induction, it suggests that AMPK pathway may function, in these conditions, as a tumor suppressor pathway.

4. Study the impact of autophagy pharmacological manipulation on cell survival and DNA damage of AML cells treated with conventional chemotherapy

In previous sections, results seem to indicate that AMPK pathway activation associated with G0/G1 cell cycle arrest and autophagy induction functions as a pro-survival mechanism in HL-60 cells. In fact, in section 3.1 we also mentioned that studies in diverse solid tumor cells described that AMPK activation associated with autophagy induction is responsible for cancer cells survival and chemoresistance. Therefore, in order to better understand if autophagy induction observed in HL-60 cells treated with cytarabine or doxorubicin is a mechanism developed to allow HL-60 cell survival, we decided to evaluate the impact of autophagy modulation on cell survival of HL-60 cells treated with the anti-leukemia agents. In earlier sections we also demonstrated that KG-1 cells submitted to doxorubicin alone or combined with cytarabine induced a slight increase in AMPK activation, cell cycle arrest in S phase and autophagy induction. Therefore, we also decided to evaluate the impact of autophagy manipulation on the viability of these cells after cytarabine and/or doxorubicin treatment. For such a purpose, in a first approach, we determined the autophagy modulators concentrations that induce a minimal impact on cell viability but promote alterations in the autophagy levels. In fact, there are no specific pharmacological inhibitors or inducers of autophagy and therefore the choice of sub-lethal concentrations are important to minimize the impact that these drugs might have in other cellular processes and maximize their effects on autophagy. The autophagy inducer selected was rapamycin, an indirect autophagy activator through inhibition of the negatively autophagy regulator mammalian target of rapamycin complex 1 (mTORC1) [198], which also exerts crucial functions on a plethora of other biological processes (reviewed in [127]). The autophagy inhibitor selected was CQ, that as previous referred is a lysosomotropic drug that raises intralysosomal pH [196] blocking the last step of autophagy pathway [197]. CQ is also known as an inducer of DNA damage [214]. Therefore, the choice of sub-lethal concentrations was important for a more accurate and reliable interpretation of the results.

4.1. HL-60 cells (AML-FAB M2 leukemia)

4.1.1. Determination of rapamycin sub-lethal concentrations that induce autophagy

To determine the sub-lethal concentrations of rapamycin, HL-60 cells were treated during 18h with different concentrations of this agent and after this time cell viability was assessed through MTS assay. The results showed that 1 μM of rapamycin induced a slight decrease in HL-60 cell viability while 3 μM of rapamycin was close to the IC_{50} concentration for this compound (Fig.23).

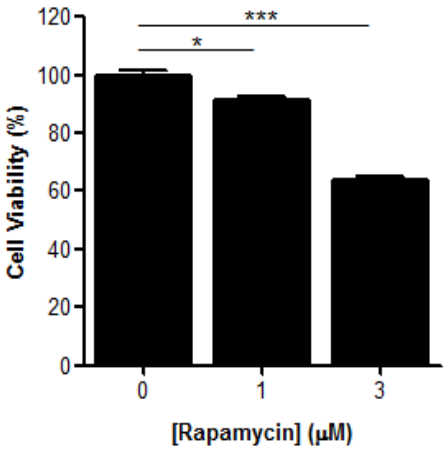

Figure 23 – Determination of HL-60 cell viability after treatment with rapamycin. Cells were incubated during 18h with different concentrations of this agent as represented, and after this time, cell viability was measured by MTS assay, as described in Material and Methods section. The results were obtained from comparison with non-treated cells (no drug) and are shown as mean+/-SEM of at least three biological replicates. The comparison between non-treated group and treated groups was performed using the Student´s *t*test and the Prism software (Graph-Pad Software, San Diego, CA). *p <0.05; ***p <0.001.

To confirm that rapamycin was inducing autophagy, LC3-II/LC3-I ratio was determined, as previously described. The results showed that, as expected, both rapamycin concentrations promoted a statistical significant increase in LC3-II/LC3-I ratio (Fig.24).

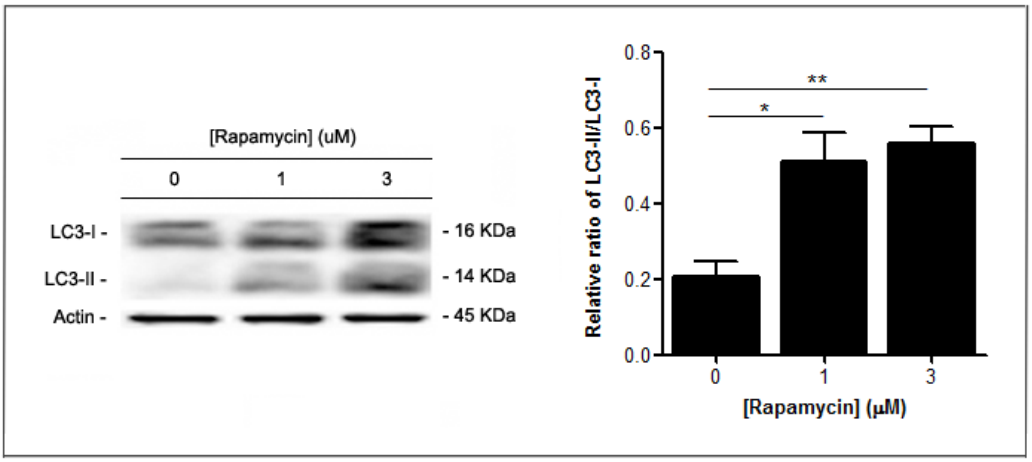

Figure 24 – LC3-I and LC3-II protein levels and densitometric analysis of LC3-II/LC3-I in HL-60 cells treated with rapamycin. Cells were incubated during 18h with different concentrations of this agent as represented and 2h before the end of the treatment CQ (4.4 µM) was added to block the autophagy flux and to allow LC3-II accumulation. After the treatment time, immunoblotting analysis of LC3 (I and II), as described in Material and Methods section, was performed to assess autophagy activity. The protein bands were quantified in the Image Lab® Software. The comparison between non-treated group and treated groups was performed using the Student´s *t*-test and the Prism software (Graph-Pad Software, San Diego, CA). Densitometric analysis is shown as mean+/-SEM of at least three biological replicates. *p <0.05; **p <0.01.

As rapamycin 1 µM was a sub-lethal concentration that promoted an increase in the autophagy activity, we chose this concentration to be used in the following experiments.

4.1.2. Determination of CQ sub-lethal concentrations that inhibit autophagy

To determine the sub-lethal concentrations of CQ, HL-60 cells were treated during 18h with different concentrations of this agent and cell viability was assessed through MTS assay. The results demonstrated that CQ concentrations between 5 µM to 15 µM had no significant effect on HL-60 cell's viability and that only the highest concentrations, 25 µM and 50 µM, induced a decrease in cell's viability (Fig.25).

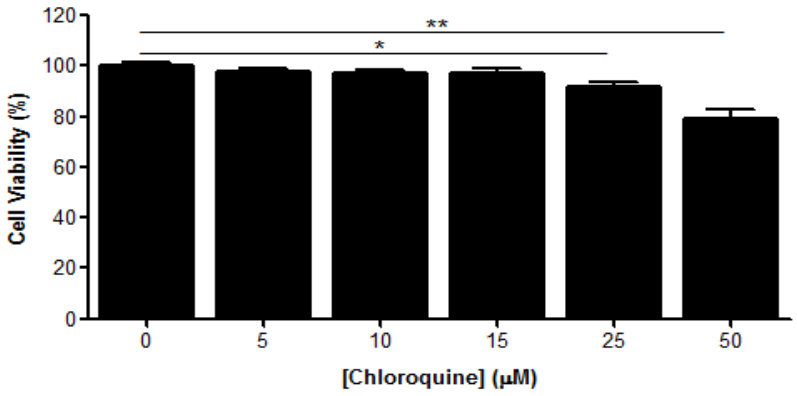

Figure 25 – Determination of HL-60 cell viability after treatment with CQ. Cells were incubated during 18h with different concentrations of this agent as represented, and after this time, cell viability was measured by MTS assay, as described in Material and Methods section. The results were obtained from comparison with non-treated cells (no drug) and are shown as mean+/-SEM of at least three biological replicates. The comparison between non-treated group and treated groups was performed using the Student´s *t*test and the Prism software (Graph-Pad Software, San Diego, CA). *p <0.05; **p <0.01.

The autophagy levels of HL-60 cells treated with the determined CQ concentrations were also evaluated. For that, cells were treated with the different drug concentrations and immunoblotting analysis of LC3 (I and II) was performed. The results demonstrated that all CQ concentrations tested induced a statistical significant increase in LC3-II/LC3-I ratio compatible with an inhibition of autophagy (Fig.26).

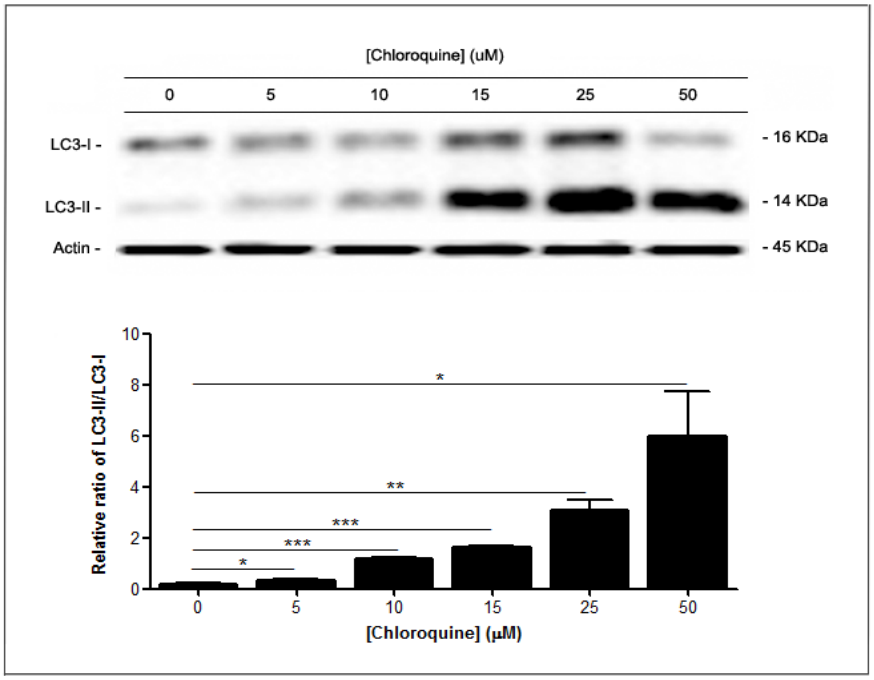

Figure 26 – LC3-I and LC3-II protein levels and densitometric analysis of LC3-II/LC3-I in HL-60 cells treated with CQ. Cells were incubated during 18h with different concentrations of this agent as represented, and after this time, immunoblotting analysis of LC3 (I and II), as described in Material and Methods section, was performed to assess autophagy activity. The protein bands were quantified in the Image Lab® Software. The comparison between non-treated group and treated groups was performed using the Student´s *t*-test and the Prism software (Graph-Pad Software, San Diego, CA). Densitometric analysis is shown as mean+/-SEM of at least three biological replicates. *p <0.05; **p <0.01; ***p <0.001.

As 10 μM of CQ could be considered a sub-lethal concentration that promotes autophagy inhibition, we selected this concentration to be used in the subsequent experiments.

4.1.3. Evaluation the impact of autophagy pharmacological manipulation on viability of cells treated with conventional chemotherapy

4.1.3.1. Evaluation of autophagy activity and cell cycle profile

To understand the role of autophagy in the viability of HL-60 cells treated with conventional chemotherapy, we started by evaluating the impact of sub-lethal concentrations of autophagy modulators in the autophagy levels of cells treated with cytarabine and/or doxorubicin. For that, cells were submitted to cytarabine and/or doxorubicin treatment combined with rapamycin or

CQ, and after this time, immunoblotting analysis of LC3 was performed to assess autophagy activity. After 16h of treatment, CQ was added to samples, excepted to those treated with CQ, to block the autophagy flux and to allow LC3-II accumulation. As in previous sections, the cell cycle profile of HL-60 cells was also analyzed after the treatment mentioned before to determine any crosstalk regulation between autophagy and cell cycle progression. The results showed that rapamycin promoted an increase in LC3-II/LC3-I ratio of HL-60 cells treated with doxorubicin alone or combined with cytarabine, however, only the combination of rapamycin with doxorubicin displayed statistical significance (Fig.27). Data also demonstrated that the combination of rapamycin with cytarabine did not affect the LC3-II/LC3-I ratio when compared to cells only treated with cytarabine (Fig.27).

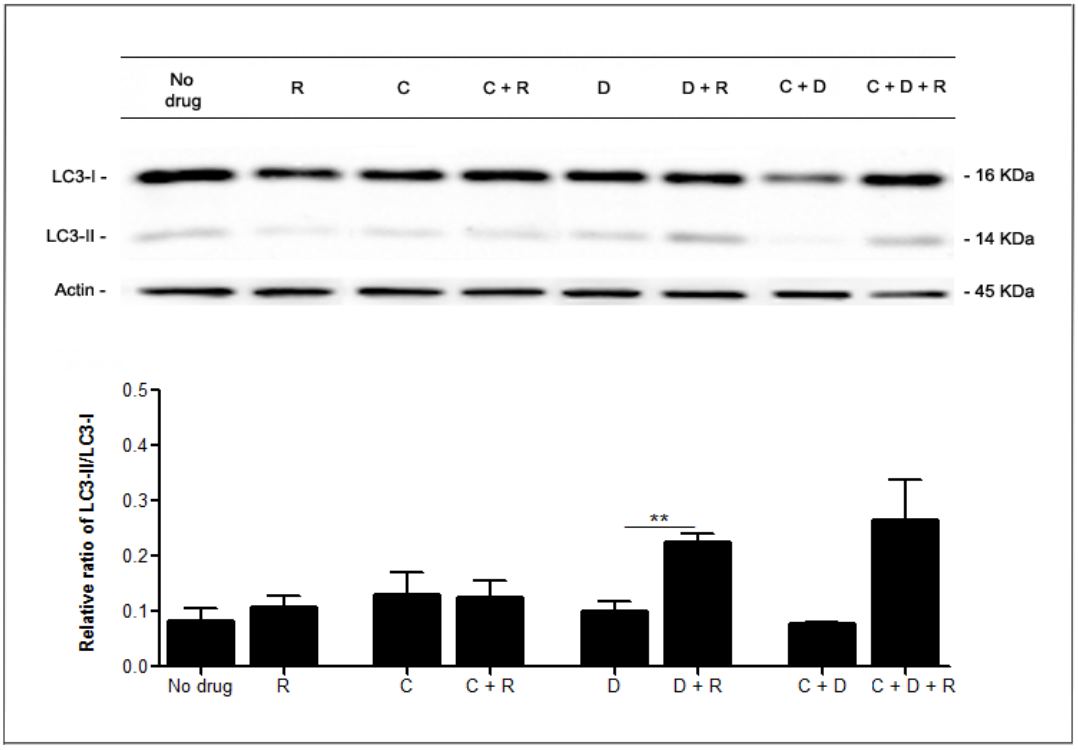

Figure 27 – LC3-I and LC3-II protein levels and densitometric analysis of LC3-II/LC3-I in HL-60 cells treated with cytarabine and/or doxorubicin combined with a sub-lethal concentration of rapamycin. Cells were incubated during 18h with each of the agents as represented and 2h before the end of the treatment CQ (4.4 μM) was added to block the autophagy flux and to allow LC3-II accumulation. After the treatment time, immunoblotting analysis of LC3 (I and II), as described in Material and Methods section, was performed to assess autophagy activity. The protein bands were quantified in the Image Lab® Software. The comparison between non-treated group and treated group and within treated groups was performed using the Student´s *t*test and the Prism software (Graph-Pad Software, San Diego, CA). Densitometric analysis is shown as mean+/-SEM of at least three

biological replicates. **p <0.01. C – cytarabine; D – doxorubicin; C+D – cytarabine combined with doxorubicin; R - rapamycin; C+R – cytarabine combined with rapamycin; D+R – doxorubicin combined with rapamycin; C+D+R – cytarabine and doxorubicin combined with rapamycin.

Regarding the cell cycle profile, results showed that rapamycin induced cell cycle arrest in S phase of HL-60 cells treated with doxorubicin alone or combined with cytarabine, being this effect more pronounced in cells treated only with doxorubicin (Fig.28). Moreover, results also revealed that the combination of rapamycin with cytarabine did not alter the cell cycle profile exhibited by cells only treated with the anti-leukemia agent (Fig.28).

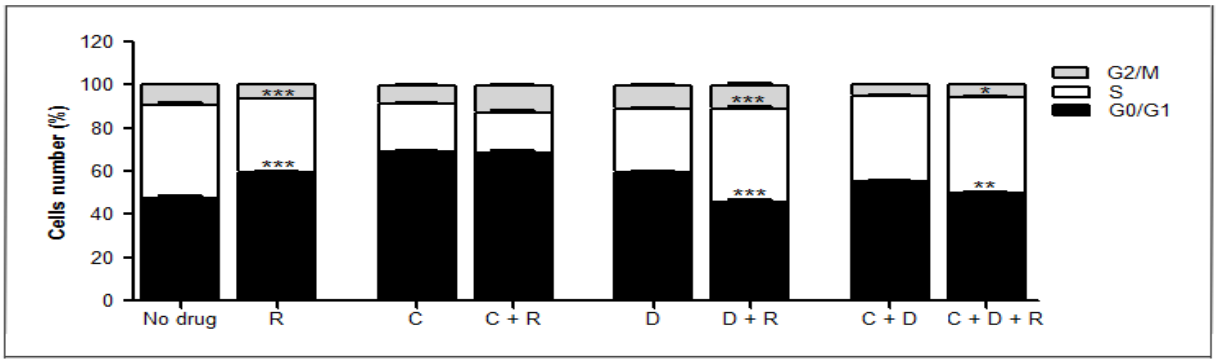

Figure 28 - Cell cycle profile of HL-60 cells treated with cytarabine and/or doxorubicin combined with a sub-lethal concentration of rapamycin. Cells were incubated during 18h with each of the agents as represented, and after this time, cell cycle profile was determined through DNA content assessment, as described in Material and Methods section. Cell cycle analysis was performed using the Modifit® Software. The comparison between non-treated group and treated group and within treated groups was performed using the Two-way ANOVA with Bonferroni post hoc test and the Prism software (Graph-Pad Software, San Diego, CA). Cell cycle analysis is shown as mean+/-SEM of at least three biological replicates. *p <0.05; **p <0.01; *** <0.001. C – cytarabine; D – doxorubicin; C+D – cytarabine combined with doxorubicin; R – rapamycin; C+R – cytarabine combined with rapamycin; D+R – doxorubicin combined with rapamycin; C+D+R – cytarabine and doxorubicin combined with rapamycin.

Altogether, these results suggested that rapamycin promotes autophagy induction associated with cell cycle arrest in S phase of HL-60 cells treated with doxorubicin alone or combined with cytarabine.

Concerning CQ, results demonstrated that this autophagy inhibitor induced a statistical significant increase in LC3-II/LC3-I ratio of HL-60 cells treated with cytarabine and/or doxorubicin (Fig.29), suggesting that in all tested conditions an evident inhibition of the autophagy process occurred.

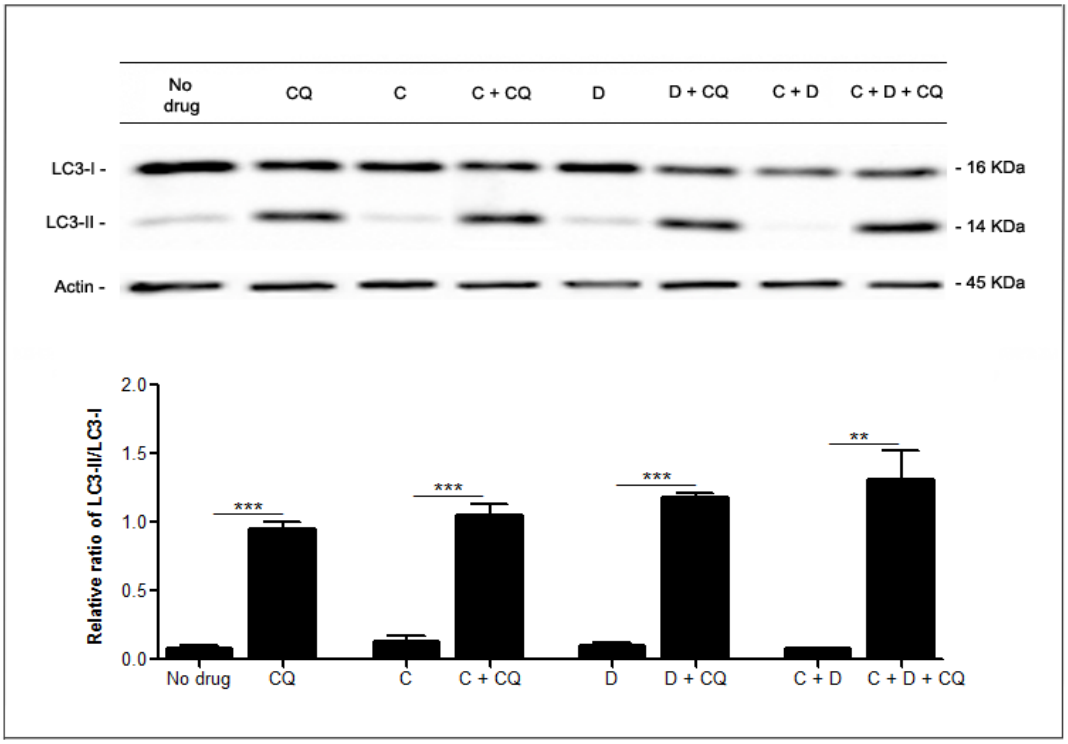

Figure 29 – LC3-I and LC3-II protein levels and densitometric analysis of LC3-II/LC3-I in HL-60 cells treated with cytarabine and/or doxorubicin combined with a sub-lethal concentration of CQ. Cells were incubated during 18h with each of the agents as represented, and after this time, immunoblotting analysis of LC3 (I and II), as described in Material and Methods section, was performed to assess autophagy activity. The protein bands were quantified in the Image Lab® Software. The comparison between non-treated group and treated group and within treated groups was performed using the Student´s *t*-test and the Prism software (Graph-Pad Software, San Diego, CA). Densitometric analysis is shown as mean+/-SEM of at least three biological replicates. **p <0.01; *** <0.001. C – cytarabine; D – doxorubicin; C+D – cytarabine combined with doxorubicin; CQ - chloroquine; C+CQ – cytarabine combined with chloroquine; D+CQ – doxorubicin combined with chloroquine; C+D+CQ – cytarabine and doxorubicin combined with chloroquine.

In addition to autophagy activity, the cell cycle profile of HL-60 cells treated with the combination of CQ with cytarabine and/or doxorubicin was also evaluated. Results showed that CQ induced a cell cycle arrest in S phase of HL-60 cells treated with cytarabine and/or

doxorubicin and that the combination of CQ with doxorubicin also promoted a cell cycle arrest in G2/M phases (Fig.30).

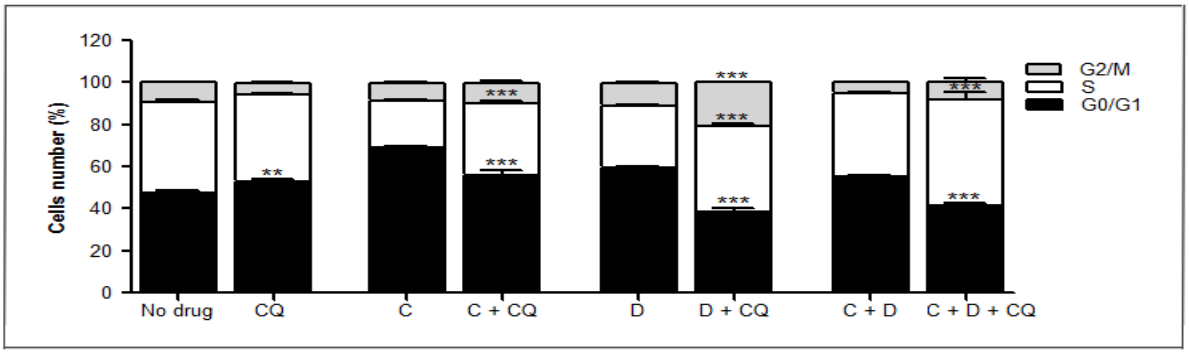

Figure 30 - Cell cycle profile of HL-60 cells treated with cytarabine and/or doxorubicin combined with a sub-lethal concentration of CQ. Cells were incubated during 18h with each of the agents as represented, and after this time, cell cycle profile was determined through DNA content assessment, as described in Material and Methods section. Cell cycle analysis was performed using the Modifit® Software. The comparison between non-treated group and treated group and within treated groups was performed using the Two-way ANOVA with Bonferroni post hoc test and the Prism software (Graph-Pad Software, San Diego, CA). Cell cycle analysis is shown as mean+/- SEM of at least three biological replicates. **p <0.01; *** <0.001. C – cytarabine; D – doxorubicin; C+D – cytarabine combined with doxorubicin; CQ - chloroquine; C+CQ – cytarabine combined with chloroquine; D+CQ – doxorubicin combined with chloroquine; C+D+CQ – cytarabine and doxorubicin combined with chloroquine.

Altogether, these results suggested that CQ induces autophagy inhibition associated with cell cycle arrest in S phase of HL-60 cells treated with cytarabine and/or doxorubicin.

In summary, the results of section 4.1.3.1 suggested the existence of a correlation between the autophagy process and the arrest in S phase of the cell cycle. Indeed, either autophagy induction or inhibition was closely associated with cell cycle arrest in S phase of HL-60 cells submitted to conventional chemotherapy.

Previous results suggested that autophagy may function as a pro-survival mechanism in HL-60 cells. Thus, it is possible that the autophagy activation associated with cell cycle arrest in S phase occurs as an attempt to promote HL-60 cell survival. Interesting, the connection between autophagy inhibition and cell cycle arrest in S phase may also suggest that this arrest occurs to

promote HL-60 cell death. Therefore, it was crucial to understand the impact that these approaches have on HL-60 cell survival.

4.1.3.2. Evaluation of cell viability

After determining the impact of the sub-lethal concentrations of rapamycin or CQ in the autophagy levels and cell cycle profile of HL-60 cells treated with conventional chemotherapy, our next step was to evaluate the effect of these autophagy modulators on the viability of HL-60 cells submitted to anti-leukemia agents. For that, cells were submitted, during 18h, to cytarabine and/or doxorubicin combined with rapamycin or CQ. After that, MTS and Annexin V/PI assays were performed to assess cell viability. Similar to that observed in section 1.1.1, these results also showed that data for cell survival obtained by MTS did not correlate with Annexin V/PI when HL-60 cells were treated with cytarabine and/or doxorubicin alone or combined with rapamycin or CQ (Fig.31 and 32). Once again, these differences between MTS and Annexin V/PI assays suggested that cytarabine and doxorubicin may interfere with mitochondrial activity of HL-60 cells.

Regarding MTS assay, data showed that rapamycin promoted a statistical significant decrease in the viability of HL-60 cells treated with doxorubicin alone or combined with cytarabine (Fig.31A). The Annexin V/PI data did not show statistical significant alterations in the viability of HL-60 cells treated with cytarabine and/or doxorubicin combined with rapamycin when compared to cells only submitted to conventional chemotherapy treatment (Fig.31B). Thus, according to Annexin V/PI assay, results indicated that the induction of autophagy (Fig.27) and cell cycle arrest in S phase (Fig.28) promoted by rapamycin do not affect the viability of HL-60 cells treated with anti-leukemia agents. One possible explanation for these results could be the fact that the concentrations of cytarabine or doxorubicin used in this study, by Annexin V/PI assay, only induced a decrease of about 30% in the viability of HL-60 cells (Fig.9B) and therefore jeopardize the detection of the effects that autophagy promotion by rapamycin have on HL-60 cell viability.

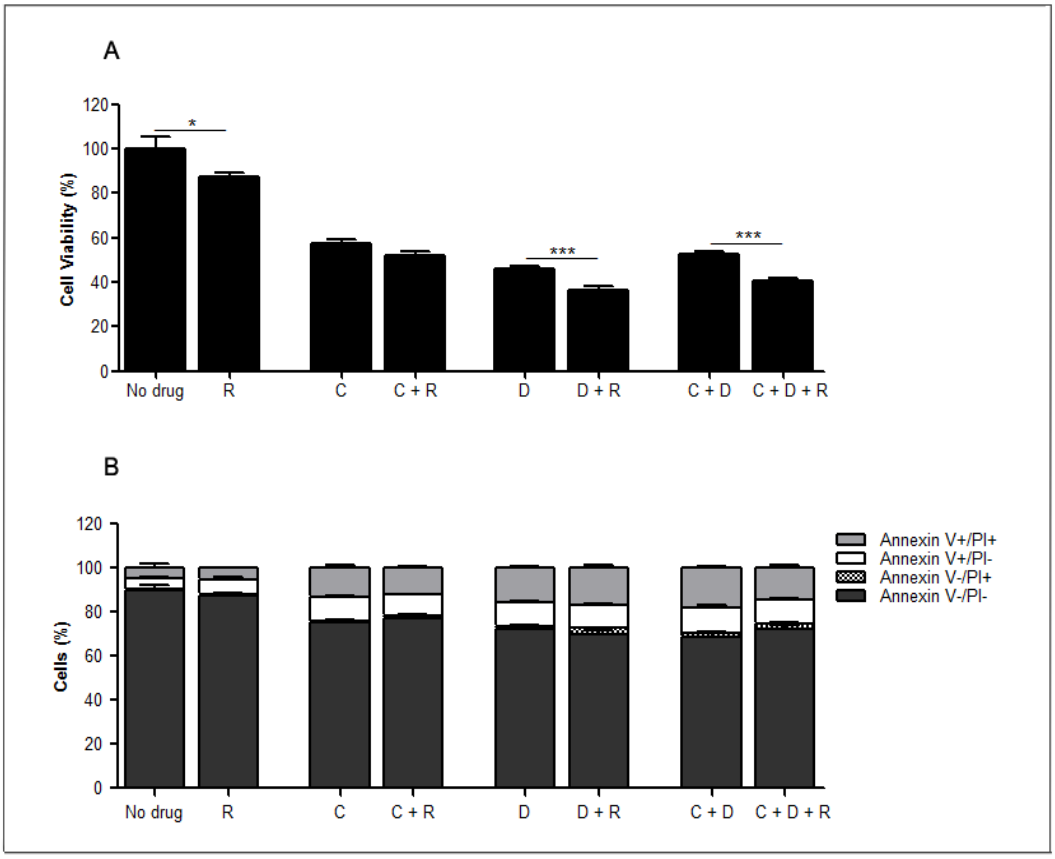

Figure 31 - Determination of HL-60 cell viability after treatment with cytarabine and/or doxorubicin combined with a sub-lethal concentration of rapamycin. Cells were incubated during 18h with each of the agents as represented, and after this time, cell viability was measured by MTS (A) and Annexin V/PI (B) assays, as described in Material and Methods section. The results of MTS and Annexin V/PI assays were obtained from comparison with non-treated cells (no drug) and are represented as mean+/-SEM of at least three biological replicates. The comparison between non-treated group and treated group and within treated groups was performed using the Student´s *t*-test for MTS results and the Two-way ANOVA with Bonferroni post hoc test for Annexin V/PI results. The statistical analysis was performed using the Prism software (Graph-Pad Software, San Diego, CA) and *p <0.05; ***p <0.001. C – cytarabine; D – doxorubicin; C+D - cytarabine combined with doxorubicin; R – rapamycin; C+R – cytarabine combined with rapamycin; D+R – doxorubicin combined with rapamycin; C+D+R – cytarabine and doxorubicin combined with rapamycin.

Regarding CQ, the MTS results showed that this autophagy inhibitor did not affect the viability of HL-60 cells treated with doxorubicin alone or combined with cytarabine, however, promoted a statistical significant increase in the viability of cells treated with cytarabine (Fig.32A). In contrast to MTS results, the Annexin V/PI data showed that combination of CQ with cytarabine and/or doxorubicin promoted a decrease in HL-60 cell's viability, however, only the combination of CQ

with cytarabine or doxorubicin promoted statistical significance (Fig.32B). Thus, according to Annexin V/PI assay and as previous hypothesized, autophagy inhibition associated with cell cycle arrest in S phase may promote the death of HL-60 cells treated with anti-leukemia agents. Moreover, these results also supported the hypothesis that autophagy may function as a pro-survival mechanism in HL-60 cells. However, in future, genetic manipulation of autophagy, such as the silencing by siRNA of some autophagy regulators such as *BECLIN1*, *ATG5* and *ATG7*, will be performed in order to confirm this hypothesis.

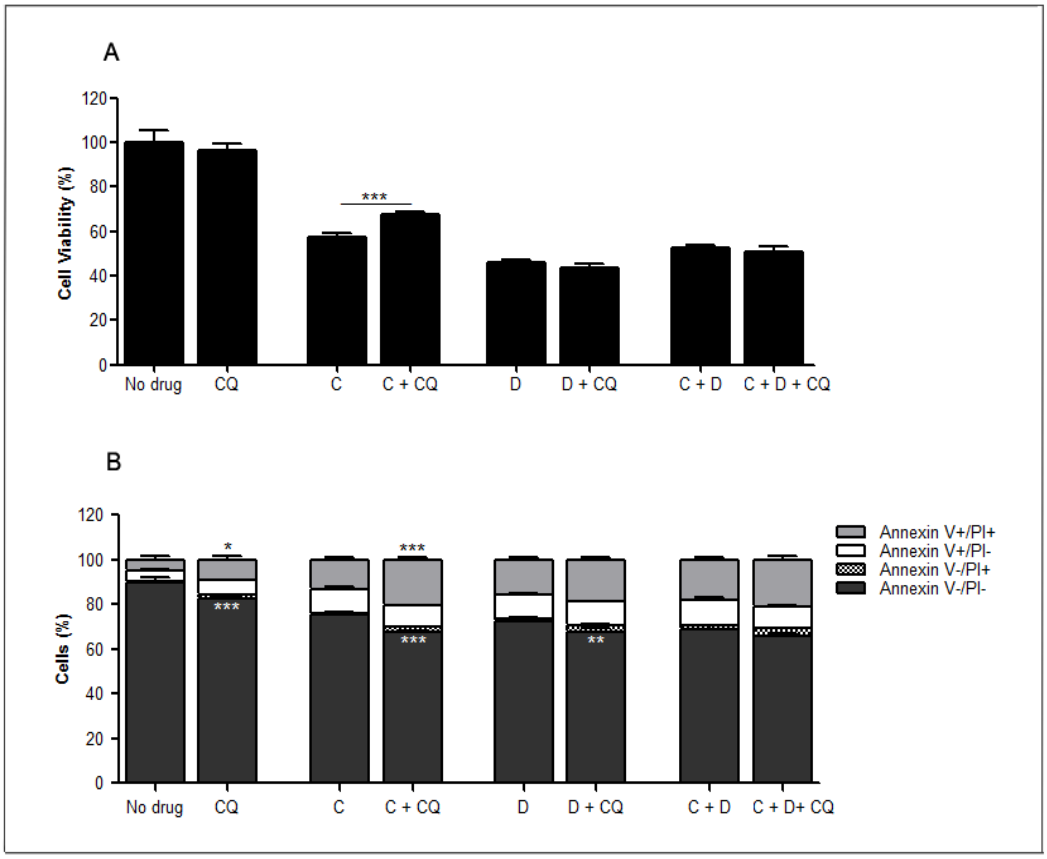

Figure 32 - Determination of HL-60 cell viability after treatment with cytarabine and/or doxorubicin combined with a sub-lethal concentration of CQ. Cells were incubated during 18h with each of the agents as represented, and after this time, cell viability was measured by MTS (A) and Annexin V/PI (B) assays, as described in Material and Methods section. The results of MTS and Annexin V/PI assays were obtained from comparison with non-treated cells (no drug) and are represented as mean+/-SEM of at least three biological replicates. The comparison between non-treated group and treated group and within treated groups was performed using the Student´s *t*test for MTS results and the Two-way ANOVA with Bonferroni post hoc test for Annexin V/PI results. The statistical analysis was performed using the Prism software (Graph-Pad Software, San Diego, CA) and *p <0.05; **p <0.01; ***p <0.001. C – cytarabine; D – doxorubicin; C+D - cytarabine combined with doxorubicin; CQ –

chloroquine; C+CQ – cytarabine combined with chloroquine; D+CQ – doxorubicin combined with chloroquine; C+D+CQ – cytarabine and doxorubicin combined with chloroquine.

4.1.4. Evaluation the impact of autophagy pharmacological manipulation on DNA damage of cells treated with conventional chemotherapy

In the previous section, we presented results suggesting that autophagy may act as a pro-survival mechanism in HL-60 cells. Therefore, in the next step we decided to evaluate if autophagy modulation impacts on DNA damage of HL-60 cells. Results showed that rapamycin promoted a decrease in pH2AX/H2AX ratio of untreated cells and of cells treated with cytarabine or doxorubicin (Fig.33). However, only the combination of rapamycin with doxorubicin displayed statistical significance (Fig.33). Data obtained also demonstrated that rapamycin combination with cytarabine plus doxorubicin did not induce any changes in pH2AX/H2AX ratio (Fig.33). Thus, our data suggested that rapamycin protects HL-60 cells from DNA damage induced by cytarabine or doxorubicin individual treatment. However, as rapamycin is a direct inhibitor of mTORC1 and its action may have pleiotropic effects on several cellular processes (reviewed in [127]), we cannot conclude if this protection is promoted by autophagy induction or by other processes affected by mTORC1 inhibition.

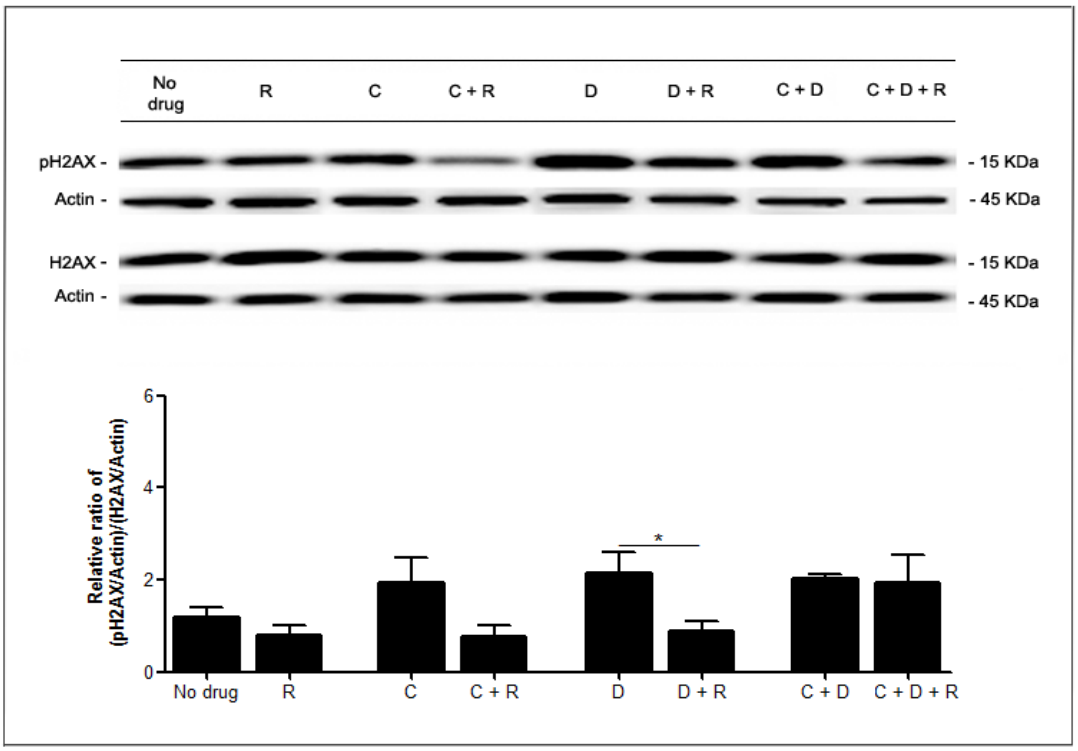

Figure 33 – pH2AX (Ser139) and total H2AX protein levels and densitometric analysis of pH2AX/H2AX in HL-60 cells treated with cytarabine and/or doxorubicin combined with a sub-lethal concentration of rapamycin. Cells were incubated during 18h with each of the agents as represented, and after this time, immunoblotting analysis of pH2AX and total H2AX, as described in Material and Methods section, was performed to assess DNA damage. The protein bands were quantified in the Image Lab® Software. The comparison between non-treated group and treated group and within treated groups was performed using the Student´s t-test and the Prism software (Graph-Pad Software, San Diego, CA). Densitometric analysis is shown as mean+/-SEM of at least three biological replicates. *p <0.05. C – cytarabine; D – doxorubicin; C+D – cytarabine combined with doxorubicin; R - rapamycin; C+R – cytarabine combined with rapamycin; D+R – doxorubicin combined with rapamycin; C+D+R – cytarabine and doxorubicin combined with rapamycin.

Regarding CQ, results demonstrated that this autophagy inhibitor promoted an increase, although without statistical significance, in pH2AX/H2AX ratio of cells treated with cytarabine and/or doxorubicin (Fig.34). Indeed, these results were somewhat expected, since studies (in rat liver cells) reported that CQ, besides the well-known effect as autophagy inhibitor [196, 197], is also an inducer of DNA damage [214]. Therefore, it is difficult to understand if the increase in DNA damage induced by the combination of CQ with cytarabine and/or doxorubicin is promoted by the inhibition of autophagy or by the genotoxic stress induced by CQ.

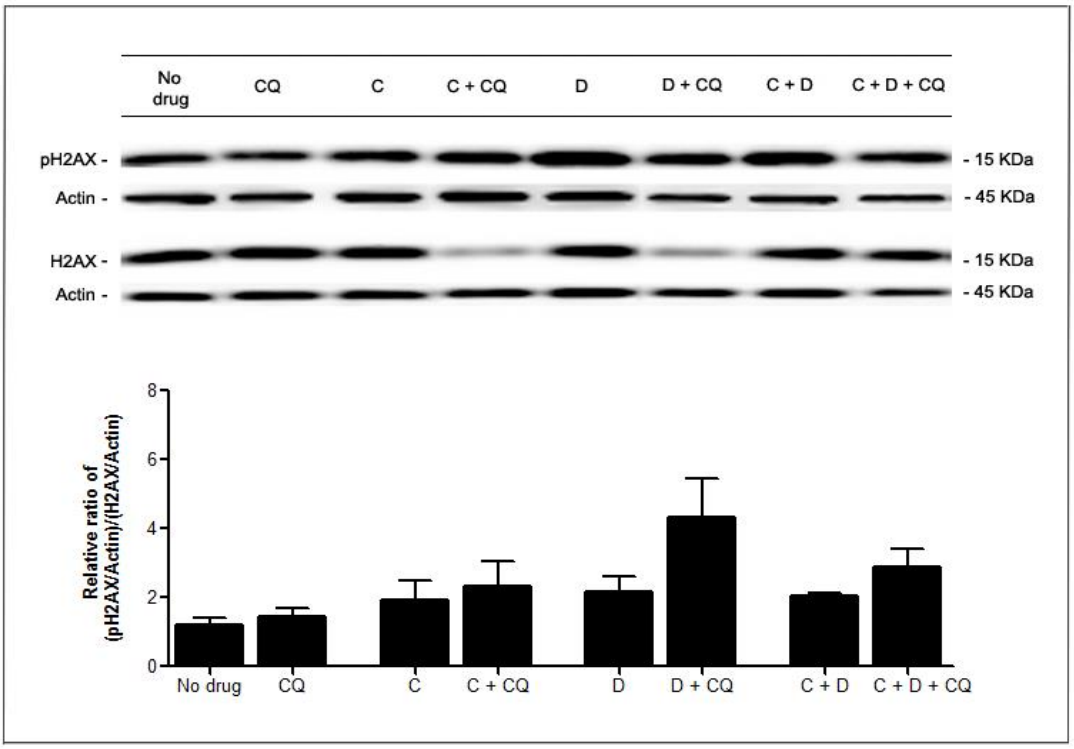

Figure 34 – pH2AX (Ser139) and total H2AX protein levels and densitometric analysis of pH2AX/H2AX in HL-60 cells treated with cytarabine and/or doxorubicin combined with a sub-lethal concentration of CQ. Cells were incubated during 18h with each of the agents as represented, and after this time, immunoblotting analysis of pH2AX and total H2AX, as described in Material and Methods section, was performed to assess DNA damage. The protein bands were quantified in the Image Lab® Software. The comparison between non-treated group and treated group and within treated groups was performed using the Student´s *t*-test and the Prism software (Graph-Pad Software, San Diego, CA). Densitometric analysis is shown as mean+/-SEM of at least three biological replicates. C – cytarabine; D – doxorubicin; C+D – cytarabine combined with doxorubicin; CQ – chloroquine; C+CQ – cytarabine combined with chloroquine; D+CQ – doxorubicin combined with chloroquine; C+D+CQ – cytarabine and doxorubicin combined with chloroquine.

Taken together, results of section 4.1.4 claim for further studies, involving genetic manipulation of autophagy, in order to understand whether autophagy induction or inhibition have impact on DNA damage levels of HL-60 cells.

4.2. KG-1 cells (erythroleukemia - FAB M6 leukemia)

4.2.1. Determination of rapamycin sub-lethal concentrations that induce autophagy

To define the sub-lethal concentrations of rapamycin that induce autophagy, KG-1 cells were submitted, during 18h, to rapamycin treatment and after this time cell viability and autophagy activity were determined through MTS assay and immunoblotting analysis of LC3, respectively. Data showed that although rapamycin 1 μM promoted a decrease in KG-1 cell viability of about 20% (Fig.35A), this was the lowest concentration that induced alterations on autophagy levels (Fig.35B).

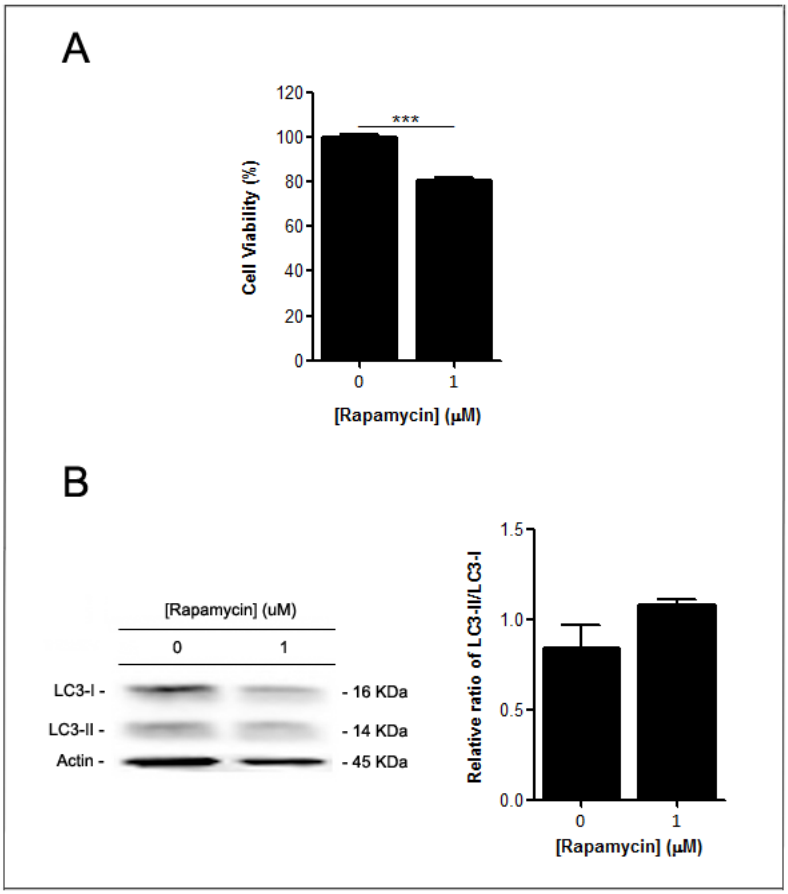

Figure 35 – Determination of cell viability (A) and LC3-I and LC3-II protein levels and densitometric analysis of LC3-II/LC3-I (B) in KG-1 cells treated with rapamycin. Cells were incubated during 18h with this agent as represented and 2h before the end of the treatment CQ (4.4 μM) was added to samples designed for LC3 protein analysis to block the autophagy flux and to allow LC3-II accumulation. After the treatment time, cell viability was measured by MTS assay and autophagy activity by immunoblotting analysis of LC3 (I and II), as described in

Material and Methods section. The MTS results were obtained from comparison with non-treated cells (no drug) and are shown as mean+/-SEM of at least three biological replicates. The protein bands were quantified in the Image Lab® Software and densitometric analysis is shown as mean+/-SEM of at least three biological replicates. For both approaches the comparison between non-treated group and treated group was performed using the Student´s *t*test and the Prism software (Graph-Pad Software, San Diego, CA). ***p <0.001.

Based on the above mentioned, we decided to choose 1 μM of rapamycin to be used in the following experiments.

4.2.2. Determination of CQ sub-lethal concentrations that inhibit autophagy

To determine the sub-lethal concentrations of CQ, KG-1 cells were treated during 18h with different concentrations of this agent and after this time cell viability was assessed through MTS assay. The results showed that KG-1 cells displayed a decrease in cell viability associated with an increase of CQ concentration with the highest concentration affecting the viability of about 20% of the cells (Fig.36).

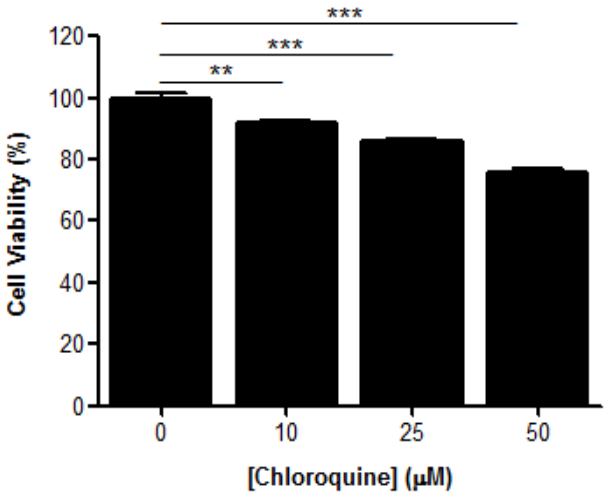

Figure 36 – Determination of KG-1 cell viability after treatment with CQ. Cells were incubated during 18h with different concentrations of this agent as represented, and after this time, cell viability was measured by MTS assay, as described in Material and Methods section. The results were obtained from comparison with non-treated cells (no drug) and are shown as mean+/-SEM of at least three biological replicates. Comparison between non-

treated group and treated groups was performed using the Student´s *t*test and the Prism software (Graph-Pad Software, San Diego, CA). **p <0.01; ***p <0.001.

In the next step, the autophagy levels of KG-1 cells treated with the different CQ concentrations were also evaluated. For that, cells were treated with different drug concentrations and immunoblotting analysis of LC3 (I and II) was performed. Data showed that all CQ concentrations tested promoted a statistical significant increase in LC3-II/LC3-I ratio compatible with autophagy inhibition (Fig.37).

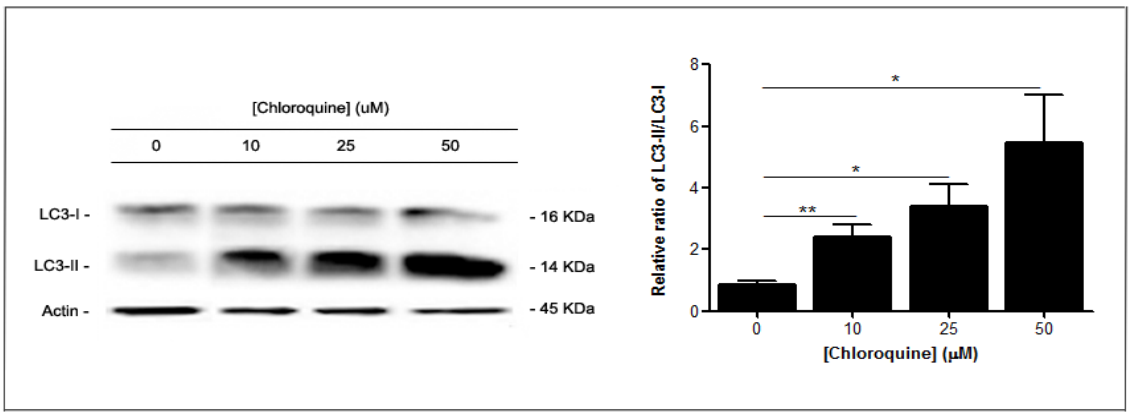

Figure 37 – LC3-I and LC3-II protein levels and densitometric analysis of LC3-II/LC3-I in KG-1 cells treated with CQ. Cells were incubated during 18h with different concentrations of this agent as represented, and after this time, immunoblotting analysis of LC3 (I and II), as described in Material and Methods section, was performed to assess autophagy activity. The protein bands were quantified in the Image Lab® Software. The comparison between non-treated group and treated groups was performed using the Student´s *t*test and the Prism software (Graph-Pad Software, San Diego, CA). Densitometric analysis is shown as mean+/-SEM of at least three biological replicates. *p <0.05; **p <0.01.

As CQ 10 µM was the concentration that exhibited less impact on KG-1 cell viability and simultaneously inhibits autophagy, we selected this concentration to be used in future experiments.

4.2.3. Evaluation the impact of autophagy pharmacological manipulation on viability of cells treated with conventional chemotherapy

4.2.3.1. Evaluation of autophagy activity and cell cycle profile

Similar to HL-60 cells, to determine the role of autophagy in the viability of KG-1 cells submitted to conventional chemotherapy treatment, we started by evaluating the impact of sub-lethal concentrations of autophagy modulators in the autophagy levels and cell cycle progression of KG-1 cells treated with cytarabine and/or doxorubicin. For that, cells were treated, during 18h, with cytarabine and/or doxorubicin combined with rapamycin or CQ, and after this time, immunoblotting analysis of LC3 and cell cycle profile analysis was performed. Results showed that rapamycin promoted a statistical significant increase in LC3-II/LC3-I ratio of KG-1 cells treated with cytarabine, while in cells treated with doxorubicin alone or combined with cytarabine rapamycin did not induce alterations (Fig.38).

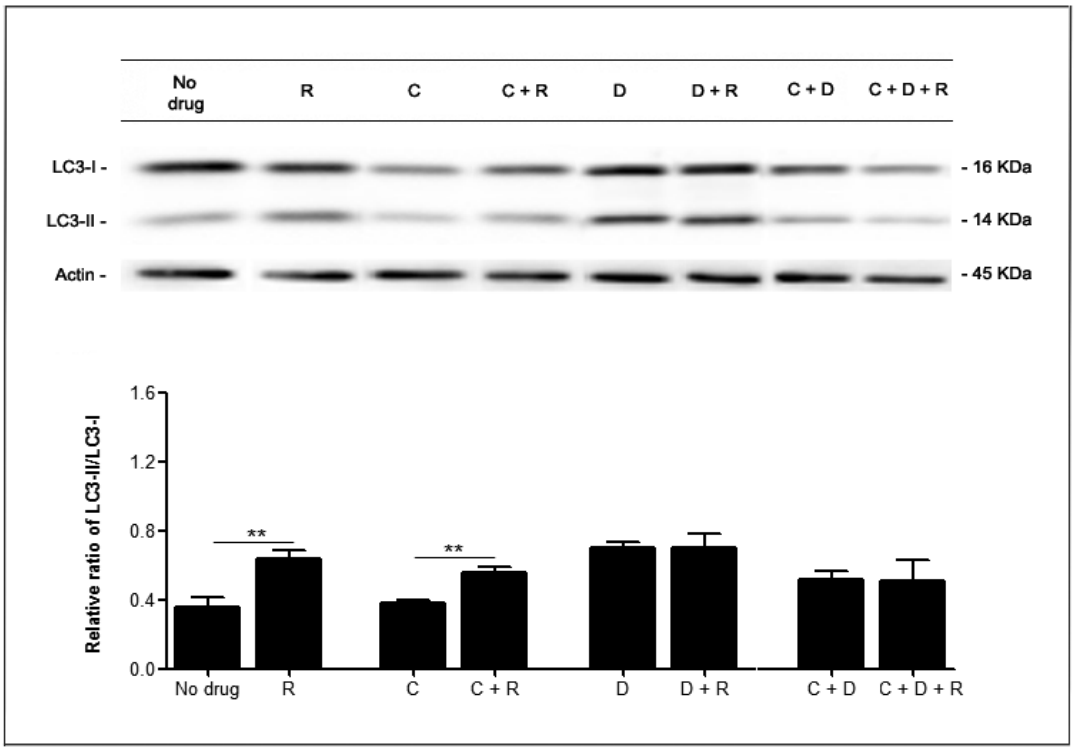

Figure 38 – LC3-I and LC3-II protein levels and densitometric analysis of LC3-II/LC3-I in KG-1 cells treated with cytarabine and/or doxorubicin combined with a sub-lethal concentration of rapamycin. Cells were incubated during 18h with each of the agents as represented and 2h before the end of the treatment CQ (4.4 μM) was added to block the autophagy flux and to allow LC3-II accumulation. After the treatment time, immunoblotting analysis of LC3 (I and II), as described in Material and Methods section, was performed to assess

autophagy activity. The protein bands were quantified in the Image Lab® Software. The comparison between non-treated group and treated group and within treated groups was performed using the Student´s *t*-test and the Prism software (Graph-Pad Software, San Diego, CA). Densitometric analysis is shown as mean+/-SEM of at least three biological replicates. **p <0.01. C – cytarabine; D – doxorubicin; C+D – cytarabine combined with doxorubicin; R - rapamycin; C+R – cytarabine combined with rapamycin; D+R – doxorubicin combined with rapamycin; C+D+R – cytarabine and doxorubicin combined with rapamycin.

Regarding cell cycle profile, data demonstrated that rapamycin induced a cell cycle arrest in S phase of KG-1 cells treated with cytarabine, while in cells submitted to doxorubicin alone or combined with cytarabine this agent did not promote major alterations (Fig.39).

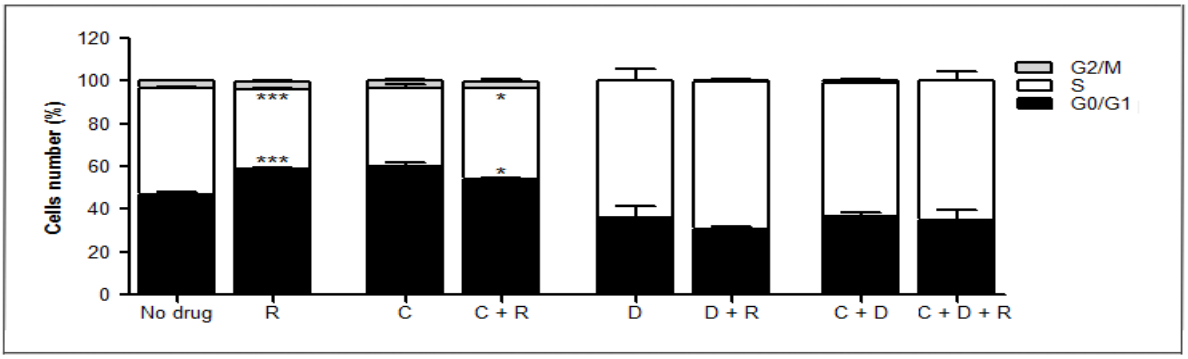

Figure 39 - Cell cycle profile of KG-1 cells treated with cytarabine and/or doxorubicin combined with a sub-lethal concentration of rapamycin. Cells were incubated during 18h with each of the agents as represented, and after this time, cell cycle profile was determined through DNA content assessment, as described in Material and Methods section. Cell cycle analysis was performed using the Modifit® Software. The comparison between non-treated group and treated group and within treated groups was performed using the Two-way ANOVA with Bonferroni post hoc test and the Prism software (Graph-Pad Software, San Diego, CA). Cell cycle analysis is shown as mean+/-SEM of at least three biological replicates. *p <0.05; *** <0.001. C – cytarabine; D – doxorubicin; C+D – cytarabine combined with doxorubicin; R - rapamycin; C+R – cytarabine combined with rapamycin; D+R – doxorubicin combined with rapamycin; C+D+R – cytarabine and doxorubicin combined with rapamycin.

Altogether, these results suggested that rapamycin promote autophagy induction associated with cell cycle arrest in S phase of KG-1 cells treated only with cytarabine.

Concerning CQ, our data showed that this autophagy inhibitor promoted a statistical significant increase in LC3-II/LC3-I ratio of KG-1 cells submitted to cytarabine and/or doxorubicin treatment, indicating that in all tested conditions an inhibition of the autophagy process took place (Fig.40).

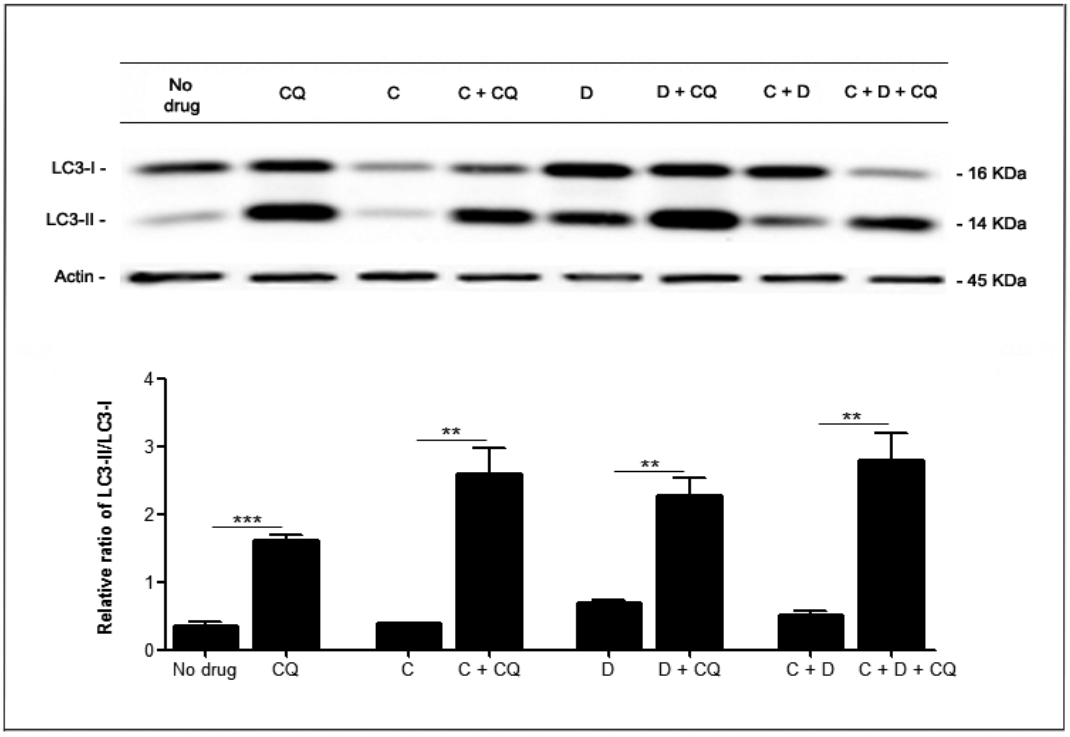

Figure 40 – LC3-I and LC3-II protein levels and densitometric analysis of LC3-II/LC3-I in KG-1 cells treated with cytarabine and/or doxorubicin combined with a sub-lethal concentration of CQ. Cells were incubated during 18h with each of the agents as represented, and after this time, immunoblotting analysis of LC3 (I and II), as described in Material and Methods section, was performed to assess autophagy activity. The protein bands were quantified in the Image Lab® Software. The comparison between non-treated group and treated group and within treated groups was performed using the Student´s *t*test and the Prism software (Graph-Pad Software, San Diego, CA). Densitometric analysis is shown as mean+/-SEM of at least three biological replicates. **p <0.01; *** <0.001. C – cytarabine; D – doxorubicin; C+D – cytarabine combined with doxorubicin; CQ - chloroquine; C+CQ – cytarabine combined with chloroquine; D+CQ – doxorubicin combined with chloroquine; C+D+CQ – cytarabine and doxorubicin combined with chloroquine.

In addition to autophagy activity, cell cycle profile of KG-1 cells treated with the combination of CQ with cytarabine and/or doxorubicin was also evaluated. Data showed that CQ induced cell

cycle arrest in S phase of KG-1 cells treated with cytarabine or doxorubicin and that the combination of CQ with cytarabine plus doxorubicin promoted cell cycle arrest in G0/G1 phases when compared to cells only treated with the anti-leukemia agents (Fig.41).

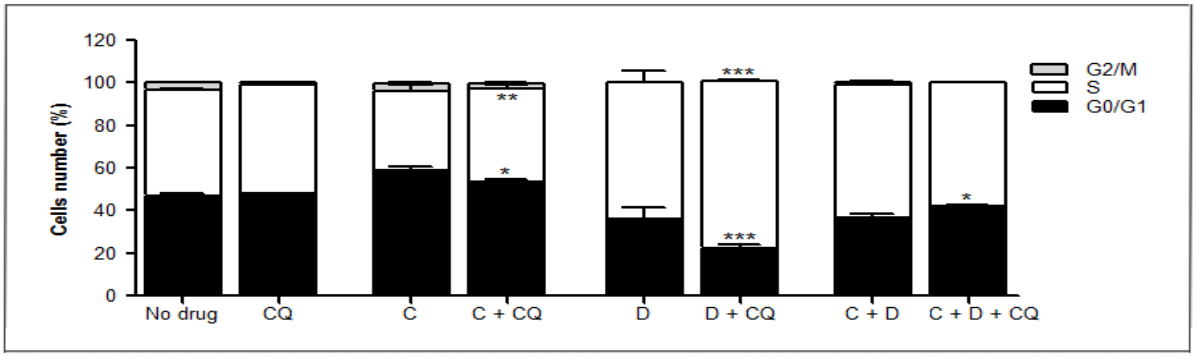

Figure 41 - Cell cycle profile of KG-1 cells treated with cytarabine and/or doxorubicin combined with a sub-lethal concentration of CQ. Cells were incubated during 18h with each of the agents as represented, and after this time, cell cycle profile was determined through DNA content assessment, as described in Material and Methods section. Cell cycle analysis was performed using the Modifit® Software. The comparison between non-treated group and treated group and within treated groups was performed using the Two-way ANOVA with Bonferroni post hoc test and the Prism software (Graph-Pad Software, San Diego, CA). Cell cycle analysis is shown as mean+/- SEM of at least three biological replicates. *p <0.05; **p <0.01; *** <0.001. C – cytarabine; D – doxorubicin; C+D – cytarabine combined with doxorubicin; CQ - chloroquine; C+CQ – cytarabine combined with chloroquine; D+CQ – doxorubicin combined with chloroquine; C+D+CQ – cytarabine and doxorubicin combined with chloroquine.

Overall, these results demonstrated that autophagy inhibition promoted by CQ is associated with cell cycle arrest in S phase of KG-1 cells treated with cytarabine or doxorubicin and cell cycle arrest in G0/G1 phases of cells treated with the anti-leukemia agent´s combination.

In summary, and identical to observed with HL-60 cells, results of section 4.2.3.1 also suggested the existence of a correlation between the autophagy process and the cell cycle arrest in S phase of KG-1 cells treated with anti-leukemia agents.

In contrast to HL-60 cells, our previous results indicated that autophagy may act as a pro-death mechanism in KG-1 cells. Thus, and contrarily to HL-60 cells, the connection between autophagy induction and S phase cell cycle arrest may occur in order to promote KG-1 cell death, while the inhibition of autophagy associated with S phase cell cycle arrest may occur to promote

KG-1 cell survival. Therefore, and similar to HL-60 cells, it was fundamental to understand the impact that these approaches have in KG-1 cell survival.

4.2.3.2 Evaluation of cell viability

Identical to HL-60 cells, after evaluating the effects of the sub-lethal concentrations of rapamycin or CQ on autophagy and cell cycle profile of KG-1 cells treated with conventional chemotherapy, our next step was to determine the impact of these autophagy modulators in the viability of KG-1 cells submitted to anti-leukemia agents. Similar to that observed in section 1.2.1, these results also showed a good correlation between MTS and Annexin V/PI assays (Fig.42A and 42B). In fact, data from both approaches demonstrated that rapamycin promoted a statistical significant decrease in the viability of KG-1 cells treated with doxorubicin alone or combined with cytarabine (Fig.42A and 42B). However, due to the effects that mTORC1 inhibition may have on other cellular processes, these results do not allow us to conclude that this decrease in KG-1 cell viability is promoted only by autophagy.

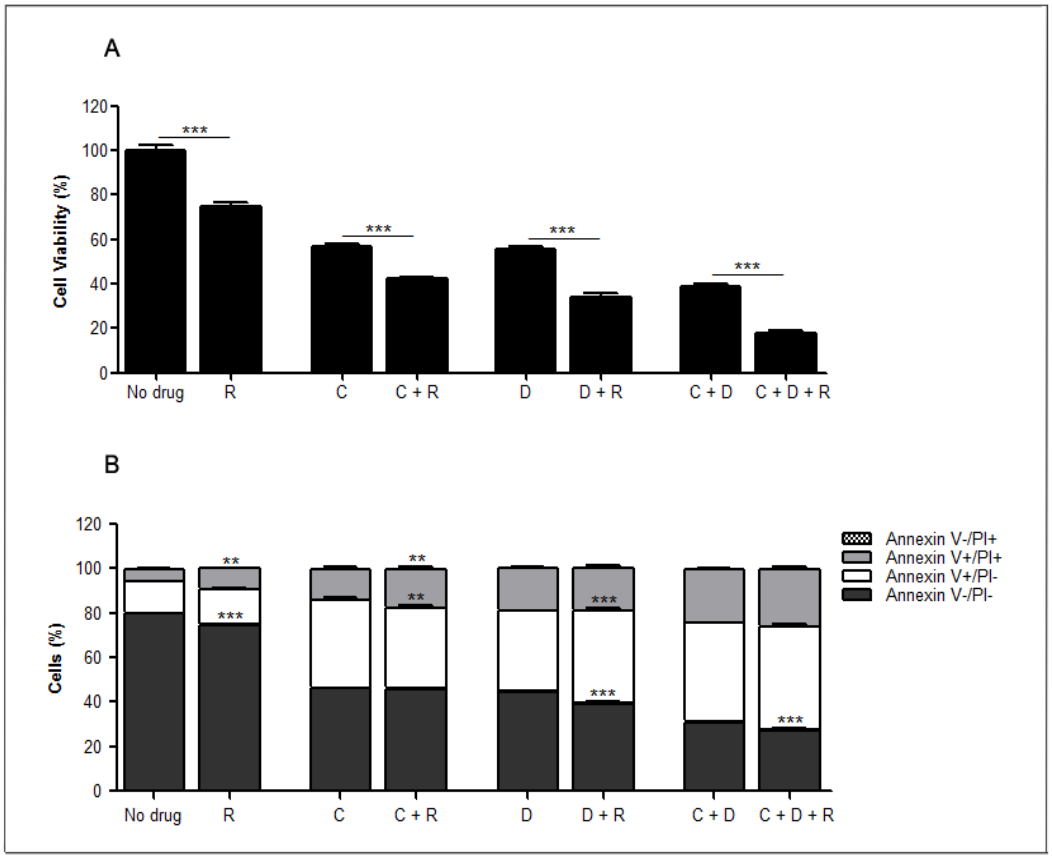

Figure 42 - Determination of KG-1 cell viability after treatment with cytarabine and/or doxorubicin combined with a sub-lethal concentration of rapamycin. Cells were incubated during 18h with each of the agents as represented, and after this time, cell viability was measured by MTS (A) and Annexin V/PI (B) assays, as described in Material and Methods section. The results of MTS and Annexin V/PI assays were obtained from comparison with non-treated cells (no drug) and are represented as mean+/-SEM of at least three biological replicates. The comparison between non-treated group and treated group and within treated groups was performed using the Student´s *t*-test for MTS results and the Two-way ANOVA with Bonferroni post hoc test for Annexin V/PI results. The statistical analysis was performed using the Prism software (Graph-Pad Software, San Diego, CA) and **p <0.01; ***p <0.001. C – cytarabine; D – doxorubicin; C+D - cytarabine combined with doxorubicin; R – rapamycin; C+R – cytarabine combined with rapamycin; D+R – doxorubicin combined with rapamycin; C+D+R – cytarabine and doxorubicin combined with rapamycin.

Regarding CQ, both MTS and Annexin V/PI results showed that this autophagy inhibitor promoted a statistical significant increase in the viability of KG-1 cells submitted to doxorubicin alone or combined with cytarabine, being this effect more evident in cells treated with doxorubicin (Fig.43A and 43B). Moreover, data obtained from both techniques also demonstrated that CQ did not induce alterations in the viability of KG-1 cells treated with

cytarabine (Fig.43A and 43B). Thus, this data indicated that autophagy inhibition associated with cell cycle arrest in S phase may promote the survival of KG-1 cells treated with anti-leukemia agents. Moreover, these results also supported the hypothesis that autophagy may function as a tumor suppressor process in KG-1 cells. However, studies involving the genetic manipulation of autophagy will be performed in future to confirm these results.

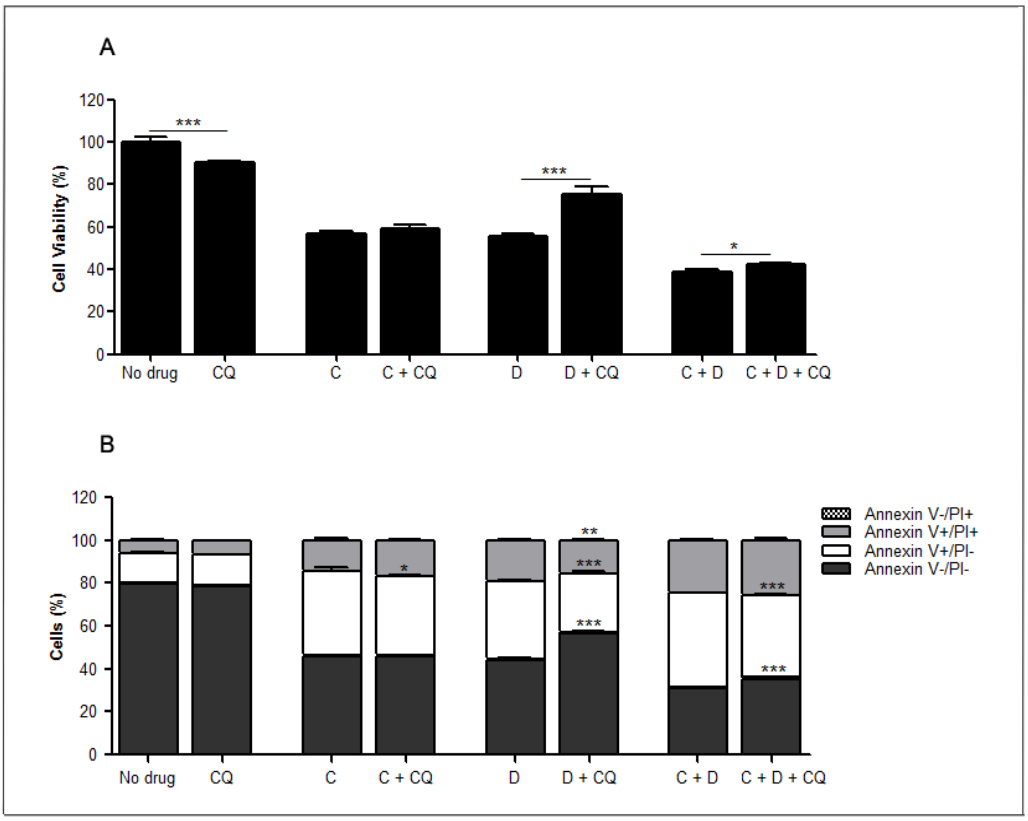

Figure 43 - Determination of KG-1 cell viability after treatment with cytarabine and/or doxorubicin combined with a sub-lethal concentration of CQ. Cells were incubated during 18h with each of the agents as represented, and after this time, cell viability was measured by MTS (A) and Annexin V/PI (B) assays, as described in Material and Methods section. The results of MTS and Annexin V/PI assays were obtained from comparison with non-treated cells (no drug) and are represented as mean+/-SEM of at least three biological replicates. The comparison between non-treated group and treated group and within treated groups was performed using the Student´s *t*test for MTS results and the Two-way ANOVA with Bonferroni post hoc test for Annexin V/PI results. The statistical analysis was performed using the Prism software (Graph-Pad Software, San Diego, CA) and *p <0.05; **p <0.01; ***p <0.001. C – cytarabine; D – doxorubicin; C+D - cytarabine combined with doxorubicin; CQ – chloroquine; C+CQ – cytarabine combined with chloroquine; D+CQ – doxorubicin combined with chloroquine; C+D+CQ – cytarabine and doxorubicin combined with chloroquine.

4.2.4. Evaluation the impact of autophagy pharmacological manipulation on DNA damage of cells treated with conventional chemotherapy

In contrast to HL-60 cells, the results described in previous sections suggested that autophagy may act as inducer of KG-1 cell death. Therefore, our next step was to determine if autophagy modulation impacts on DNA damage of KG-1 cells. Results showed that rapamycin promoted a decrease in pH2AX/H2AX ratio of untreated cells or cells treated with cytarabine and/or doxorubicin (Fig.44). However, as referred above, control cells displayed a high endogenous pH2AX/H2AX ratio (Fig.44). Thus, and similar to observed for HL-60 cells, this data suggested that rapamycin decreases the DNA damage levels of KG-1 cells treated with cytarabine and/or doxorubicin. However, and as previous mentioned, the effect that mTORC1 inhibition may have on diverse cellular processes do not allow us to associate this decrease only with autophagy.

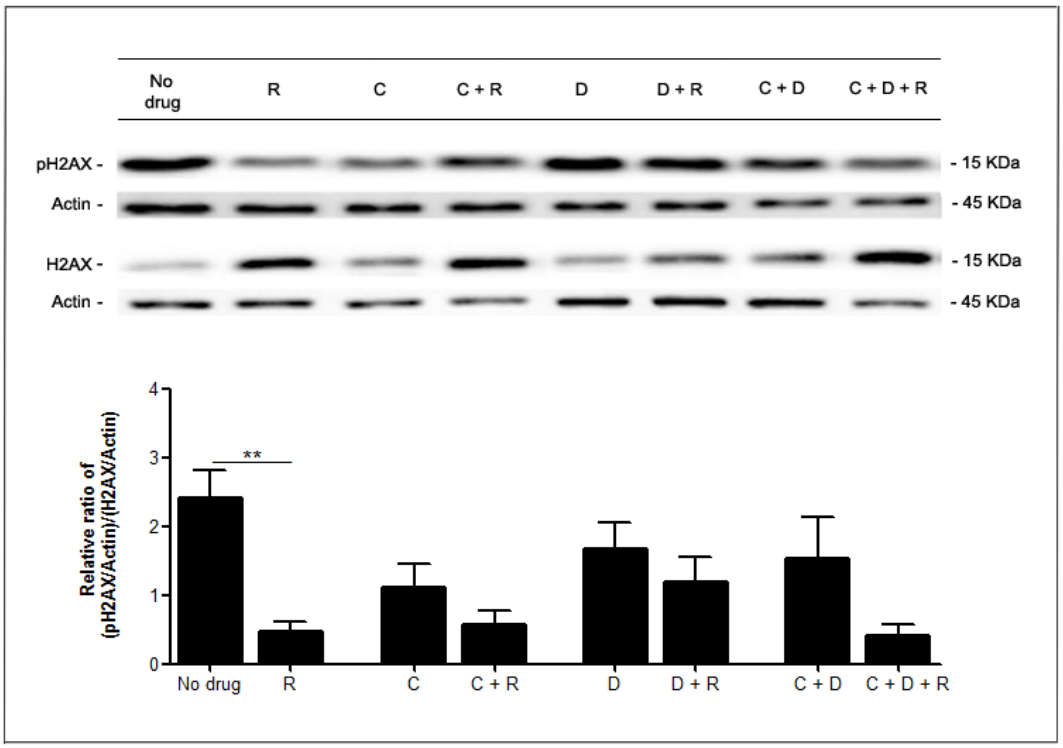

Figure 44 – pH2AX (Ser139) and total H2AX protein levels and densitometric analysis of pH2AX/H2AX in KG-1 cells treated with cytarabine and/or doxorubicin combined with a sub-lethal concentration of rapamycin. Cells were incubated during 18h with each of the agents as represented, and after this time, immunoblotting analysis of pH2AX and total H2AX, as described in Material and Methods section, was performed to assess DNA damage. The protein bands were quantified in the Image Lab® Software. The comparison

between non-treated group and treated group and within treated groups was performed using the Student´s *t*-test and the Prism software (Graph-Pad Software, San Diego, CA). Densitometric analysis is shown as mean+/-SEM of at least three biological replicates. **p <0.01. C – cytarabine; D – doxorubicin; C+D – cytarabine combined with doxorubicin; R - rapamycin; C+R – cytarabine combined with rapamycin; D+R – doxorubicin combined with rapamycin; C+D+R – cytarabine and doxorubicin combined with rapamycin.

Concerning CQ, results demonstrated that this autophagy inhibitor promoted an increase in pH2AX/H2AX ratio of KG-1 cells treated with cytarabine or doxorubicin and a decrease in cells treated with the combination of these two anti-leukemia agents (Fig.45). However, in none of the tested conditions statistical significance was obtained (Fig.45). Thus, similar to HL-60 cells, this data do not allow us to conclude if autophagy inhibition may interfere with DNA damage levels of KG-1 cells.

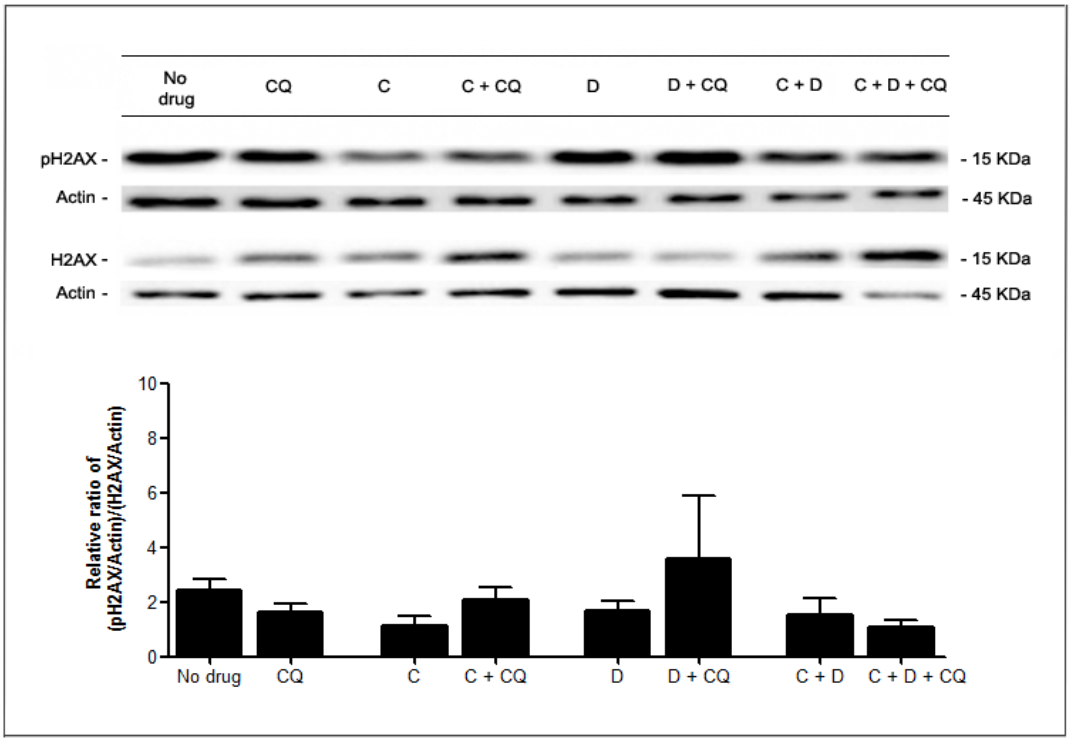

Figure 45 – pH2AX (Ser139) and total H2AX protein levels and densitometric analysis of pH2AX/H2AX in KG-1 cells treated with cytarabine and/or doxorubicin combined with a sub-lethal concentration of CQ. Cells were incubated during 18h with each of the agents as represented, and after this time, immunoblotting analysis of pH2AX and total H2AX, as described in Material and Methods section, was performed to assess DNA damage. The protein bands were quantified in the Image Lab® Software. The comparison between non-treated group and treated group and within treated groups was performed using the Student´s *t*-test and the Prism

software (Graph-Pad Software, San Diego, CA). Densitometric analysis is shown as mean+/-SEM of at least three biological replicates. C – cytarabine; D – doxorubicin; C+D – cytarabine combined with doxorubicin; CQ – chloroquine; C+CQ – cytarabine combined with chloroquine; D+CQ – doxorubicin combined with chloroquine; C+D+CQ – cytarabine and doxorubicin combined with chloroquine.

Taken together, results of section 4.2.4 indicated that further studies are needed to understand if autophagy activation or inhibition has impact on DNA damage levels of KG-1 cells.

A summary of the results obtained is presented in table 7 and 8 for HL-60 and KG-1 cells, respectively. In summary, our results suggested that anti-leukemia agents induce DNA damage in HL-60 cells, which promote AMPK pathway activation, cell cycle arrest in G0/G1 phases and autophagy. The fact that the drugs combination, more efficient in eradicating HL-60 cells (by Annexin V/PI), is associated with a lower activation of AMPK suggests that this pathway functions as a pro-survival mechanism. In addition, the inhibition of autophagy through CQ promoted a decrease in the viability of HL-60 cells (by Annexin V/PI) indicating that one of the outcomes of AMPK activation could be responsible for HL-60 cell survival. Surprisingly, all the treatment combinations that display higher efficiency in killing HL-60 cells are associated with an arrest of cells in S phase and further studies have to be performed to understand the interconnections and the coordinated regulation of AMPK, autophagy and cell cycle (Table 7).

Our data also indicated that HL-60 and KG-1 cells respond differently to conventional chemotherapy treatment. Indeed, KG-1 cells display high levels of endogenous DNA damage, as previously described [211], that jeopardizes the analysis of chemotherapy effects on DNA damage. However, and in contrast to HL-60 cells, increased AMPK activation, cell cycle arrest in S phase and autophagy induction was observed in the most efficient treatments such as doxorubicin alone or combined with cytarabine, suggesting that AMPK in KG-1 cells might function as a tumor suppressor pathway. In addition, the inhibition of autophagy through CQ promoted an increase in the viability of KG-1 cells treated with anti-leukemia agents, suggesting that autophagy could be one of the AMPK outcomes responsible for its tumor suppression function (Table 8).

Altogether, these results suggested that, contrarily to occur in clinical, different strategies should be applied for AML-FAB M2 and AML-FAB M6 leukemia patients' treatment. Particularly,

the combination of conventional chemotherapy with AMPK and/or autophagy inhibitors seem to be a good approach for AML-FAB M2 leukemia treatment, while, on other hand, the combination of anti-leukemia agents with AMPK and/or autophagy activators could be a good strategy to apply in AML-FAB M6 leukemia.

Table 7 - An overview of the results obtained with HL-60 cells.

HL-60										
		C			D			C + D		
			+ R	+ CQ		+ R	+ CQ		+ R	+ CQ
Viability	MTS	57±1.7%*	52±1.8%	68±1.2%*	46±1.4%*	36±1.8%*	44±1.5%	52±1.1%*	41±1.0%*	51±2.1%
	Annexin V/PI	75±1.4%*	77±1.0%	67±1.0%*	72±1.5%*	70±1.7%	68±1.4%*	68±1.4%*	72±1.8%	66±1.6%
pH2AX/H2AX		+	-	++	+	-*	++	+*	N/C	++
pAMPK/AMPK		+++*	ND	ND	++*	ND	ND	+	ND	ND
pp27/p27		N/C	ND	ND	N/C	ND	ND	N/C	ND	ND
Cell cycle		G0/G1 phases (+++)*	N/C	S phase*	G0/G1 phases (++)*	S phase*	S phase* and G2/M phases*	G0/G1 phases (+)* and S phase (+)*	S phase (++)*	S phase (++)*
Autophagy		++	N/C	-*	+	++*	-*	N/C	+	-*

The letters and symbols exhibited in the previous table represent: C (cytarabine); D (doxorubicin); C+D (cytarabine combined with doxorubicin); R (rapamycin); CQ (chloroquine); + (increase); - (decrease); N/C (not changed); ND (not determined); * (results with statistical significance).

Table 8 - An overview of the results obtained with KG-1 cells.

KG-1										
		C			D			C + D		
			+ R	+ CQ		+ R	+ CQ		+ R	+ CQ
Viability	MTS	57±1.5%*	42±1.0%	59±1.9%	56±1.1%*	34±1.7%	75±3.7%	39±1.1%*	17.7±1.2%	42±0.9%
	Annexin V/PI	46±0.5%*	46±0.2%	46±0.4%	45±0.7%*	39±1.4%	57±1.4%	31±0.5%*	26.7±1.7%	35±0.9%
pH2AX/H2AX		N/C	-	+	N/C	-	+	N/C	-	-
pAMPK/AMPK		+	ND	ND	++	ND	ND	+++	ND	ND
pp27/p27		N/C	ND	ND	N/C	ND	ND	N/C	ND	ND
Cell cycle		G0/G1 phases*	S phase*	S phase*	S phase (+)*	N/C	S phase (++)*	S phase (+)*	N/C	G0/G1 phase*
Autophagy		N/C	+*	-*	++*	N/C	-*	+	N/C	-*

The letters and symbols exhibited in the previous table represent: C (cytarabine); D (doxorubicin); C+D (cytarabine combined with doxorubicin); R (rapamycin); CQ (chloroquine); + (increase); - (decrease); N/C (not changed); ND (not determined); * (results with statistical significance).

As current acute myeloid leukemia (AML) therapies present poor outcomes among old patients, it becomes crucial to elucidate the mechanisms underlying AML cell´s resistance/susceptibility to conventional chemotherapy in order to develop more effective treatments. Malignant cells are characterized by high nuclear DNA replication rates and consequent extreme proliferation, when compared to surrounded healthy cells [74], and therefore several anticancer agents act as inducers of DNA damage [76]. However, recently studies reported that the DNA damage induced by some of these agents activates a DNA damage response (DDR) involving the activation of crucial proteins, such as AMP-activated protein kinase (AMPK), that culminates in autophagy induction as a pro-survival mechanism [135, 184-186]. Cytarabine and doxorubicin, chemotherapeutic agents used in AML treatment, are described as inducers of DNA damage [80, 81, 89-91] and DDR [101-103]. However, their effects on AMPK activation in AML cells are still elusive. Our preliminary data showed that these anti-leukemia agents promoted cell cycle arrest in G0/G1 and S phases associated with autophagy induction in AML cells. Therefore, this master project aimed to associate those events with the occurrence of DNA damage induced by conventional chemotherapy in AML cells. The work hypothesis was based on the fact that DNA damage, which activates a DDR, could culminate in cell cycle arrest and autophagy induction as a pro-survival mechanism conferring chemoresistance to AML cells. To validate this hypothesis, two distinct AML cell lines, HL-60, an *in vitro* model of AML with differentiation, and KG-1, an *in vitro* model of erythroleukemia, were used. Cell lines are advantageous models that allow the reduction of human burden associated with ethical considerations, as well as, the decrease of the variability between samples. Moreover, continuous proliferation of AML cells permits to study leukemia *in vitro* whereas non-immortalized hematopoietic cells cannot survive in these conditions during long time periods. However, studies using cell lines have important limitations such as: these models do not recapitulate the complexity of primary tumor cells and the cellular interactions with the environment niches are not reviewed in these *in vitro* studies [215]. Nevertheless, these models are very useful to identify targets to be explored in patient's sample contexts.

The occurrence of DNA damage and DDR elicited by the anti-leukemia agents was evaluated using the half maximal inhibitory concentration (IC_{50}) values of cytarabine and doxorubicin. In fact, these concentrations are the most commonly used in testing drugs cytotoxicity in tumor cell lines

[203, 204]. MTS and Annexin V/PI assays were the approaches used to determine these concentrations, however, in contrast to KG-1 cells, a good correlation between these methods was not obtained in HL-60 cells. Particularly, the drugs concentration that correspond to IC_{50} values by MTS only promoted a decrease of about 30% in the viability of HL-60 cells by Annexin V/PI assay. MTS is a metabolic assay that allows the indirect determination of the number of viable cells by the ability of mitochondria to reduce tetrazolium salt into formazan [200]. On the other hand, Annexin V/PI assay is a more accurate method that permits this determination through the use of Annexin V, a molecule that binds with high affinity to phosphatidylserine (PE) allowing the identification of plasma membrane symmetry alterations, and propidium iodide (PI), a membrane impermeable compound that only intercalates with nucleic acids when cells have compromised/disintegrated plasma membrane [201, 202]. Cytarabine [208] and doxorubicin [209] have been described as affecting mitochondrial function of HL-60 cells. Therefore, these anti-leukemia agents could interfere with mitochondrial activity of HL-60 cells impairing the reduction of tetrazolium salt into formazan, leading to an overestimation of the drugs cytotoxicity. In fact, over the last years, studies have emerging reporting that some drugs have the capacity to interfere with mitochondrial activity affecting the reduction of tetrazolium salt and resulting in erroneous cytotoxicity conclusions [205-207]. Our data suggested that the IC_{50} values of cytarabine or doxorubicin determined by MTS assay for HL-60 cells are not real IC_{50} values, however, we decided to use these concentrations throughout this work since these are the most commonly used concentrations chosen for cytotoxicity studies performed in HL-60 cells [203, 204]. Nonetheless, in future, the determination of IC_{50} values for cytarabine or doxorubicin in HL-60 cells will be performed by Annexin V/PI assay and all parameters studied in this thesis will be repeated using these concentrations.

Annexin V/PI results for HL-60 cells and MTS and Annexin V/PI results for KG-1 cells also showed that the combination of cytarabine with doxorubicin increases the killing of cells when compared to the individual treatments, suggesting that this combination generates a synergistic cytotoxic effect. However, the most accurate procedure to study synergism between drugs is through the determination of a ratio between these agents in order to find the most effective combination, which is achieved using specific software analysis such as CalcuSyn [210]. Therefore, in future, this analysis will also be performed to determine the combinations that have the highest synergistic effect.

The strategy for studying DNA damage in AML cell´s response to conventional chemotherapy was based on the evaluation of histone H2AX phosphorylation at Ser139, since this event is the most commonly used biomarker to detect genotoxic stress [109-111]. As expected, our data showed that cytarabine and/or doxorubicin promoted DNA damage in HL-60 cells, being that the higher cytotoxic effect promoted by drugs combination seemed to result in a more pronounced DNA damage induction. In contrast, KG-1 cells appeared to exhibit endogenous DNA damage and anti-leukemia agents did not seem to affect this DNA damage levels. In fact, previous work showed that KG-1 cells display signs of endogenous DNA damage and that high doses of irradiation did not promote alterations in these levels [211]. Thus, our data raises two hypotheses: either anti-leukemia agents do not promote DNA damage in KG-1 cells or it is not detectable due to the high endogenous DNA damage levels displayed by these cells. To complement and validate results obtained with both cell lines, additional methodologies to evaluate the occurrence of DNA damage, such as TUNEL (terminal deoxyribonucleotidyl transferase-mediated deoxyuridine triphosphate nick end labeling) assay [216], can be applied in future.

Studies have shown that the DNA damage induced by some anticancer agents promotes the activation of AMPK pathway [184-186]. Our results on HL-60 cells suggest that cytarabine or doxorubicin alone induce AMPK activation. Interesting the combination of both drugs resulted in a less AMPK activation when compared to individual treatments, suggesting that AMPK activation may function as a pro-survival mechanism in these cells. Cytarabine and doxorubicin are described as inducers of ATR and ATM (through phosphorylation at Ser1981) activation, respectively [101, 103]. However, once activated, ATR or ATM may phosphorylate AMPK directly [118] or mediated through LKB1 phosphorylation [120]. Therefore, in future, further studies should be accomplished in order to understand if the activation of AMPK observed in HL-60 cells treated with anti-leukemia agents is promoted by ATR or ATM directly or mediated through LKB1 phosphorylation. These studies may include: immunoblotting analysis of ATR, ATM (Ser1981) and LKB1 (Thr366) and knockdown of ATR, ATM or LKB1 by siRNA [120].

In addition to DNA damage, AMPK is also an important sensor of cellular energy status that is activated by a rise in the AMP: ATP ratio, promoted either by a reduction in ATP production or an increase in ATP consumption (reviewed in [136]). Results about the induction of DNA damage promoted by cytarabine and/or doxorubicin in KG-1 cells were inconclusive, however, AMPK could also be activated in response to an increase in AMP: ATP ratio promoted by these agents.

In fact, data suggested that cytarabine and/or doxorubicin promote AMPK activation in KG-1 cells, being that the higher cytotoxic effect promoted by drugs combination resulted in a more evident AMPK activation. Thus, it would be interesting to determine the ATP levels in KG-1 cells submitted to anti-leukemia agents in order to correlate these levels with AMPK activation.

Studies in solid tumors cells have shown that the activation of AMPK leads to autophagy induction as a tumor pro-survival mechanism [184-186]. Nonetheless, other studies, namely in lymphoma cells, demonstrated that AMPK activation associated with autophagy induction acts as a pro-death mechanism [187, 188]. Interesting, our data suggested that while in HL-60 cells the activation of AMPK promoted by anti-leukemia agents leads to a moderate autophagy induction and G0/G1 cell cycle arrest as a pro-survival mechanism, in KG-1 cells this activation seems to result in autophagy induction and S phase cell cycle arrest as a pro-death mechanism.

Once activated AMPK is described as phosphorylating the cyclin-dependent kinase inhibitor (CDKI) p27, which results in its exportation from nucleus to cytoplasm where it induces autophagy [135, 141]. However, contrarily to expected, our results suggested that both in HL-60 and KG-1 cells the activation of AMPK by anti-leukemia agents did not result in p27 phosphorylation, suggesting that phosphorylated p27 is not involved in the slight induction of autophagy observed in these cells. Nonetheless, to complement and corroborate this data, additional approaches, such as immunohistochemistry for the detection of phosphorylated p27 and total p27, will be performed in order to evaluate the subcellular localization of these molecules. In addition to phosphorylated p27, AMPK could also impact on autophagy in other different ways, such as: through directly phosphorylation of ULK1 [143] or through phosphorylation of raptor [142]. Therefore, to clarify how AMPK activation could promote autophagy in AML cells, immunoblotting analysis of these proteins may be executed in the future.

Our results also suggested that cytarabine and/or doxorubicin induce AMPK activation associated with G0/G1 cell cycle arrest in HL-60 cells. As p27 is a CDKI that functions in nucleus to negatively regulate Cdk2 promoting G0/G1 cell cycle arrest [134], it is possible that the G0/G1 cell cycle arrest observed in HL-60 cells treated with conventional chemotherapy be induced by this CDKI. Thus, this aspect may be clarified through an immunohistochemistry in order to detect and confirm p27 nuclear localization. p53 plays an important role in the maintenance of genome integrity and it is well described as inducer of G0/G1 cell cycle arrest in response to DNA damage (reviewed in [144]). However, this protein is not involved in the G0/G1 cell cycle arrest observed in HL-60 cells, since these cells have a null-p53 phenotype [217, 218].

Interesting, KG-1 cells also lack the expression of *P53* mRNA [217]. However, while in HL-60 cells most of the *P53* gene is deleted and no aberrant *P53* mRNA species is detected [217], in KG-1 cells wild-type *P53* mRNA is not expressed because these cells have mutations in *P53* gene [219]. In fact, deletions or mutations in this gene were detected in other types of AML cell lines, suggesting that inactivation of the *P53* gene may be a common feature in AML cells and that may play an important role in the establishment of these cells [219]. The Cdc25A (Cell division cycle 25 homolog A) phosphatase is another protein that could be involved in the G0/G1 cell cycle arrest promoted by cytarabine and/or doxorubicin in HL-60 cells. In response to DNA damage Cdc25A is phosphorylated and suffers ubiquitin-proteasome mediated degradation, which impairs the dephosphorylation of Cdk2 leading to its inhibition and consequent G0/G1 cell cycle arrest (reviewed in [144]). Thus, to determine if the G0/G1 cell cycle arrest promoted by conventional chemotherapy could be mediated by a mechanism that involves Cdc25A degradation, immunoblotting analysis of Cdc25A can be performed in future approaches. The degradation of Cdc25A is also involved in S phase cell cycle arrest (reviewed in [144]) and therefore immunoblotting analysis of this protein may also be done to understand if the S phase cell cycle arrest induced by doxorubicin alone or combined with cytarabine in KG-1 cells is promoted by this event.

To complement and validate results showing that AMPK is a crucial player in HL-60 cells response to conventional chemotherapy, we intent to pharmacologically manipulate AMPK through metformin, an AMPK activator, or compound C, an AMPK inhibitor. To confirm results obtained, genetic approaches, such as the silencing by siRNA of AMPK, will also be performed. The same approaches will be executed in KG-1 cells to confirm the role of AMPK in the cell cycle arrest and autophagy induction as a pro-death mechanism.

Autophagy has been described as playing a dual role in cancer therapeutic context, namely in hematological malignancies. Studies have reported that autophagy may function as a pro-survival mechanism in response to chemotherapy. For example, the inhibition of autophagy by pharmacological inhibitors or genetic knockdown of autophagy genes enhanced the death of chronic myeloid leukemia (CML) cells by Imatinib [179]. However, studies also described a role as a pro-death mechanism for autophagy. For example, morphinone, vitamin K2 and Eupalinin A were reported as inducing autophagic cell death in HL-60 AML cell line [183]. These findings point for a role of autophagy in cancer cells response to chemotherapy but also suggest that the impact of autophagy on the multiple cancer cells is different. In fact, our results also supported

this dual role of autophagy. The pharmacological inhibition of autophagy potentiated the cytotoxic effects of the anti-leukemia therapy in HL-60 cells, but in KG-1 cells this inhibition enhanced cell survival. Therefore, these results suggested that while in HL-60 cells autophagy may function as a pro-survival mechanism, in KG-1 cells may act as a pro-death mechanism. Data of pharmacological activation of autophagy limits our conclusions on the role of autophagy in AML cells survival due to the fact that rapamycin induces autophagy through direct inhibition of the mammalian target of rapamycin complex 1 (mTORC1), which may exert crucial functions in other several cellular processes (reviewed in [127]). Thus, the genetic manipulation of autophagy through the silencing by siRNA of some autophagy regulators, such as *BECLIN1*, *ATG5* and *ATG7*, will be performed to confirm obtained results.

In conclusion, our findings suggested that AMPK pathway activation culminating in cell cycle arrest and autophagy induction plays an important role in AML cells response to conventional chemotherapy (Fig.47). Nevertheless, our results showed that HL-60 and KG-1 cells respond differently to anti-leukemia therapy. In fact, while in HL-60 cells AMPK activation associated with G0/G1 cell cycle arrest and autophagy induction promoted by DNA damage (Fig.47A) seems to function as a pro-survival mechanism, in KG-1 cells the AMPK activation associated with S phase cell cycle arrest and autophagy induction (Fig.47B) seems to act as a pro-death mechanism. Thus, this data points for AMPK as a potential therapeutic target, which in combination with conventional chemotherapy may be a successful strategy to eradicate AML cells.

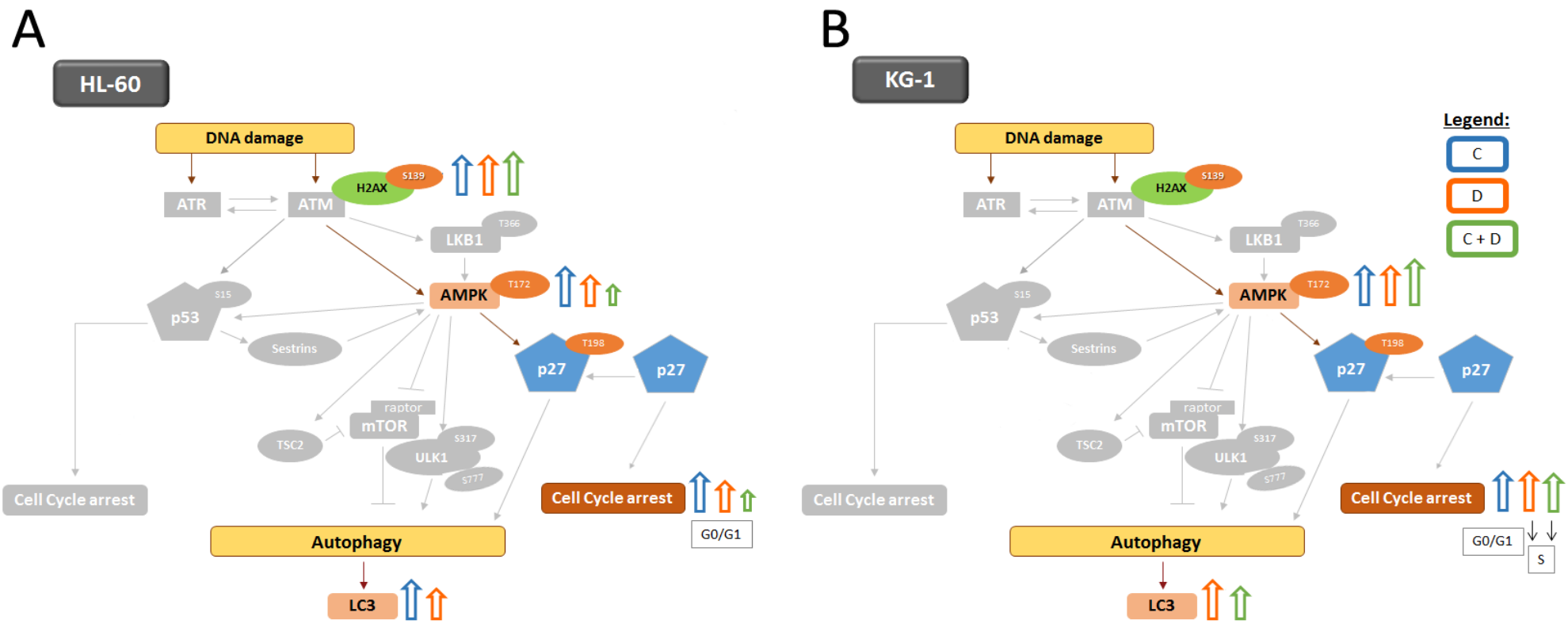

Figure 47 - Schematic representation of the results obtained with HL-60 (A) and KG-1 (B) cells during this master project. In HL-60 cells, cytarabine or doxorubicin promoted H2AX phosphorylation at Ser139, AMPK phosphorylation at Thr172 and G0/G1 cell cycle arrest. The combination of both drugs resulted in a more pronounced H2AX phosphorylation, less AMPK phosphorylation and G0/G1 cell cycle arrest and no impact on autophagy. Nonetheless, cytarabine and/or doxorubicin did not promote p27 phosphorylation at Thr198. In KG-1 cells, cytarabine and/or doxorubicin did not promote H2AX phosphorylation at Ser139, but induced AMPK phosphorylation and cell cycle arrest. Doxorubicin alone or combined with cytarabine promoted AMPK phosphorylation associated with S phase cell cycle arrest and autophagy induction. Similar to HL-60 cells, the phosphorylation of p27 at Thr198 was also not observed in KG-1 cells treated with cytarabine and/or doxorubicin. C - cytarabine; D - doxorubicin; C+D - cytarabine combined with doxorubicin.

REFERENCES

1. Passegue, E., et al., *Normal and leukemic hematopoiesis: are leukemias a stem cell disorder or a reacquisition of stem cell characteristics?* Proc Natl Acad Sci U S A, 2003. **100 Suppl 1**: p. 11842-9.
2. Passegue, E. and I.L. Weisman, *Leukemic stem cells: where do they come from?* Stem Cell Rev, 2005. **1**(3): p. 181-8.
3. Jordan, C.T. and M.L. Guzman, *Mechanisms controlling pathogenesis and survival of leukemic stem cells.* Oncogene, 2004. **23**(43): p. 7178-87.
4. Mittal, P., *The Acute Leukemias.* Hospital Physician, 2001: p. 37-44.
5. Lowenberg, B., J.R. Downing, and A. Burnett, *Acute myeloid leukemia.* N Engl J Med, 1999. **341**(14): p. 1051-62.
6. Estey E, D.H., *Acute myeloid leukemia.* Lancet, 2006. **368**: p. 1894-1907.
7. Shipley, J.L. and J.N. Butera, *Acute myelogenous leukemia.* Exp Hematol, 2009. **37**(6): p. 649-58.
8. Caceres-Cortes, J.R., *Blastic Leukaemias (AML): A Biologist's View.* Cell Biochem Biophys, 2012.
9. Horton, S.J. and B.J. Huntly, *Recent advances in acute myeloid leukemia stem cell biology.* Haematologica, 2012. **97**(7): p. 966-74.
10. Appelbaum, F.R., *Acute myeloid leukemia in adults.* Clinical oncology, 2004. **2004**: p. 2825-2848.
11. Pedersen-Bjergaard, J., et al., *Causality of myelodysplasia and acute myeloid leukemia and their genetic abnormalities.* Leukemia, 2002. **16**(11): p. 2177-84.
12. Leone, G., et al., *Therapy related leukemias: susceptibility, prevention and treatment.* Leuk Lymphoma, 2001. **41**(3-4): p. 255-76.
13. Felix, C.A., *Secondary leukemias induced by topoisomerase-targeted drugs.* Biochim Biophys Acta, 1998. **1400**(1-3): p. 233-55.
14. Greenlee, R.T., et al., *Cancer statistics, 2001.* CA Cancer J Clin, 2001. **51**(1): p. 15-36.
15. Forman, D., et al., *Cancer prevalence in the UK: results from the EUROPREVAL study.* Ann Oncol, 2003. **14**(4): p. 648-54.
16. Jemal, A., et al., *Cancer statistics, 2002.* CA Cancer J Clin, 2002. **52**(1): p. 23-47.
17. Jemal, A., et al., *Cancer statistics, 2010.* CA Cancer J Clin, 2010. **60**(5): p. 277-300.
18. Deschler, B. and M. Lubbert, *Acute myeloid leukemia: epidemiology and etiology.* Cancer, 2006. **107**(9): p. 2099-107.
19. SEER Cancer Statistics Review, -., National Cancer Institute. Bethesda, MD, www.seer.cancer.gov/csr/1975_2010/, based on November 2010 SEER data submission, posted to the SEER website 2011.
20. Kumar, C.C., *Genetic abnormalities and challenges in the treatment of acute myeloid leukemia.* Genes Cancer, 2011. **2**(2): p. 95-107.

21. Bennett, J.M., et al., *Proposals for the classification of the acute leukaemias. French-American-British (FAB) co-operative group.* Br J Haematol, 1976. **33**(4): p. 451-8.
22. Harris, N., Jaffe, E., Diebold, J., et al., *WHO classification of neoplastic disease of the hematopoietic and lymphoid tissues: report of the clinical advisory committee meeting-Airlie House, Virginia.* J Clin Oncol, 1999. **17**: p. 3835-3849.
23. Bennett, J.M., et al., *Proposed revised criteria for the classification of acute myeloid leukemia. A report of the French-American-British Cooperative Group.* Ann Intern Med, 1985. **103**(4): p. 620-5.
24. Cheson, B.D., et al., *Report of the National Cancer Institute-sponsored workshop on definitions of diagnosis and response in acute myeloid leukemia.* J Clin Oncol, 1990. **8**(5): p. 813-9.
25. Vardiman, J.W., N.L. Harris, and R.D. Brunning, *The World Health Organization (WHO) classification of the myeloid neoplasms.* Blood, 2002. **100**(7): p. 2292-302.
26. Vardiman, J.W., et al., *The 2008 revision of the World Health Organization (WHO) classification of myeloid neoplasms and acute leukemia: rationale and important changes.* Blood, 2009. **114**(5): p. 937-51.
27. Vardiman, J.W., *The World Health Organization (WHO) classification of tumors of the hematopoietic and lymphoid tissues: an overview with emphasis on the myeloid neoplasms.* Chem Biol Interact, 2010. **184**(1-2): p. 16-20.
28. Yin, C.C., L.J. Medeiros, and C.E. Bueso-Ramos, *Recent advances in the diagnosis and classification of myeloid neoplasms–comments on the 2008 WHO classification.* Int J Lab Hematol, 2010. **32**(5): p. 461-76.
29. Martens, J.H. and H.G. Stunnenberg, *The molecular signature of oncofusion proteins in acute myeloid leukemia.* FEBS Lett, 2010. **584**(12): p. 2662-9.
30. Look, A.T., *Oncogenic transcription factors in the human acute leukemias.* Science, 1997. **278**(5340): p. 1059-64.
31. Redner, R.L., J. Wang, and J.M. Liu, *Chromatin remodeling and leukemia: new therapeutic paradigms.* Blood, 1999. **94**(2): p. 417-28.
32. Mitelman, F., B. Johansson, and F. Mertens, *The impact of translocations and gene fusions on cancer causation.* Nat Rev Cancer, 2007. **7**(4): p. 233-45.
33. Uribesalgo, I. and L. Di Croce, *Dynamics of epigenetic modifications in leukemia.* Brief Funct Genomics, 2011. **10**(1): p. 18-29.
34. Sell, S., *Leukemia: stem cells, maturation arrest, and differentiation therapy.* Stem Cell Rev, 2005. **1**(3): p. 197-205.
35. Meyers, S., N. Lenny, and S.W. Hiebert, *The t(8;21) fusion protein interferes with AML-1B-dependent transcriptional activation.* Mol Cell Biol, 1995. **15**(4): p. 1974-82.
36. Frank, R., et al., *The AML1/ETO fusion protein blocks transactivation of the GM-CSF promoter by AML1B.* Oncogene, 1995. **11**(12): p. 2667-74.
37. Lutterbach, B., et al., *The inv(16) encodes an acute myeloid leukemia 1 transcriptional corepressor.* Proc Natl Acad Sci U S A, 1999. **96**(22): p. 12822-7.
38. Lutterbach, B. and S.W. Hiebert, *Role of the transcription factor AML-1 in acute leukemia and hematopoietic differentiation.* Gene, 2000. **245**(2): p. 223-35.

39. Mrozek, K., H. Dohner, and C.D. Bloomfield, *Influence of new molecular prognostic markers in patients with karyotypically normal acute myeloid leukemia: recent advances.* Curr Opin Hematol, 2007. **14**(2): p. 106-14.
40. Tallman, M.S., D.G. Gilliland, and J.M. Rowe, *Drug therapy for acute myeloid leukemia.* Blood, 2005. **106**(4): p. 1154-63.
41. Lowenberg, B., J.D. Griffin, and M.S. Tallman, *Acute myeloid leukemia and acute promyelocytic leukemia.* Hematology Am Soc Hematol Educ Program, 2003. **2003**: p. 82-101.
42. Stone, R.M., M.R. O'Donnell, and M.A. Sekeres, *Acute myeloid leukemia.* Hematology Am Soc Hematol Educ Program, 2004. **2004**: p. 98-117.
43. Roboz, G.J., *Novel approaches to the treatment of acute myeloid leukemia.* Hematology Am Soc Hematol Educ Program, 2011. **2011**: p. 43-50.
44. Cheson, B.D., et al., *Revised recommendations of the International Working Group for Diagnosis, Standardization of Response Criteria, Treatment Outcomes, and Reporting Standards for Therapeutic Trials in Acute Myeloid Leukemia.* J Clin Oncol, 2003. **21**(24): p. 4642-9.
45. Erba, H.P., *Has there been progress in the treatment of older patients with acute myeloid leukemia?* Best Pract Res Clin Haematol., 2010. **23**: p. 495-501.
46. Dombret, H., E. Raffoux, and C. Gardin, *Acute myeloid leukemia in the elderly.* Semin Oncol, 2008. **35**(4): p. 430-8.
47. Pollyea, D.A., H.E. Kohrt, and B.C. Medeiros, *Acute myeloid leukaemia in the elderly: a review.* Br J Haematol, 2011. **152**(5): p. 524-42.
48. Kohrt, H.E. and S.E. Coutre, *Optimizing therapy for acute myeloid leukemia.* J Natl Compr Canc Netw, 2008. **6**(10): p. 1003-16.
49. Cassileth, P.A., et al., *Chemotherapy compared with autologous or allogeneic bone marrow transplantation in the management of acute myeloid leukemia in first remission.* N Engl J Med, 1998. **339**(23): p. 1649-56.
50. Burnett, A.K., et al., *Randomised comparison of addition of autologous bone-marrow transplantation to intensive chemotherapy for acute myeloid leukaemia in first remission: results of MRC AML 10 trial. UK Medical Research Council Adult and Children's Leukaemia Working Parties.* Lancet, 1998. **351**(9104): p. 700-8.
51. Jones, C.V. and E.A. Copelan, *Treatment of acute myeloid leukemia with hematopoietic stem cell transplantation.* Future Oncol, 2009. **5**(4): p. 559-68.
52. Dohner, H., et al., *Diagnosis and management of acute myeloid leukemia in adults: recommendations from an international expert panel, on behalf of the European LeukemiaNet.* Blood, 2010. **115**(3): p. 453-74.
53. O'Donnell, M.R., et al., *Acute myeloid leukemia.* J Natl Compr Canc Netw, 2011. **9**(3): p. 280-317.
54. Estey, E., *Acute myeloid leukemia and myelodysplastic syndromes in older patients.* J Clin Oncol, 2007. **25**(14): p. 1908-15.
55. Yanada, M. and T. Naoe, *Acute myeloid leukemia in older adults.* Int J Hematol, 2012. **96**(2): p. 186-93.

56. Stapnes, C., et al., *Targeted therapy in acute myeloid leukaemia: current status and future directions.* Expert Opin Investig Drugs, 2009. **18**(4): p. 433-55.
57. Licht, J.D., *Reconstructing a disease: what essential features of the retinoic acid receptor fusion oncoproteins generate acute promyelocytic leukemia?* Cancer Cell, 2006. **9**: p. 73-74.
58. Villa, R., et al., *Epigenetic gene silencing in acute promyelocytic leukemia.* Biochem Pharmacol, 2004. **68**(6): p. 1247-54.
59. Horlein, A.J., et al., *Ligand-independent repression by the thyroid hormone receptor mediated by a nuclear receptor co-repressor.* Nature, 1995. **377**(6548): p. 397-404.
60. Chen, J.D. and R.M. Evans, *A transcriptional co-repressor that interacts with nuclear hormone receptors.* Nature, 1995. **377**(6548): p. 454-7.
61. Kamei, Y., et al., *A CBP integrator complex mediates transcriptional activation and AP-1 inhibition by nuclear receptors.* Cell, 1996. **85**(3): p. 403-14.
62. Chakravarti, D., et al., *Role of CBP/P300 in nuclear receptor signalling.* Nature, 1996. **383**(6595): p. 99-103.
63. Kwok, C., et al., *Forced homo-oligomerization of RARalpha leads to transformation of primary hematopoietic cells.* Cancer Cell, 2006. **9**(2): p. 95-108.
64. Sternsdorf, T., et al., *Forced retinoic acid receptor alpha homodimers prime mice for APL-like leukemia.* Cancer Cell, 2006. **9**(2): p. 81-94.
65. Castaigne, S., et al., *All-trans retinoic acid as a differentiation therapy for acute promyelocytic leukemia. I. Clinical results.* Blood, 1990. **76**(9): p. 1704-9.
66. Warrell, R.P., Jr., et al., *Differentiation therapy of acute promyelocytic leukemia with tretinoin (all-trans-retinoic acid).* N Engl J Med, 1991. **324**(20): p. 1385-93.
67. Degos, L., et al., *Treatment of first relapse in acute promyelocytic leukaemia with all-trans retinoic acid.* Lancet, 1990. **336**(8728): p. 1440-1.
68. Sanz, M.A., *Treatment of acute promyelocytic leukemia.* Hematology Am Soc Hematol Educ Program, 2006. **2006**: p. 147-55.
69. Fenaux, P., et al., *A randomized comparison of all transretinoic acid (ATRA) followed by chemotherapy and ATRA plus chemotherapy and the role of maintenance therapy in newly diagnosed acute promyelocytic leukemia. The European APL Group.* Blood, 1999. **94**(4): p. 1192-200.
70. Douer, D., *ATO: the forefront of APL treatment?* Blood, 2006. **107**: p. 2588-2589.
71. Douer, D. and M.S. Tallman, *Arsenic trioxide: new clinical experience with an old medication in hematologic malignancies.* J Clin Oncol, 2005. **23**(10): p. 2396-410.
72. Sanz, M.A., P. Fenaux, and F. Lo Coco, *Arsenic trioxide in the treatment of acute promyelocytic leukemia. A review of current evidence.* Haematologica, 2005. **90**(9): p. 1231-5.
73. Shen, Z.X., et al., *All-trans retinoic acid/As2O3 combination yields a high quality remission and survival in newly diagnosed acute promyelocytic leukemia.* Proc Natl Acad Sci U S A, 2004. **101**(15): p. 5328-35.
74. Bentley, N.J. and A.M. Carr, *DNA structure-dependent checkpoints in model systems.* Biol Chem, 1997. **378**(11): p. 1267-74.

75. McIntosh, E.M. and R.H. Haynes, *dUTP pyrophosphatase as a potential target for chemotherapeutic drug development.* Acta Biochim Pol, 1997. **44**(2): p. 159-71.
76. Gmeiner, W.H., et al., *Cytarabine-induced destabilization of a model Okazaki fragment.* Nucleic Acids Res, 1998. **26**(10): p. 2359-65.
77. Lamba, J.K., *Genetic factors influencing cytarabine therapy.* Pharmacogenomics, 2009. **10**(10): p. 1657-74.
78. Higashigawa, M., et al., *Membrane transport of 1-beta-D-arabinofuranosylcytosine and accumulation of 1-beta-D-arabinofuranosylcytosine 5'-triphosphate in P388 murine leukemic cells resistant to vincristine.* Leuk Res, 1991. **15**(4): p. 255-62.
79. Wang, L.M., J.C. White, and R.L. Capizzi, *The effect of ara-C-induced inhibition of DNA synthesis on its cellular pharmacology.* Cancer Chemother Pharmacol, 1990. **25**(6): p. 418-24.
80. Ross, D.D., et al., *Mechanistic implications of alterations in HL-60 cell nascent DNA after exposure to 1-beta-D-arabinofuranosylcytosine.* Cancer Chemother Pharmacol, 1992. **31**(1): p. 61-70.
81. Thompson, H.C. and R.D. Kuchta, *Arabinofuranosyl nucleotides are not chain-terminators during initiation of new strands of DNA by DNA polymerase alpha-primase.* Biochemistry, 1995. **34**(35): p. 11198-203.
82. Cortes-Funes, H. and C. Coronado, *Role of anthracyclines in the era of targeted therapy.* Cardiovasc Toxicol, 2007. **7**(2): p. 56-60.
83. Minotti, G., et al., *Anthracyclines: molecular advances and pharmacologic developments in antitumor activity and cardiotoxicity.* Pharmacol Rev, 2004. **56**(2): p. 185-229.
84. Phillips, D.R., P.C. Greif, and R.C. Boston, *Daunomycin-DNA dissociation kinetics.* Mol Pharmacol, 1988. **33**(2): p. 225-30.
85. Cutts, S.M., et al., *The power and potential of doxorubicin-DNA adducts.* IUBMB Life, 2005. **57**(2): p. 73-81.
86. Swift, L.P., et al., *Doxorubicin-DNA adducts induce a non-topoisomerase II-mediated form of cell death.* Cancer Res, 2006. **66**(9): p. 4863-71.
87. Cutts, S.M., et al., *Recent advances in understanding and exploiting the activation of anthracyclines by formaldehyde.* Curr Med Chem Anticancer Agents, 2005. **5**(5): p. 431-47.
88. Yokochi, T. and K.D. Robertson, *Doxorubicin inhibits DNMT1, resulting in conditional apoptosis.* Mol Pharmacol, 2004. **66**(6): p. 1415-20.
89. Wilstermann, A.M. and N. Osheroff, *Stabilization of eukaryotic topoisomerase II-DNA cleavage complexes.* Curr Top Med Chem, 2003. **3**(3): p. 321-38.
90. Sordet, O., et al., *Apoptosis induced by topoisomerase inhibitors.* Curr Med Chem Anticancer Agents, 2003. **3**(4): p. 271-90.
91. Larsen, A.K., A.E. Escargueil, and A. Skladanowski, *Catalytic topoisomerase II inhibitors in cancer therapy.* Pharmacol Ther, 2003. **99**(2): p. 167-81.
92. Cowell, I.G. and C.A. Austin, *Mechanism of generation of therapy related leukemia in response to anti-topoisomerase II agents.* Int J Environ Res Public Health, 2012. **9**(6): p. 2075-91.

93. Nyberg, K.A., et al., *Toward maintaining the genome: DNA damage and replication checkpoints.* Annu Rev Genet, 2002. **36**: p. 617-56.
94. Osborn, A.J., S.J. Elledge, and L. Zou, *Checking on the fork: the DNA-replication stress-response pathway.* Trends Cell Biol, 2002. **12**(11): p. 509-16.
95. Sancar, A., et al., *Molecular mechanisms of mammalian DNA repair and the DNA damage checkpoints.* Annu Rev Biochem, 2004. **73**: p. 39-85.
96. Zhou, B.B. and S.J. Elledge, *The DNA damage response: putting checkpoints in perspective.* Nature, 2000. **408**(6811): p. 433-9.
97. Bakkenist, C.J. and M.B. Kastan, *Initiating cellular stress responses.* Cell, 2004. **118**(1): p. 9-17.
98. Zou, L. and S.J. Elledge, *Sensing DNA damage through ATRIP recognition of RPA-ssDNA complexes.* Science, 2003. **300**(5625): p. 1542-8.
99. Cimprich, K.A. and D. Cortez, *ATR: an essential regulator of genome integrity.* Nat Rev Mol Cell Biol, 2008. **9**(8): p. 616-27.
100. Hirao, A., et al., *DNA damage-induced activation of p53 by the checkpoint kinase Chk2.* Science, 2000. **287**(5459): p. 1824-7.
101. Zhao, H. and H. Piwnica-Worms, *ATR-mediated checkpoint pathways regulate phosphorylation and activation of human Chk1.* Mol Cell Biol, 2001. **21**(13): p. 4129-39.
102. Cruet-Hennequart, S., et al., *Doxorubicin induces the DNA damage response in cultured human mesenchymal stem cells.* Int J Hematol, 2012. **96**(5): p. 649-56.
103. Kurz, E.U., P. Douglas, and S.P. Lees-Miller, *Doxorubicin activates ATM-dependent phosphorylation of multiple downstream targets in part through the generation of reactive oxygen species.* J Biol Chem, 2004. **279**(51): p. 53272-81.
104. Fram, R.J. and D.W. Kufe, *DNA strand breaks caused by inhibitors of DNA synthesis: 1-beta-D-arabinofuranosylcytosine and aphidicolin.* Cancer Res, 1982. **42**(10): p. 4050-3.
105. Bakkenist, C.J. and M.B. Kastan, *DNA damage activates ATM through intermolecular autophosphorylation and dimer dissociation.* Nature, 2003. **421**(6922): p. 499-506.
106. Stiff, T., et al., *ATR-dependent phosphorylation and activation of ATM in response to UV treatment or replication fork stalling.* EMBO J, 2006. **25**(24): p. 5775-82.
107. Hurley, P.J. and F. Bunz, *ATM and ATR: components of an integrated circuit.* Cell Cycle, 2007. **6**(4): p. 414-7.
108. Rogakou, E.P., et al., *Megabase chromatin domains involved in DNA double-strand breaks in vivo.* J Cell Biol, 1999. **146**(5): p. 905-16.
109. Kuo, L.J. and L.X. Yang, *Gamma-H2AX - a novel biomarker for DNA double-strand breaks.* In Vivo, 2008. **22**(3): p. 305-9.
110. Sharma, A., K. Singh, and A. Almasan, *Histone H2AX phosphorylation: a marker for DNA damage.* Methods Mol Biol, 2012. **920**: p. 613-26.
111. Rogakou, E.P., et al., *DNA double-stranded breaks induce histone H2AX phosphorylation on serine 139.* J Biol Chem, 1998. **273**(10): p. 5858-68.

112. Foray, N., et al., *A subset of ATM- and ATR-dependent phosphorylation events requires the BRCA1 protein.* EMBO J, 2003. **22**(11): p. 2860-71.
113. Lee, J.H., et al., *53BP1 promotes ATM activity through direct interactions with the MRN complex.* EMBO J, 2010. **29**(3): p. 574-85.
114. Banin, S., et al., *Enhanced phosphorylation of p53 by ATM in response to DNA damage.* Science, 1998. **281**(5383): p. 1674-7.
115. Canman, C.E., et al., *Activation of the ATM kinase by ionizing radiation and phosphorylation of p53.* Science, 1998. **281**(5383): p. 1677-9.
116. Sapkota, G.P., et al., *Ionizing radiation induces ataxia telangiectasia mutated kinase (ATM)-mediated phosphorylation of LKB1/STK11 at Thr-366.* Biochem J, 2002. **368**(Pt 2): p. 507-16.
117. Fu, X., et al., *Etoposide induces ATM-dependent mitochondrial biogenesis through AMPK activation.* PLoS One, 2008. **3**(4): p. e2009.
118. Sanli, T., et al., *Ionizing radiation activates AMP-activated kinase (AMPK): a target for radiosensitization of human cancer cells.* Int J Radiat Oncol Biol Phys, 2010. **78**(1): p. 221-9.
119. Sanz, P., *AMP-activated protein kinase: structure and regulation.* Curr Protein Pept Sci, 2008. **9**(5): p. 478-92.
120. Luo, L., et al., *ATM and LKB1 dependent activation of AMPK sensitizes cancer cells to etoposide-induced apoptosis.* Cancer Lett, 2012. **328**(1): p. 114-9.
121. Jenne, D.E., et al., *Peutz-Jeghers syndrome is caused by mutations in a novel serine threonine kinase.* Nat Genet, 1998. **18**(1): p. 38-43.
122. Hemminki, A., et al., *A serine/threonine kinase gene defective in Peutz-Jeghers syndrome.* Nature, 1998. **391**(6663): p. 184-7.
123. Levine, A.J., *p53, the cellular gatekeeper for growth and division.* Cell, 1997. **88**(3): p. 323-31.
124. Zhang, Y. and Y. Xiong, *Control of p53 ubiquitination and nuclear export by MDM2 and ARF.* Cell Growth Differ, 2001. **12**(4): p. 175-86.
125. Budanov, A.V. and M. Karin, *p53 target genes sestrin1 and sestrin2 connect genotoxic stress and mTOR signaling.* Cell, 2008. **134**(3): p. 451-60.
126. Inoki, K., et al., *Rheb GTPase is a direct target of TSC2 GAP activity and regulates mTOR signaling.* Genes Dev, 2003. **17**(15): p. 1829-34.
127. Laplante, M. and D.M. Sabatini, *mTOR signaling in growth control and disease.* Cell, 2012. **149**(2): p. 274-93.
128. Ma, X.M. and J. Blenis, *Molecular mechanisms of mTOR-mediated translational control.* Nat Rev Mol Cell Biol, 2009. **10**(5): p. 307-18.
129. Hay, N. and N. Sonenberg, *Upstream and downstream of mTOR.* Genes Dev, 2004. **18**(16): p. 1926-45.
130. Jung, C.H., et al., *mTOR regulation of autophagy.* FEBS Lett, 2010. **584**(7): p. 1287-95.
131. Hay, N., *p53 strikes mTORC1 by employing sestrins.* Cell Metab, 2008. **8**(3): p. 184-5.

132. Kim, H.S., et al., *Inhibition of AMP-activated protein kinase sensitizes cancer cells to cisplatin-induced apoptosis via hyper-induction of p53.* J Biol Chem, 2008. **283**(7): p. 3731-42.
133. Rashid, A., et al., *Resveratrol enhances prostate cancer cell response to ionizing radiation. Modulation of the AMPK, Akt and mTOR pathways.* Radiat Oncol, 2011. **6**: p. 144.
134. Slingerland, J. and M. Pagano, *Regulation of the cdk inhibitor p27 and its deregulation in cancer.* J Cell Physiol, 2000. **183**(1): p. 10-7.
135. Alexander, A. and C.L. Walker, *The role of LKB1 and AMPK in cellular responses to stress and damage.* FEBS Lett, 2011. **585**(7): p. 952-7.
136. Hardie, D.G., *New roles for the LKB1–>AMPK pathway.* Curr Opin Cell Biol, 2005. **17**(2): p. 167-73.
137. Alessi, D.R., K. Sakamoto, and J.R. Bayascas, *LKB1-dependent signaling pathways.* Annu Rev Biochem, 2006. **75**: p. 137-63.
138. Shaw, R.J., et al., *The tumor suppressor LKB1 kinase directly activates AMP-activated kinase and regulates apoptosis in response to energy stress.* Proc Natl Acad Sci U S A, 2004. **101**(10): p. 3329-35.
139. Jones, R.G., et al., *AMP-activated protein kinase induces a p53-dependent metabolic checkpoint.* Mol Cell, 2005. **18**(3): p. 283-93.
140. Inoki, K., T. Zhu, and K.L. Guan, *TSC2 mediates cellular energy response to control cell growth and survival.* Cell, 2003. **115**(5): p. 577-90.
141. Liang, J., et al., *The energy sensing LKB1-AMPK pathway regulates p27(kip1) phosphorylation mediating the decision to enter autophagy or apoptosis.* Nat Cell Biol, 2007. **9**(2): p. 218-24.
142. Gwinn, D.M., et al., *AMPK phosphorylation of raptor mediates a metabolic checkpoint.* Mol Cell, 2008. **30**(2): p. 214-26.
143. Zhao, M. and D.J. Klionsky, *AMPK-dependent phosphorylation of ULK1 induces autophagy.* Cell Metab, 2011. **13**(2): p. 119-20.
144. Lukas, J., C. Lukas, and J. Bartek, *Mammalian cell cycle checkpoints: signalling pathways and their organization in space and time.* DNA Repair (Amst), 2004. **3**(8-9): p. 997-1007.
145. Bartek, J. and J. Lukas, *Mammalian G1- and S-phase checkpoints in response to DNA damage.* Curr Opin Cell Biol, 2001. **13**(6): p. 738-47.
146. Ward, I.M., X. Wu, and J. Chen, *Threonine 68 of Chk2 is phosphorylated at sites of DNA strand breaks.* J Biol Chem, 2001. **276**(51): p. 47755-8.
147. Maya, R., et al., *ATM-dependent phosphorylation of Mdm2 on serine 395: role in p53 activation by DNA damage.* Genes Dev, 2001. **15**(9): p. 1067-77.
148. Shinozaki, T., et al., *Functional role of Mdm2 phosphorylation by ATR in attenuation of p53 nuclear export.* Oncogene, 2003. **22**(55): p. 8870-80.
149. Mailand, N., et al., *Rapid destruction of human Cdc25A in response to DNA damage.* Science, 2000. **288**(5470): p. 1425-9.

150. Falck, J., et al., *The ATM-Chk2-Cdc25A checkpoint pathway guards against radioresistant DNA synthesis.* Nature, 2001. **410**(6830): p. 842-7.
151. Sherr, C.J. and J.M. Roberts, *CDK inhibitors: positive and negative regulators of G1-phase progression.* Genes Dev, 1999. **13**(12): p. 1501-12.
152. Stewart, Z.A. and J.A. Pietenpol, *p53 Signaling and cell cycle checkpoints.* Chem Res Toxicol, 2001. **14**(3): p. 243-63.
153. Niculescu, A.B., 3rd, et al., *Effects of p21(Cip1/Waf1) at both the G1/S and the G2/M cell cycle transitions: pRb is a critical determinant in blocking DNA replication and in preventing endoreduplication.* Mol Cell Biol, 1998. **18**(1): p. 629-43.
154. Falck, J., et al., *The DNA damage-dependent intra-S phase checkpoint is regulated by parallel pathways.* Nat Genet, 2002. **30**(3): p. 290-4.
155. Donzelli, M. and G.F. Draetta, *Regulating mammalian checkpoints through Cdc25 inactivation.* EMBO Rep, 2003. **4**(7): p. 671-7.
156. Mailand, N., et al., *Regulation of G(2)/M events by Cdc25A through phosphorylation-dependent modulation of its stability.* EMBO J, 2002. **21**(21): p. 5911-20.
157. Pietenpol, J.A. and Z.A. Stewart, *Cell cycle checkpoint signaling: cell cycle arrest versus apoptosis.* Toxicology, 2002. **181-182**: p. 475-81.
158. Sanchez, Y., et al., *Conservation of the Chk1 checkpoint pathway in mammals: linkage of DNA damage to Cdk regulation through Cdc25.* Science, 1997. **277**(5331): p. 1497-501.
159. Matsuoka, S., M. Huang, and S.J. Elledge, *Linkage of ATM to cell cycle regulation by the Chk2 protein kinase.* Science, 1998. **282**(5395): p. 1893-7.
160. Lopez-Girona, A., et al., *Nuclear localization of Cdc25 is regulated by DNA damage and a 14-3-3 protein.* Nature, 1999. **397**(6715): p. 172-5.
161. Flatt, P.M., et al., *p53 regulation of G(2) checkpoint is retinoblastoma protein dependent.* Mol Cell Biol, 2000. **20**(12): p. 4210-23.
162. Chan, T.A., et al., *14-3-3Sigma is required to prevent mitotic catastrophe after DNA damage.* Nature, 1999. **401**(6753): p. 616-20.
163. Jin, S., et al., *GADD45-induced cell cycle G2-M arrest associates with altered subcellular distribution of cyclin B1 and is independent of p38 kinase activity.* Oncogene, 2002. **21**(57): p. 8696-704.
164. Xiao, G., *Autophagy and NF-kappaB: fight for fate.* Cytokine Growth Factor Rev, 2007. **18**(3-4): p. 233-43.
165. Yang, Z. and D.J. Klionsky, *An overview of the molecular mechanism of autophagy.* Curr Top Microbiol Immunol, 2009. **335**: p. 1-32.
166. He, C. and D.J. Klionsky, *Regulation mechanisms and signaling pathways of autophagy.* Annu Rev Genet, 2009. **43**: p. 67-93.
167. Glick, D., S. Barth, and K.F. Macleod, *Autophagy: cellular and molecular mechanisms.* J Pathol, 2010. **221**(1): p. 3-12.
168. Mizushima, N., T. Yoshimori, and B. Levine, *Methods in mammalian autophagy research.* Cell, 2010. **140**(3): p. 313-26.

169. Fleming, A., et al., *Chemical modulators of autophagy as biological probes and potential therapeutics.* Nat Chem Biol, 2011. **7**(1): p. 9-17.
170. Rabinowitz, J.D. and E. White, *Autophagy and metabolism.* Science, 2010. **330**(6009): p. 1344-8.
171. Hippert, M.M., P.S. O'Toole, and A. Thorburn, *Autophagy in cancer: good, bad, or both?* Cancer Res, 2006. **66**(19): p. 9349-51.
172. Dalby, K.N., et al., *Targeting the prodeath and prosurvival functions of autophagy as novel therapeutic strategies in cancer.* Autophagy, 2010. **6**(3): p. 322-9.
173. Murrow, L. and J. Debnath, *Autophagy as a stress-response and quality-control mechanism: implications for cell injury and human disease.* Annu Rev Pathol, 2012. **8**: p. 105-37.
174. Mizushima, N., et al., *Autophagy fights disease through cellular self-digestion.* Nature, 2008. **451**(7182): p. 1069-75.
175. Yang, Z.J., et al., *The role of autophagy in cancer: therapeutic implications.* Mol Cancer Ther, 2011. **10**(9): p. 1533-41.
176. Tseng, H.C., et al., *Sensitizing effect of 3-methyladenine on radiation-induced cytotoxicity in radio-resistant HepG2 cells in vitro and in tumor xenografts.* Chem Biol Interact, 2011. **192**(3): p. 201-8.
177. Sasaki, K., et al., *Chloroquine potentiates the anti-cancer effect of 5-fluorouracil on colon cancer cells.* BMC Cancer, 2010. **10**: p. 370.
178. Sotelo, J., E. Briceno, and M.A. Lopez-Gonzalez, *Adding chloroquine to conventional treatment for glioblastoma multiforme: a randomized, double-blind, placebo-controlled trial.* Ann Intern Med, 2006. **144**(5): p. 337-43.
179. Bellodi, C., et al., *Targeting autophagy potentiates tyrosine kinase inhibitor-induced cell death in Philadelphia chromosome-positive cells, including primary CML stem cells.* J Clin Invest, 2009. **119**(5): p. 1109-23.
180. Amaravadi, R.K., et al., *Autophagy inhibition enhances therapy-induced apoptosis in a Myc-induced model of lymphoma.* J Clin Invest, 2007. **117**(2): p. 326-36.
181. Kanzawa, T., et al., *Arsenic trioxide induces autophagic cell death in malignant glioma cells by upregulation of mitochondrial cell death protein BNIP3.* Oncogene, 2005. **24**(6): p. 980-91.
182. Bursch, W., et al., *Active cell death induced by the anti-estrogens tamoxifen and ICI 164 384 in human mammary carcinoma cells (MCF-7) in culture: the role of autophagy.* Carcinogenesis, 1996. **17**(8): p. 1595-607.
183. Puissant, A., G. Robert, and P. Auberger, *Targeting autophagy to fight hematopoietic malignancies.* Cell Cycle, 2010. **9**(17): p. 3470-8.
184. Harhaji-Trajkovic, L., et al., *AMPK-mediated autophagy inhibits apoptosis in cisplatin-treated tumour cells.* J Cell Mol Med, 2009. **13**(9B): p. 3644-54.
185. Xie, B.S., et al., *Autophagy inhibition enhances etoposide-induced cell death in human hepatoma G2 cells.* Int J Mol Med, 2011. **27**(4): p. 599-606.
186. Li, D.D., et al., *The inhibition of autophagy sensitises colon cancer cells with wild-type p53 but not mutant p53 to topotecan treatment.* PLoS One, 2012. **7**(9): p. e45058.

187. Shi, W.Y., et al., *Therapeutic metformin/AMPK activation blocked lymphoma cell growth via inhibition of mTOR pathway and induction of autophagy.* Cell Death Dis, 2012. **3**: p. e275.
188. Huo, H.Z., et al., *AMP-activated protein kinase (AMPK)/Ulk1-dependent autophagic pathway contributes to C6 ceramide-induced cytotoxic effects in cultured colorectal cancer HT-29 cells.* Mol Cell Biochem, 2013. **378**(1-2): p. 171-81.
189. Green, A.S., et al., *The LKB1/AMPK signaling pathway has tumor suppressor activity in acute myeloid leukemia through the repression of mTOR-dependent oncogenic mRNA translation.* Blood, 2010. **116**(20): p. 4262-73.
190. Borthakur G. AM., et al., *High Expression of Autophagy Related Proteins Negatively Impacts Clinical Outcomes in Acute Myelogenous Leukemia–Time to Target Autophagy to Improve Therapy Outcomes?* American Society of Hematology, 2011.
191. Min, Y.H., et al., *Elevated S-phase kinase-associated protein 2 protein expression in acute myelogenous leukemia: its association with constitutive phosphorylation of phosphatase and tensin homologue protein and poor prognosis.* Clin Cancer Res, 2004. **10**(15): p. 5123-30.
192. Yokozawa, T., et al., *Prognostic significance of the cell cycle inhibitor p27Kip1 in acute myeloid leukemia.* Leukemia, 2000. **14**(1): p. 28-33.
193. Dalton, W.T., Jr., et al., *HL-60 cell line was derived from a patient with FAB-M2 and not FAB-M3.* Blood, 1988. **71**(1): p. 242-7.
194. Birnie, G.D., *The HL60 cell line: a model system for studying human myeloid cell differentiation.* Br J Cancer Suppl, 1988. **9**: p. 41-5.
195. Hyun, J.W., et al., *Leukemic cell line, KG-1 has a functional loss of hOGG1 enzyme due to a point mutation and 8-hydroxydeoxyguanosine can kill KG-1.* Oncogene, 2000. **19**(39): p. 4476-9.
196. Poole, B. and S. Ohkuma, *Effect of weak bases on the intralysosomal pH in mouse peritoneal macrophages.* J Cell Biol, 1981. **90**(3): p. 665-9.
197. Glaumann, H. and J. Ahlberg, *Comparison of different autophagic vacuoles with regard to ultrastructure, enzymatic composition, and degradation capacity–formation of crinosomes.* Exp Mol Pathol, 1987. **47**(3): p. 346-62.
198. Ballou, L.M. and R.Z. Lin, *Rapamycin and mTOR kinase inhibitors.* J Chem Biol, 2008. **1**(1-4): p. 27-36.
199. Kurose, A., et al., *Effects of hydroxyurea and aphidicolin on phosphorylation of ataxia telangiectasia mutated on Ser 1981 and histone H2AX on Ser 139 in relation to cell cycle phase and induction of apoptosis.* Cytometry A, 2006. **69**(4): p. 212-21.
200. Goodwin, C.J., et al., *Microculture tetrazolium assays: a comparison between two new tetrazolium salts, XTT and MTS.* J Immunol Methods, 1995. **179**(1): p. 95-103.
201. Gorczyca, W., *Cytometric analyses to distinguish death processes.* Endocr Relat Cancer, 1999. **6**(1): p. 17-9.
202. van Engeland, M., et al., *Annexin V-affinity assay: a review on an apoptosis detection system based on phosphatidylserine exposure.* Cytometry, 1998. **31**(1): p. 1-9.

203. Pu, Q.Q. and W.R. Bezwoda, *Induction of alkylator (melphalan) resistance in HL60 cells is accompanied by increased levels of topoisomerase II expression and function.* Mol Pharmacol, 1999. **56**(1): p. 147-53.
204. Colado, E., et al., *The effect of the proteasome inhibitor bortezomib on acute myeloid leukemia cells and drug resistance associated with the CD34+ immature phenotype.* Haematologica, 2008. **93**(1): p. 57-66.
205. Hsu, S., et al., *Green tea polyphenols induce differentiation and proliferation in epidermal keratinocytes.* J Pharmacol Exp Ther, 2003. **306**(1): p. 29-34.
206. Devika, P.T. and P. Stanely Mainzen Prince, *(-)Epigallocatechin-gallate (EGCG) prevents mitochondrial damage in isoproterenol-induced cardiac toxicity in albino Wistar rats: a transmission electron microscopic and in vitro study.* Pharmacol Res, 2008. **57**(5): p. 351-7.
207. Wang, P., S.M. Henning, and D. Heber, *Limitations of MTT and MTS-based assays for measurement of antiproliferative activity of green tea polyphenols.* PLoS One, 2010. **5**(4): p. e10202.
208. Kim, C.N., et al., *Overexpression of Bcl-X(L) inhibits Ara-C-induced mitochondrial loss of cytochrome c and other perturbations that activate the molecular cascade of apoptosis.* Cancer Res, 1997. **57**(15): p. 3115-20.
209. Tao, Z., et al., *Inhibition of cellular respiration by doxorubicin.* Chem Res Toxicol, 2006. **19**(8): p. 1051-8.
210. Chou, T.C., *Drug combination studies and their synergy quantification using the Chou-Talalay method.* Cancer Res, 2010. **70**(2): p. 440-6.
211. Boehrer, S., et al., *Suppression of the DNA damage response in acute myeloid leukemia versus myelodysplastic syndrome.* Oncogene, 2009. **28**(22): p. 2205-18.
212. Mizushima, N., and T. Yoshimori, *How to interpret LC3 immunoblotting.* Autophagy 3, 2007: p. 542-5.
213. Alvino, G.M., et al., *Replication in hydroxyurea: it's a matter of time.* Mol Cell Biol, 2007. **27**(18): p. 6396-406.
214. Farombi, E.O., *Genotoxicity of chloroquine in rat liver cells: protective role of free radical scavengers.* Cell Biol Toxicol, 2006. **22**(3): p. 159-67.
215. Kennedy, J.A. and F. Barabe, *Investigating human leukemogenesis: from cell lines to in vivo models of human leukemia.* Leukemia, 2008. **22**(11): p. 2029-40.
216. Kumari, S., et al., *DNA DAMAGE: DETECTION STRATEGIES.* EXCLI Journal 2008, 2008. **7**: p. 44-62.
217. Wolf, D. and V. Rotter, *Major deletions in the gene encoding the p53 tumor antigen cause lack of p53 expression in HL-60 cells.* Proc Natl Acad Sci U S A, 1985. **82**(3): p. 790-4.
218. Planchon, S.M., et al., *Beta-lapachone-mediated apoptosis in human promyelocytic leukemia (HL-60) and human prostate cancer cells: a p53-independent response.* Cancer Res, 1995. **55**(17): p. 3706-11.
219. Sugimoto, K., et al., *Frequent mutations in the p53 gene in human myeloid leukemia cell lines.* Blood, 1992. **79**(9): p. 2378-83.